McGill University

Montreal

CALCIFICATION IN INTERVERTEBRAL DISC DEGENERATION AND SCOLIOSIS

by Gergana Ivanova Hristova

Division of Experimental Surgery

Faculty of Medicine

McGill University

Montreal

A thesis submitted to McGill University in partial fulfillment of the requirements of the degree of Master of Science

November 2009

TABLE OF CONTENTS

ABSTRACT

In degenerative and scoliotic intervertebral discs (IVD), calcification is a pathological process that may lead to impairment of the nutrient supply and a disturbance in disc metabolism. However, the process of calcification in disc degeneration and scoliosis is not well understood. The purpose of this study was to assess the calcification markers in IVD of patients with degenerative disc disease and adolescent idiopathic scoliosis. For this purpose, 34 IVDs from 16 adult patients with degenerative disc disease and 25 IVDs from 9 adolescent patients with adolescent idiopathic scoliosis were obtained after surgery or autopsy. The concave and the convex parts of the scoliotic discs were analyzed separately. Von Kossa staining was performed to visualize calcium deposits, while type X collagen expression, which is associated with endochondral ossification, was measured by immunohistochemistry and Western blot. Alkaline phosphatase (ALP) activity and calcium and inorganic phosphate (Pi) concentrations were used as markers of the calcification process. Results showed the presence of calcium deposits and type X collagen only in degenerative and scoliotic intervertebral discs, but not in control discs. Results also demonstrated a large individual variability in ALP activity and calcium and Pi concentrations in degenerative and scoliotic discs. Moreover, the level of the calcification markers was consistently higher in degenerative and scoliotic discs than in control discs. The results suggest that disc degeneration in adults involves mineral deposition and that mineralization in adolescent idiopathic scoliosis discs might reflect an ongoing premature degenerative process.

RÉSUMÉ

Dans les disques intervertébraux (DIV) dégénérés et de scoliose, la calcification est un processus pathologique qui peut mener à une diminution de l'apport nutritif et à un débalancement du métabolisme. Cependant, le processus de calcification de ces disques est très peu connu. Le but de la présente étude était d'évaluer le potentiel de calcification des DIVs de patients avec une maladie dégénérative des disques (MDD) ou avec une scoliose idiopathique chez l'adolescent (SIA). Pour ce faire 34 DIVs provenant de 16 adultes avec MDD et 25 DIVs de 9 patients avec SIA ont été obtenus après chirurgie ou autopsie. Les côtés convexe et concaves des disques scoliotiques on été analysés séparément. Une coloration de Von Kossa a été faite afin de visualiser les dépôts de calcium alors que l'expression du collagène de type X, associé à l'ossification endochondrale, a été mesurée par immunohistochimie et par buvardage de type Western. L'activité de la phosphatase alcaline (PA) ainsi que les concentrations de calcium et de phosphate inorganique (Pi) ont servi d'indicateurs du potentiel de calcification. Les résultats montrent la présence de dépôts de calcium et de collagène de type X uniquement dans les DIVs des patients ayant une MDD ou une SIA, mais non dans les disques témoins. Les résultats montrent également une grande variabilité individuelle de l'activité de la PA ainsi que des concentrations de calcium et de Pi. De plus, les niveaux de ces marqueurs du potentiel de calcification était plus élevés dans les disques dégénérés et scoliotiques que dans les disques témoins. Les résultats suggèrent que la dégénération du disque intervertébral adulte est associée à une déposition de minéraux et que la minéralisation du disque scoliotique pourrait refléter un processus de dégénération prématurée.

LIST OF FIGURES

LIST OF TABLES

LIST OF ABBREVIATIONS

AF – annulus fibrosus

AIS – adolescent idiopathic scoliosis

ALP – alkaline phosphatase

BSA – bovine serum albumin

Ca^{2+} – calcium

Col X – type X collagen

DAB – 3,3'-diaminobenzidine

DDD – degenerative disc disease

ECM – extracellular matrix

EP – cartilage endplate

HA - hydroxyapatite

IVD – intervertebral disc

kDa – kilodaltons

MVs – matrix vesicles

NP – nucleus pulposus

Pi – inorganic phosphate

PPi – inorganic pyrophosphate

SDS – sodium dodecyl sulfate

SDS-PAGE – sodium dodecyl sulfate-polyacrylamide gel electrophoresis

VB – vertebral body

ACKNOWLEDGEMENTS

I would like to acknowledge the valuable help of all those who contributed to the conducting and completion of this study. Dr. Peter Roughley greatly contributed to the study with his continuous advice, guidance and encouragement at all stages of the project. He devoted his time and his attention to any kind of questions I had. His valuable suggestions and deep understanding are sincerely appreciated. I would like to thank also to my supervisors Dr. John Antoniou and Dr. Fackson Mwale for giving me the wonderful chance to work in medical research and for their guidance and continuous help throughout the whole period of my studies and work on the project. I am deeply thankful to them for the opportunity to learn so much during my work in the lab. I would like to acknowledge the continuous help of Dr. Alain Petit and Laura Epure from the Orthopedics Research Lab. They were always there for me for any kinds of requests I had during the whole process of conducting the study, and finally, during the period of preparation of this thesis. I would also like to acknowledge the contribution of Dr. Jean Ouellet and Dr. Peter Jarzem, the two orthopedics surgeons who provided the intervertebral discs for the study and were always helpful with their valuable ideas and suggestions regarding the study. Their help during the initiation and the progress of the project are highly appreciated. Also, I would like to thank to my family, who continuously supported me even from the long distance between us and to all my friends in Canada and abroad. Here, I would like to mention the name of Audley Legore and to express my special gratefulness to him for being such an experienced scientist while giving me advice and such a great friend of mine, always helping me and motivating me during my studies. I would also like to express my thankfulness to McGill University for providing me the wonderful opportunity to study and learn so much and to CIHR for the funding.

I. INTRODUCTION

1. The Human Spine – Structure and Function

1.1. The Human Vertebral Column

The human spine is an anatomical structure situated in the dorsal area of the torso. It constitutes an important part of the locomotor system and provides the necessary structure for proper position and functioning of internal organs. It is composed of the spinal cord, a nervous tissue transmitting neural signals between the brain and the rest of the body, and the vertebral column, which constitutes the protective and supportive structure of the spinal cord. The vertebral column can be divided in 3 sections: the vertebrae, the sacrum and the coccyx. The vertebrae remains distinct within themselves throughout life and are then named true or movable vertebrae. They formed the cervical (C1-C7), the thoracic (T1-T12), and the lumbar (L1-L5) parts of the column (Fig 1) and are numerated starting from the cranium. Thus the first cervical vertebra is designated as C1 and the last one as C7. In the same manner thoracic vertebrae are designated as T1 to T12 and lumbar are designated as L1 to L5. The sacrum and the coccyx are fused vertebrae and are also named false or fixed vertebrae. The five sacral vertebrae form the upper bone of the sacrum, a compact anatomical structure and are designated as S1 to S5. Finally, the four coccygeal vertebrae form the terminal bone of the coccyx (Standring, 2008).

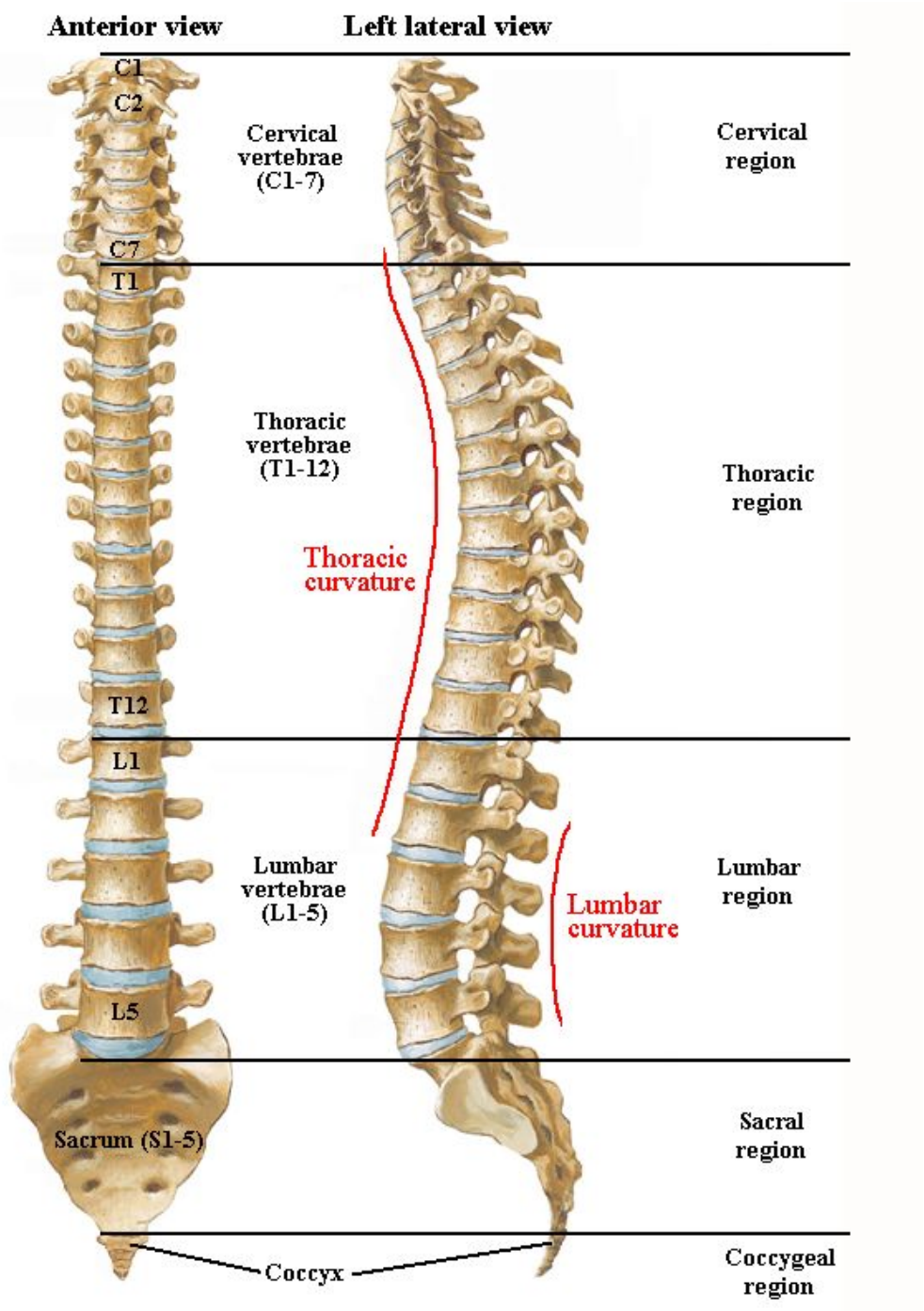

Figure 1. Normal human vertebral column (adapted from: www.indyspinemd.com)

Figure represents sagittal and lateral views of the vertebral column. Different anatomical regions of the vertebral column are designated, namely cervical, thoracic, lumbar, sacral and coccygeal regions.

1.2. The Intervertebral Disc

The true or movable vertebrae, with the exception of C1 and C2, are separated by intervertebral discs (IVDs). An IVD is also present between the last lumbar vertebra (L5) and the sacrum. Indeed, the human spine possesses twenty-three (23) IVDs that separate the vertebrae and provide flexibility (Roughley, 2004). They are identified by specifying the particular vertebrae they separate. For example, the disc between the fourth and fifth lumbar vertabrae is called “L4–L5” or “L4-5”. Each IVD forms a cartilaginous joint to allow specific and limited movement of the vertebrae and acts as a ligament to hold the vertebrae together. As such, each vertebra is interconnected to the next adjacent vertebra by an IVD, ligaments, and muscles (Buckwalter, 1995). The size of the IVDs increases from the cervical to lumbar regions and account for 20% to 30% of the length of the spine. The IVD is composed of three main elements, namely, an inner nucleus pulposus (NP), an outer annulus fibrosus (AF), which surrounds it, and a cartilaginous endplate (EP) that attach the discs to the vertebrae (Hayes, Benjamin, & Ralphs, 2001) (Fig. 2).

The central portion of the disc contains the NP which, during the intrauterine developmental period, is composed of cells from the primitive notochord (Standring, 2008). Later on during adulthood, it consists of chondrocyte-like cells that are sparsely dispersed within an extracellular matrix (ECM) that contains loose fibers surrounded by a mucoprotein gel that has the consistency of jelly. These fibers are made up of type II collagen and elastin molecules and form an irregular network (Akeson, Woo, Taylor, Ghosh, & Bushell, 1977).

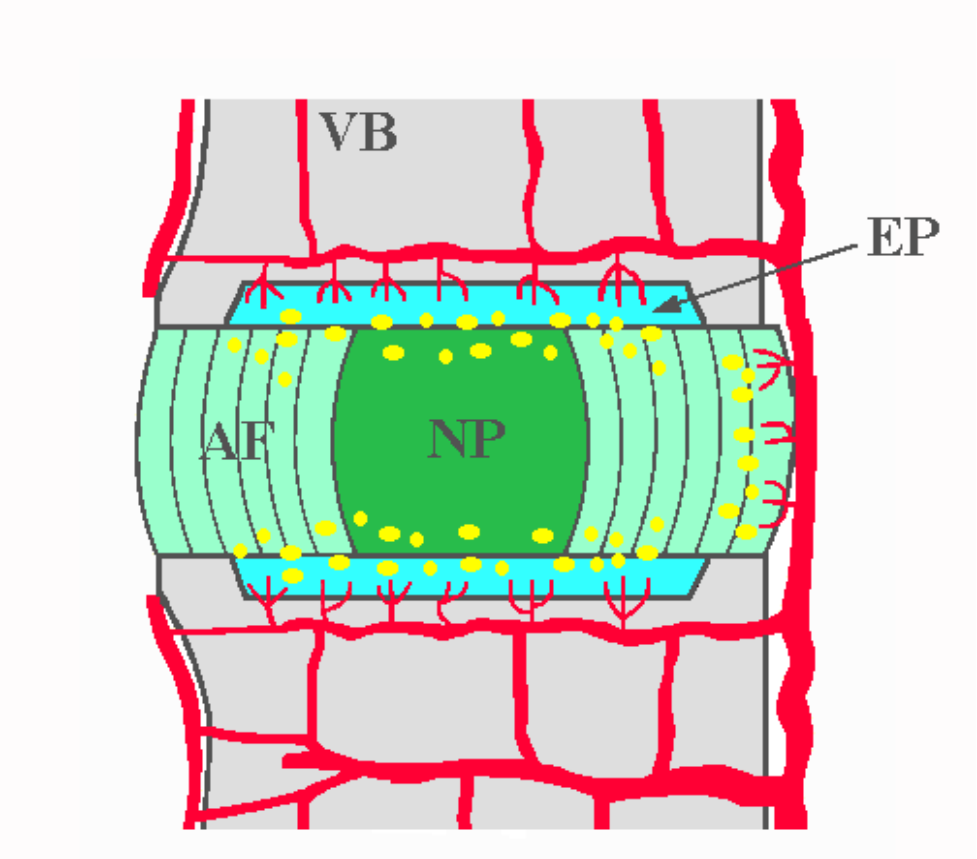

Figure 2. Structure of the intervertebral disc (adapted from: www.chirogeek.com)

Figure represents the intervertebral disc (IVD) situated between two adjacent vertebral bodies (VB in gray color). The three main elements of the IVD are represented as follows: endplate (EP) in blue; annulus fibrosus (AF) in light green; nucleus pulposus (NP) in dark green. Blood vessels are represented in red color. Different substances diffusing through the disc are represented as yellow dots.

The fiber network of the NP is suspended in water rich gel. This gel is comprised of proteoglycans which trap and hold water within the disc. The major proteoglycan of the disc is aggrecan which, because of its high anionic glycosaminoglycan content (chondroitin sulfate and keratin sulfate), exhibits osmotic properties which provide the high water content of the nucleus and hence its ability to resist compression (Watanabe, Yamada, & Kimata, 1998). The nucleus, therefore, acts

as a shock absorber, absorbing the impact of the body's daily activities and keeping the two vertebrae separated. NP cells mainly respond to hydrostatic pressure by synthesizing mostly proteoglycans and type II collagen fibrils (Adams & Roughley, 2006). The proteoglycan content of the disc is maximal in the young adult and declines thereafter, presumably because of proteolysis (Antoniou, et al., 1996). Cell density also declines, especially in the nucleus, during aging and is extremely low in the adult (Boos, et al., 2002).

The AF is composed of concentric layers of fibro-cartilage called lamellae and intertwined annular bands (Fig. 2). These annular bands are arranged in a specific pattern to resist sheer forces placed on the spine (Standring, 2008). Individual lamellae of the AF consist primarily of type I collagen fibers. The strong annular fibers of AF constrain the NP and distribute pressure evenly across the disc. As a result, the swelling of the nucleus due to the proteoglycan is limited radially by the collagen fibrils of the annulus and axially by the cartilage endplates and vertebral bodies, thereby providing the ability of the IVD to withstand the compressive loads resulting from the body’s weight and its bending (Roughley, 2004). AF cells predominantly respond to deformation by synthesizing type I collagen fibers. The cells in the peripheral annulus are spindle shaped and become more rounded and cartilage-like in the innermost rings where the aggrecan content also increases (Akeson, et al., 1977).

The vertebral EPs (Fig. 2) are cartilaginous plates that supply food (nutrients) to the inner two-thirds of the annulus and the entire nucleus (J. P. Urban, Smith, & Fairbank, 2004). In adult discs, blood vessels are normally restricted to the endplate (EP) and the outmost layers of the annulus. The transport of metabolites occurs predominantly by diffusion and bulk fluid flow, especially in terms of the metabolic supply to the nucleus and inner two-thirds of the annulus. Diffusion is the main

mechanism of circulation of small molecules within the disc, whereas, the bulk fluid flow is an important mechanism for the movement of large molecules (Ferguson, Ito, & Nolte, 2004). Deficiencies in metabolite transport appear to limit both the density and metabolic activity of disc cells (J. P. Urban, et al., 2004). As a consequence, discs have only a limited ability to recover from any metabolic or mechanical injury.

2. Degenerative Disc Disease

2.1. Description of Degenerative Disc Disease

Usually, IVD aging involves a process of slow and steady degeneration. The changes that occur throughout life are due to preprogrammed events, such as notochordal cell loss, mesenchymal cell senescence, calcification of the vertebral EPs, and loss of the vasculature which disturbs the IVD nutrition. This in turn alters or decreases the synthetic capabilities of the disc cells. In addition, normal turnover of disc matrix molecules is impaired as a consequence of the large size and avascular nature of the growing disc. This leads to the accumulation of degradation products that further disturb the IVD metabolism (Roughley, 2004). However, in some cases this process rapidly accelerates and leads to the development of degenerative disc disease (DDD), which often causes chronic pain and different degrees of disability. Degenerative changes in IVD could be accelerated and enhanced by adverse biomechanical loading patterns of the disc (Iatridis, MacLean, Roughley, & Alini, 2006) that promote disc degeneration process either by initiating degeneration or by influencing cell-mediated remodeling events that occur in response to the mechanical stimuli caused by daily activities (Setton & Chen, 2006).

2.2. Grading of Degenerative Disc Disease

Normal IVD anatomy and physiology are usually discussed in terms of the collagen fibrils of the AF and the aggrecan molecule of the NP (Meakin & Hukins, 2000). The ability of the nucleus to resist compression is closely related to the ability of the proteoglycans to retain water. This ability, however, decreases with age as the aggrecan content declines. The catabolic processes that continuously occur in the disc matrix and the decreased abilities to replace degraded collagen and aggrecan molecules with new intact molecules lead to functional impairment and degenerative structural changes in IVD tissue (Roughley, 2004). In general, the IVD degeneration involves dehydration and biochemical and structural changes of the discs (Feng, Danfelter, Stromqvist, & Heinegard, 2006).

Degenerative IVD are characterized by progressively increasing morphological changes in IVD macrostructure (Fig. 3), including increased lamellar disorganization and fissures (Roberts, Evans, Trivedi, & Menage, 2006). As a result the disc loses its ability to act as a shock absorber between the vertebrae. Disc space loss resulting from the decreased water content of the disc is a typical feature of disc degeneration. As there is minimal blood supply to the discs, it lacks the ability to heal or self-repair.

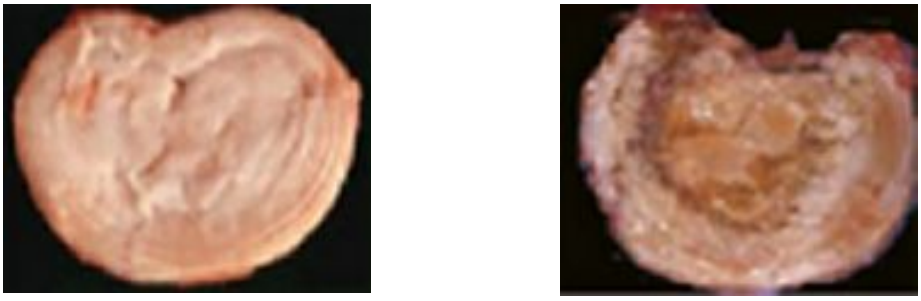

Normal IVD Degenerative IVD

Figure 3. **Morphological aspects of normal and degenerative intervertebral discs** (IVDs) (www.physiol.ox.ac.uk) Figure represents a transversal view of a normal IVD (left) compared to degenerative IVD (right).

A standard method for assessment of IVD degeneration is the Thompson grade. It is a five-category grading scheme for assessing the gross morphology of mid-sagittal sections of the human lumbar IVD (Thompson, et al., 1990). Grade I indicates a structurally and functionally intact IVD. The NP is characterized as a bulging gel, the AF consists of discrete fibrous lamellas, and the EP is hyaline and uniformly thick. The vertebral body (VB) is also intact with rounded margins. Grade II is related to the occurrence of white fibrous tissue peripherally in the NP. Mucinous material between AF lamellas can be also observed. The thickness of the EP is irregular and the vertebral body's margins are pointed. Grade III is related to even more pronounced changes in the NP, which is transformed into consolidated fibrous tissue. In AF the changes involve extensive mucinous infiltration and loss of the annular-nuclear demarcation. Focal defects in EP cartilage can be observed, as well as early chondrophytes or osteophytes at vertebral body margins. Grade IV is associated with the appearance of horizontal clefts in the NP that are parallel to the EP. It is also associated with focal disruptions in the AF. Degenerative changes in the EP are seen as fibro-cartilage extending from subchondral bone as well as irregularity and focal sclerosis of the subchondral bone. Finally, Grade V indicates the most advanced disc degeneration. The observed IVD clefts extend through the NP and the AF. The EP is affected by diffuse sclerosis. The size of the vertebral body's osteophytes is greater than 2 mm.

IVD degeneration can be analyzed in terms of the IVD structural failure. This approach allows the consideration of all other aspects of the degenerative discs, either as predisposing factors for the IVD disruption, or as its consequences (Adams & Roughley, 2006).

2.3. Biochemical Changes in Degenerative Intervertebral Discs

Many different factors influence disc degeneration, including genetic inheritance, disturbed metabolite transport, altered levels of enzyme activity, cell senescence and death, changes in IVD matrix macromolecules and water content, and IVD structural failure. Genetic inheritance, including polymorphic variations in susceptibility genes, is only a risk factor for future environmentally triggered degenerative events. This is implied by the observation that the unfavorable genetic inheritance is present from birth, but the disc degeneration becomes pronounced 40 years later and predominantly in lower lumbar discs. Biochemical changes influence IVD tissue stiffness and strength which could also be a contributing factor to the process of disc degeneration.

2.3.1. Proteoglycans and Collagens

Different types of structural matrix molecules, such as proteoglycans and collagens, are present in the IVD and changes in their metabolism are associated with degenerative disc disease. The degradation of these matrix molecules can impair disc cell metabolism (D. G. Anderson, Li, & Balian, 2005). Molecular changes can also be seen as increased production of cytokines and matrix-degrading enzymes. Indeed, proteoglycan fragmentation may start as early as during childhood (Buckwalter, 1995). It progresses with advancement in age. In parallel, the overall proteoglycan and water content of the disc decreases, especially in the NP (Antoniou, et al., 1996). In fact, the loss of proteoglycan fragments in the disc is a slow process due to the entrapment of the NP by the fibrous AF and the EP (J. P. Urban & Roberts, 2003). As long as the proteoglycan fragments remain entrapped in the disc, they can fulfill a functional role similar to that of the intact proteoglycan. However, aging is associated

with a stiffer and weaker AF. Aging is also associated with an increase in collagen content can as well as a tendency for replacement of the fine type II collagen fibrils in the inner annulus by type I collagen fibers (Adams & Roughley, 2006). Reduced matrix turnover in older discs enables collagen molecules and fibrils to become increasingly cross-linked with each other, thereby, stabilizing the cross-linking (Duance, et al., 1998).

2.3.2. Intervertebral Disc Calcification in Degenerative Disc Disease

IVD calcification in patients with disc degeneration can be observed in all disc locations (Fig. 4), namely, the EP, AF, and NP. A study of the IVD calcification of the spine in an elderly population suggests an increased prevalence of calcification in elderly persons, especially in the AF and the lower thoracic spine (Chanchairujira, et al., 2004). The IVD calcification has also been shown to be advancing with the progress of the disc degeneration process (Noltenius & Prescher, 1977). In a study of degenerative pathologies of vertebral column disc degeneration is described to be followed by proliferation of fibrous tissue and blood vessels which stimulates the formation of ossifying trabeculae within the AF or NP (Resnick, 1985). A series of studies of disc degeneration has been performed in sand rat model of DDD as the IVD degeneration in sand rats is similar to that in humans, and occurs spontaneously with aging (Gruber, Johnson, Norton, & Hanley, 2002). It has been demonstrated that in both sand rats and humans the cartilage EP undergoes calcification with aging and is replaced by bone (Gruber, et al., 2005), which is associated with impediment of the nutrient flow into the disc and subsequent IVD damage (Bernick & Cailliet, 1982). The studies based on the sand rat model of IVD degeneration have detected a positive correlation between the degree of EP calcification and the advancement in IVD

degeneration. This observation supports the hypothesis that EP calcification is involved in the progress of disc degeneration by decreasing nutrient availability to the disc (Gruber, Gordon, Williams, Norton, & Hanley, 2007).

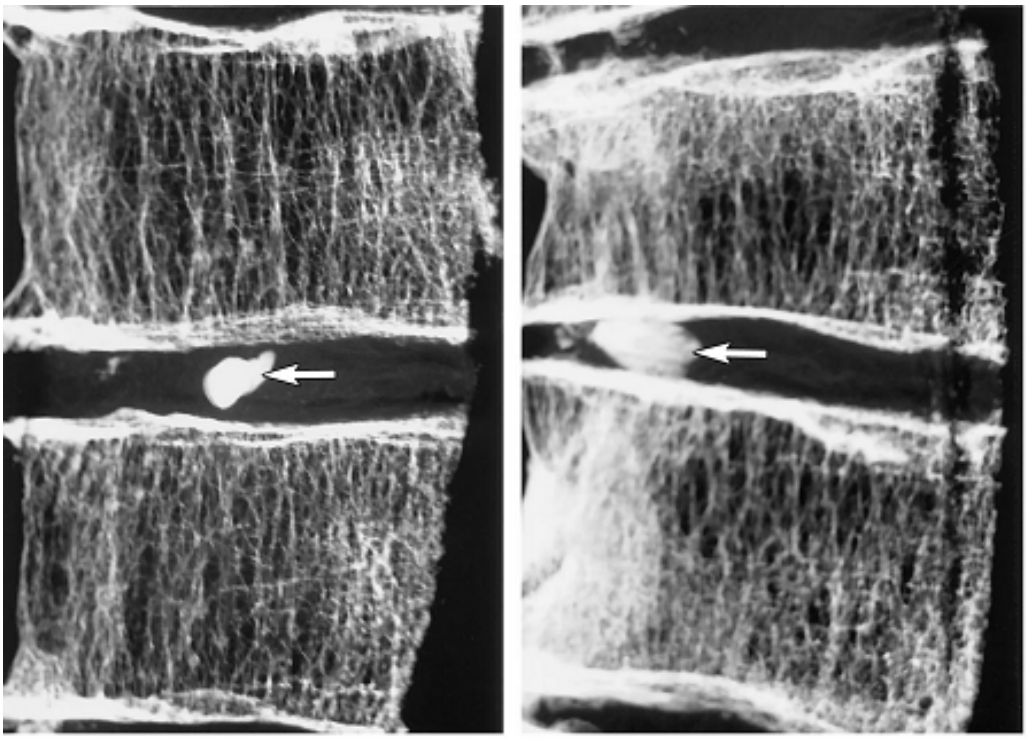

A) **B)**

Figure 4. **X-ray radiographs of the spine showing intervertebral disc calcification in nucleus pulposus and annulus fibrosus**. (Chanchairujira et al. 2004). Figure represents a lateral radiography of two adjacent lumbar vertebrae with the intervertebral disc between them (visualized as a dark space between the two vertebral bodies). **A)** The white arrow indicates a bright area within the projection of nucleus pulposus of the intervertebral disc which represents calcified intervertebral disc tissue. **B)** The white arrow indicates a bright area within the projection of annulus fibrosus of the intervertebral disc which represents calcified intervertebral disc tissue.

3. Scoliosis

3.1. Description and Classification of Scoliosis

Scoliosis is a condition that involves complex lateral and rotational curvature and deformity of the spine. The different curvatures are described as thoracic, lumbar, thoraco-lumbar in relation to their localization and as double when two curves are present (Fig. 5). The rotational component is often the phenomenon that attracts the attention to the spinal curvature. The rotational component is usually manifested as a rib hump, prominent scapula, waist asymmetry, or lumbar fullness. Other symptoms of scoliosis can include uneven shoulder levels, asymmetric size or location of breast in females, and unequal distance between arms and body.

One method of classifying the different types of scoliosis is according to its cause. For instance, if the curvature is secondary to a structural bony abnormality, it is termed as congenital scoliosis. If it is caused by a neurologic disturbance or muscle disease (myopathy for example), it is described as neuromuscular scoliosis. If no cause can be determined, this type of scoliosis is termed idiopathic scoliosis. The idiopathic type is the most common type of scoliosis. Proposed etiologies for idiopathic scoliosis include abnormalities in melatonin, growth hormone, platelets, and posterior column such as impaired proprioception and vibratiory sensibility (Skinner, 2005). Idiopathic scoliosis can also be classified according to the patient's age of onset. When this criterion for classification is used, idiopathic scoliosis can be subdivided into the following subtypes: infantile (under 3 years of age), juvenile (from 4 to 10 years of age), adolescent (from 11 years to age of skeletal maturity), and adult (after skeletal maturity).

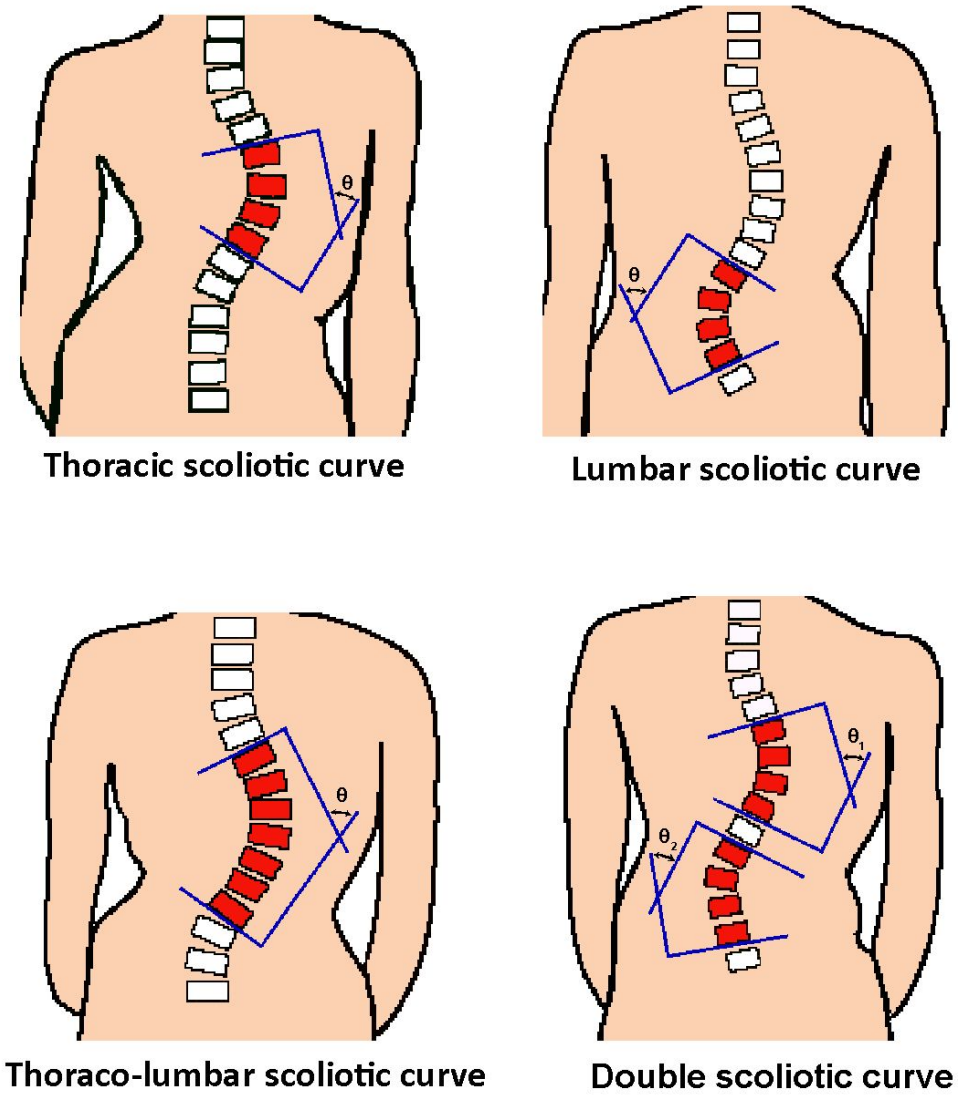

Figure 5. **Schematic representation of the different types of scoliotic curves** (adapted from www.health.uab.edu & www.healthsystem.virginia.edu). Figure represents schematically four different types of scoliotic curvature, namely thoracic, thoraco-lumbar, lumbar and double scoliotic curves, as well as the standard way for measuring of the degree of scoliotic deformity which is the Cobb angle (θ). The Cobb angle is defined as the angle between two lines drawn perpendicularly to the upper endplate of the uppermost vertebra and the lower endplate of the lowest vertebra involved in the curve. In patients with double curves, the Cobb angles for both curves are assessed (θ_1 and θ_2).

The adolescent idiopathic scoliosis (AIS) is the most commonly observed form of scoliosis: its incidence in the general population varied between 1 to 3%. AIS is a pathological entity of unknown etiology, which appears to be multifactorial. AIS occurs more frequently in females than in males and presents itself or worsens during the adolescence growth spurt, before reaching skeletal maturity. Importantly, the incidence is greater in the children of women with scoliosis and particularly in the daughters of these women (Skinner, 2005). This suggests a genetic predisposition for the development of AIS as well as an influence of gender on the incidence of the disease. However, the development of AIS has not been related to nutritional or postural factors, the practice of sports, use of backpacks or carrying a heavy book bag.

3.2. Scoliotic Curvature

The natural history of spinal curvatures is affected by factors such as the magnitude and the type of the curve, the age and the growth potential of the patient, the patient's gender, and the underlying cause of the problem. The curvature in scoliosis is named according to the side of the convexity, as well as the level of the apex, which is the most rotated vertebral body (VB) in the curve (Table 1). The right thoracic curve is the most common types of curves in cases of AIS, followed by the double curve (right thoracic and left lumbar) and the right thoraco-lumbar curve. When the curve occurs as a primary phenomenon, it is considered to be structural. As a consequence of the development of a primary curve, a secondary curve could also be developed. It allows the head to be centered over the pelvis, and is known as the compensatory curve. Compensatory curves usually are of lesser magnitude, more flexible, and less rotated. If the compensatory curve becomes less flexible and with

more pronounced rotation, it might be difficult to determine which curve is the primary one and both curves might be considered structural (Skinner, 2005).

Table 1. Types of scoliotic curves according to the level of the apex (Skinner, 2005).

Curve	**Apex**
Cervical	C1 through C6
Cervico-thoracic	C7 or T1
Thoracic	T2 through T11
Thoraco-lumbar	T12 or L1
Lumbar	L2 through L4
Lumbo-sacral	L5 or lower

A standard method for assessing the scoliotic curvature of the spine quantitatively is the measurement of the Cobb angle. The Cobb angle is the angle between two lines, drawn perpendicular to the upper EP of the uppermost vertebra involved in the curvature and the lower EP of the lowest vertebra involved in the scoliotic curvature. For patients who have two curves, Cobb angles are followed for both curves. The approach to measuring of the Cobb angle is schematically represented on Figure 5, where the Cobb angle is denoted as θ or θ_1 and θ_2 when two

scoliotic curves exist and both Cobb angles are measured. The European Spine Society indicates that scoliosis should be considered as a clinical problem when it involves a lateral curvature or deviation (right or left) of the spine greater than 10º and is associated with vertebral rotation (www.eurospine.org/p31000269.html).

Scoliotic curves greater than 10° affect 2-3% of the population of the United States (National Scoliosis Foundation: www.scoliosis.org/info.php). The prevalence of curves that is less than 20° is about equal in males and females. However, females are eight times more likely to progress to a curve of higher magnitude (www.scoliosis.org/info.php). Scoliotic curves that are greater than 20° affect approximately one in 2500 people. Curves that are convex to the right are more common than those to the left. Single or "C" curves are slightly more common than double or "S" curve patterns (www.answers.com/topic/scoliosis). Males are more likely to have infantile or juvenile scoliosis, but there is a high female predominance of adolescent scoliosis.

With curve progression, the deformity can become severe which could disturb the proper spatial position of internal organs and thus their proper blood supply and physiological functioning. With thoracic curves measuring more than 60°-90°, cardiopulmonary function can become compromised, and secondary restrictive lung disease may result from the chest deformity. Curve progression is most common during skeletal growth. However, moderate curves of 40°-50° should be observed for their progression during adulthood. The degree of curve progression in adulthood varies widely among different patients. The average extent of progression is approximately 1° per year. The routinely used approach to follow the curve progression is by taking radiographs every 2-5 years. This approach is considered to

be satisfactory, especially for patients with AIS who have reached skeletal maturity and do not demonstrate other clinical signs of progression (Skinner, 2005).

3.3. Scoliotic Intervertebral Disc

Scoliotic IVDs are morphologically different from unaffected discs, showing convex and concave parts as a result of the scoliotic deformity (Fig. 6). However, there is no generally accepted scientific theory that explains the causes underlying the IVD changes in AIS. It is generally considered that asymmetrical loading is involved in the progression of AIS since high hydrostatic pressures are observed with asymmetrical stress from concave to convex sides. The changes are then probably a secondary response to altered mechanical loading (Roberts, Menage, & Eisenstein, 1993).

The abnormalities of the scoliotic IVD could influence both disc and EP cellular activity. In addition, disc cells could be influenced through nutritional changes as a consequence of EP calcification (Castelein, van Dieen, & Smit, 2005; Meir, Fairbank, Jones, McNally, & Urban, 2007; Stokes, Burwell, & Dangerfield, 2006; Stokes, Clark, Farnum, & Aronsson, 2007). However, some studies suggest that structural changes may be of prime importance in the progression of scoliosis, although not necessarily an initiating factor (Harrington, et al., 1997; Ponseti, Pedrini, Wynne-Davies, & Duval-Beaupere, 1976; Takahashi, et al., 2007).

Changes that take place in the scoliotic discs are related to the type of collagens being produced. In scoliotic discs, more type I collagen and more minor collagens (types III, VI, IX, and X) are present than in normal discs. Gross remodeling of collagen bundles of annular lamellae also occurs. The elastic fiber network, which is well organized among the lamellae in the normal disc, is very sparse and quite

disorganized in the scoliotic disc. The proteoglycan and water contents are also reduced particularly toward the concavity of the curve (Roberts, et al., 1993). Lower cell viability is observed towards the convex side of the scoliotic curve. The greatest difference in cell viability is detected between the concave and convex sides of the apical disc (Bibby, Fairbank, Urban, & Urban, 2002).

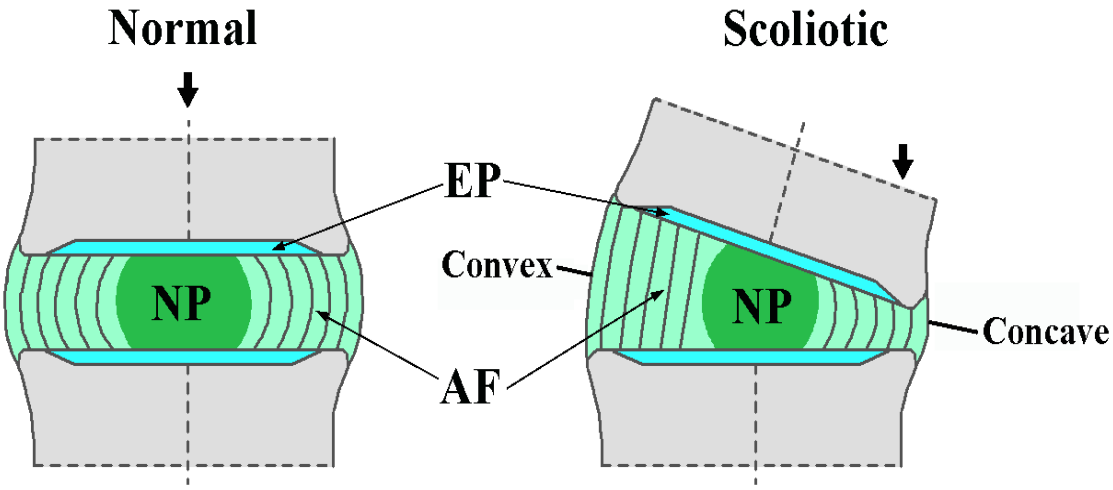

Figure 6. **Schematic representation of normal versus scoliotic intervertebral discs** (adapted from: www.maths.nottingham.ac.uk). Figure represents schematically a scoliotic intervertebral disc (right) in comparison with a normal intervertebral disc (left). For both discs, the endplates (EP) are represented in blue color, the annulus fibrosus (AF) – in light green color, the nucleus pulposus (NP) – in dark green color, and the vertebral bodies are represented in gray color. The concave and convex sides of the scoliotic intervertebral disc are also indicated.

Calcification of the cartilaginous EPs and of their adjacent IVDs could be commonly observed in AIS (Girodias, Azouz, & Marton, 1991; Roberts, et al., 1993; Ventura, Huguet, Salvador, Terricabras, & Cabrera, 1995). Similarly to the

observations in disc degeneration, calcification in scoliosis could involve all disc locations, namely, EP, AF and NP. In most cases, the EP is heavily calcified. This EP calcification may interfere with the flow of nutrients and metabolites through the endplate to and from the disc. Usually, the IVD calcification in scoliotic discs is positively related to the degree of scoliotic deformity.

4. Calcification in the Human Skeleton

4.1. Apatite Formation

Calcification of extracellular matrix (ECM) in the human skeleton is a process of deposition of inorganic calcium phosphates in crystalline forms (Christoffersen & Landis, 1991). Alkaline phosphatase (ALP) is the enzyme that plays an active role in initiating the calcification process (Miller & DeMarzo, 1988). ALP is a well-known biochemical marker of mineralization. The identity of all its substrates is not clearly established (Balcerzak, et al., 2003; Borras & Comes, 2009). During mineral formation, the ALP hydrolyzes several phosphate substrates, including PPi (Ketteler & Floege, 2006; Narisawa, Frohlander, & Millan, 1997), which is a known inhibitor of apatite formation (Balcerzak, et al., 2003). In normal physiological conditions, ALP hydrolyzes the PPi yielding inorganic monophosphate ions (Pi) used for incorporation into mineral crystals (H. C. Anderson, et al., 2004). Thus, the released Pi forms apatite in the presence of calcium (Ca^{2+}) in the extracellular fluid (Fig. 7).

In general sense, the term apatite is used to designate a group of phosphate minerals, such as hydroxyapatite (HA), fluorapatite, chlorapatite and bromapatite for instance. The minerals from the apatite group represent a considerable part of the few minerals that are produced by living organisms. In multicellular biological systems, after being produced by the living organism, apatite is often stored and included in the

composition of the body as an inorganic or mineral phase. In human body, apatite is the major mineral constituent of the bone structure (Kopylov, Jonsson, Thorngren, & Aspenberg, 1996; LeGeros, 2002). It confers the bone and other calcified tissues their mechanical strength and rigidity.

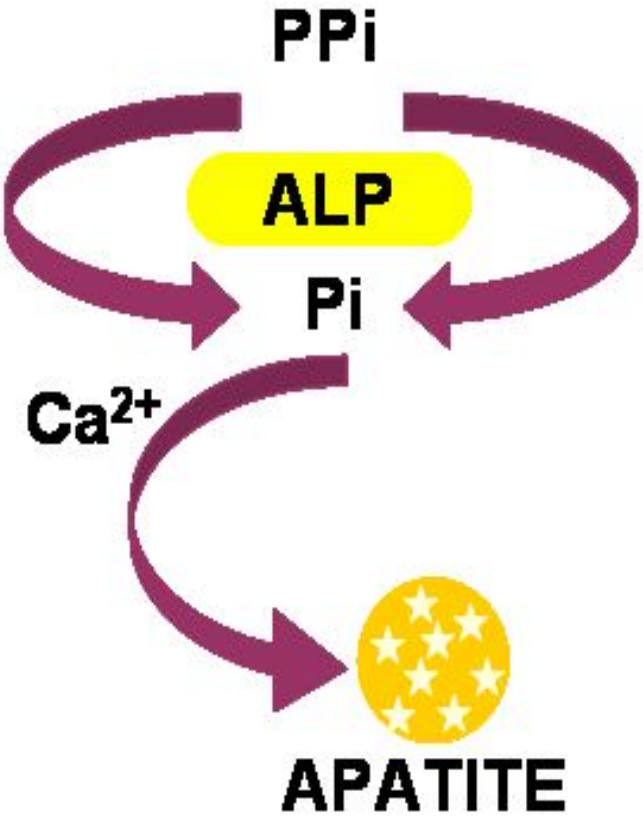

Figure 7. **Formation of apatite by alkaline phosphatase** (adapted from: Garimella et al., 2004). Figure represents schematically the process of hydrolysis of the inorganic pyrophosphate (PPi) by the alkaline phosphatase (ALP). The product of this enzymatic reaction is inorganic phosphate (Pi) which in the presence of calcium (Ca^{2+}) in the extracellular fluid yields apatite.

4.2. Endochondral Ossification

Under normal non-pathological conditions, calcification in the human skeleton occurs in the epiphyseal growth plate. It is the cartilage plate in the long bones of children and adolescents where the longitudinal growth of these bones takes place. Cartilage growth in the epiphyseal growth plate is continuous. On its diaphyseal side it matures, calcifies, and then is resorbed and replaced by bone. This process is known as endochondral ossification and is involved in the process of longitudinal growth of the bone (Mwale, Tchetina, Wu, & Poole, 2002; Roberts, Menage, Duance, Wotton, & Ayad, 1991; Stokes, et al., 2007). During endochondral ossification, chondrocytes differentiate through a series of well-defined morphological zones within the epiphyseal growth cartilage. As a result it can be histologically divided into distinct zones of different cell populations. Each cell population is characterized by distinct cell size shape and function, and is part of a different stage of cartilage maturation (Fig. 8). The zone of proliferation provides a renewable source of chondrocytes for longitudinal bone growth. After exiting the cell cycle, these maturing chondrocytes secrete a matrix composed of aggrecan and type II collagen, as well as other matrix components. Encapsulated in this matrix, the chondrocytes undergo hypertrophy and start producing type X collagen and alkaline phosphatase. In the epiphyseal growth cartilage, the process of calcification starts at the border between the hypertrophic and calcifying (ossification) zones. A considerable part of biosynthetic capacity of hypertrophic chondrocytes is involved in the synthesis of type X collagen (Gebhard, et al., 2004; Schmid, Popp, & Linsenmayer, 1990), which is thought to be involved in calcification during endochondral ossification. In the ossification zone, the matrix that surrounds the hypertrophic chondrocytes becomes mineralized and undergoes an apoptotic death. Thus, the ossification zone is replaced by trabecular bones.

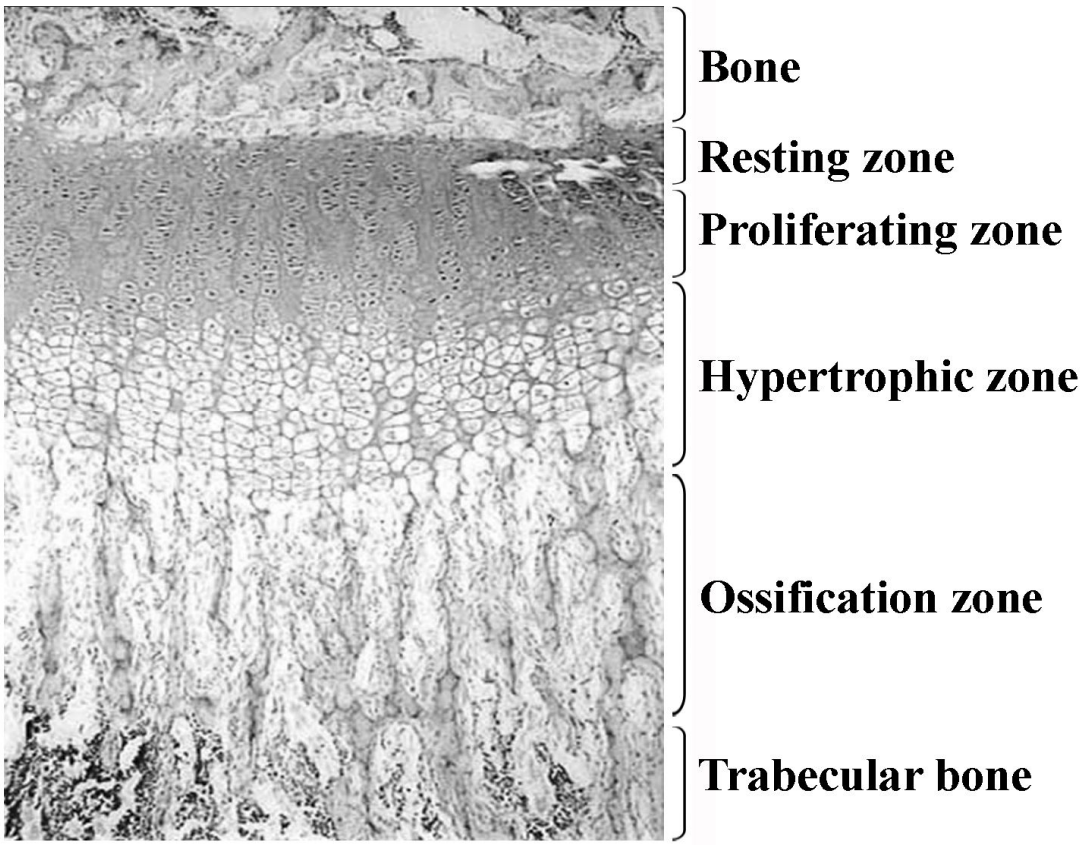

Figure 8: **Morphological zones within the epiphyseal growth plate** (adapted from: www.bioscience.org). Figure represents an image of a histologically prepared and analyzed section of the epiphyseal growth plate from the proximal tibia of a two week old mouse. The section is stained with hematoxylin and eosin. The image is obtained by a light microscope and is represented in the gray color scale. The upper side of the image corresponds to the epiphyseal side of the bone, whereas the lower side of the image represents the diaphyseal side. At the right side of the image are indicated the different histo-morphological zones of the epiphyseal growth plate in their consecutive order.

During the process of skeletal growth, the cartilaginous EP of the IVD acts as an epiphyseal growth plate (Roberts, et al., 1993). Calcification in the epiphyseal growth plate is a normal physiological process and is involved in the basic developmental phenomenon of skeletal growth and bone formation. However, calcification in mature EP cartilage, AF, and NP of IVDs is a pathological process which disturbs the nutrient transport and supply of the disc (Bibby, et al., 2002; Roberts, Urban, Evans, & Eisenstein, 1996; J. P. Urban, et al., 2004; M. R. Urban, Fairbank, Etherington, et al., 2001). Moreover, some cells of the scoliotic AFs and NPs exhibit an hypertrophic chondrocyte phenotype. Taken together, these results strongly suggest that calcification may be implicated in the pathogenesis of scoliosis and disc degeneration (Aigner, Gresk-otter, Fairbank, von der Mark, & Urban, 1998).

In scientific literature two basic mechanisms of initiating calcification have been described (Hsu, 1994). The first mechanism considers that the calcium and Pi ion product must reach the threshold of precipitation by means of Pi accumulation, which can be provided by the ALP activity. According to the other mechanism the calcium and Pi ion product can remain at physiological levels, however, some nucleating agents must induce the precipitation, such as the extracellular matrix vesicles (MVs) found in the growth plate cartilage (H. C. Anderson, 1989; Wuthier, et al., 1992). MVs are associated with some constituents which are considered to be favorable for calcium phosphate deposition, such as ALP (Matsuzawa & Anderson, 1971) and collagen type X (Wu, Genge, Lloyd, & Wuthier, 1991).

During endochondral ossification, mineralization in cartilage (epiphyseal growth plate) is described to be initiated in MVs, containing relatively high concentrations of calcium and Pi. Thus they create an optimal environment to induce the formation of apatite (Balcerzak, et al., 2003). ALP is highly enriched in MVs (Ali,

Sajdera, & Anderson, 1970) and is concentrated at their outer surfaces where it is anchored to the membrane lipid bilayer (Harrison, Shapiro, & Golub, 1995; Matsuzawa & Anderson, 1971), whereas the deposition of hydroxyapatite crystals is described to occur on the inner side of the MV-membrane (Wuthier, 1982). MVs are produced by budding from the cellular membrane of chondrocytes (Borg, Runyan, & Wuthier, 1978; Ornoy & Langer, 1978). Numerous studies have detected MVs to be present the calcifying growth plate cartilage (Bonucci, 1992). The cartilage EP of the IVD in humans, which acts as a growth plate, can be expected to calcify in a similar manner. However, in the AF and NP of the IVD, the presence of MVs has not been demonstrated.

5. Objectives of the Study

The main objectives of this study are to assess the calcification markers in IVDs of adult patients with degenerative disc disease and of adolescent patients suffering from adolescent idiopathic scoliosis, as well as to compare the calcification markers and type X collagen expression in concave and convex parts of the scoliotic IVDs. The specific aims are:

1) To visualize and quantify the calcification process in degenerative IVDs;
2) To visualize and quantify the calcification process in scoliotic IVDs and to compare the calcification markers in the concave and convex parts of the scoliotic IVDs;
3) To visualize type X collagen in degenerative and scoliotic IVDs and to compare the level of its expression in the concave and convex parts of the scoliotic IVDs.

6. Clinical Relevance

IVD mineralization and particularly the calcification of the EP is frequently viewed as a phenomenon which disturbs blood circulation and limit the effective diffusion of fluids and nutrients toward and outward the disc. As a biological structure the IVD has a low degree of vascularization and a low ability to heal and self-repair. This problem can be further exacerbated by mineralization. Calcification of IVD tissue and the impediment of disc metabolism caused by this process can be implicated in the pathogenesis of different IVD pathologies, such as IVD degeneration and scoliosis. For this reason elucidation of the mechanisms of IVD calcification is essential for understanding the different pathogenetic aspects of these pathologies and designing strategies for preventing their occurrence and progression. At the same time the success of some approaches for IVD repair is also highly dependent on the efficient circulation and nutrition of the disc. In this regard, revealing the mechanisms of IVD calcification and the possibilities for counteracting it can be crucial for developing of successful strategies for IVD repair.

II. METHODS

1. Source of Tissue

All the experiments in the present study involving human subjects were performed in accordance with the principles of Helsinki using IRB-approved protocols.

1.1. Degenerative Intervertebral Discs

Nineteen IVDs (including the EP, AF and NP) from fourteen different patients with DDD were analyzed (Table 2). The discs were extracted from patients who underwent operations for surgical management of the DDD and removal of the degenerative IVDs. The ages of the patients ranged from 23 to 55-years. The mean age of the patients was 39 years. The specimens were collected from the Montreal General Hospital and frozen in -80º C. The levels of the analyzed degenerative IVDs varied between L1–L2 and L5–S1. Prior to the dissection and processing of the discs, the post-operatively collected degenerative IVDs were graded morphologically using the Thompson grade (Thompson, et al., 1990). All discs were classified as Grade IV and Grade V which indicate advanced or severe disc degeneration.

1.2. Scoliotic Intervertebral Discs

Twenty one IVDs (including the EP, AF, and NP) of eight different patients that underwent operations for surgical management of adolescent idiopathic scoliosis (AIS) were analyzed (Table 3). The age of the patients varied from 11-year-old to 21-year-old. The mean age of the patients was 16 years. The Cobb angles of the different patients varied between 40 and 78 degrees. All the specimens were collected from the Montreal Children's Hospital and frozen in -80º C. The analyzed scoliotic IVD were between T11–T12 and L4–L5 disc levels.

Table 2: Intervertebral disc tissue for analysis of calcification in degenerative disc disease.

Degenerative IVDs		Control IVDs	
Age of patient	IVD level in the spine	Age of patient	IVD level in the spine
23	L3-L4	38	T12-L1
	L4-L5		L1-L2
26	L5-S1		L2-L3
30	L4-L5		L3-L4
	L5-S1		L4-L5
34	L4-L5		L5-S1
	L5-S1	48	T9-T10
34	L4-L5		T10-T11
39	L3-L4		T11-T12
40	L4-L5		T12-L1
	L5-S1		L1-L2
40	L4-L5		L2-L3
	L5-S1		L3-L4
42	L5-S1		L4-L5
45	L4-L5		L5-S1
45	L5-S1		
46	L4-L5		
50	L4-L5		
55	L5-S1		

Table 3: Intervertebral disc tissue for analysis of calcification in adolescent idiopathic scoliosis.

Scoliotic IVDs			Control IVDs	
Cobb angle of the patient	Age of patient	IVD level in the spine	Age of patient	IVD level in the spine
40º	13	L4-L5	15	L2-L3
52º	21	T11-T12		L3-L4
		T12-L1		L4-L5
		L1-L2		L5-S1
55º	16	L2-L3		
		L3-L4		
		L4-L5		
56º	11	T11-T12		
		T12-L1		
		L1-L2		
58º	17	T11-T12		
		T12-L1		
		L1-L2		
61º	13	T11-T12		
66º	14	T11-T12		
		T12-L1		
		L1-L2		
78º	19	T11-T12		
		T12-L1		
		L1-L2		
		L2-L3		

1.3. Control Intervertebral Discs

Control IVDs were obtained post mortem from autopsy specimens (from Transplant Quebec) and frozen in -80º C. As control for the degenerative discs, fifteen IVDs (EP, AF, and NP) were obtained at autopsy from two adult donors, 38-year old and 48-year old (Table 2), who died of acute death. In order to asses the age-related degenerative process in the control IVDs, the degree of degeneration of all control IVDs was assessed morphologically using the Thompson grade (Thompson, et al., 1990). The control IVDs were classified as Grade I and Grade II, which indicate no morphologically detectable degenerative process or low degree of degeneration respectively. The levels of the control discs were between T9–T10 and L5–S1. As control for the scoliotic discs, four IVDs (EP, AF, and NP) were obtained from a 15-year-old donor (Table 3) who also died of acute death. The discs were Grade I on the Thompson grade and were between levels L2–L3 and L5–S1.

2. Processing and Analysis of the Intervertebral Discs

2.1. Dissection of the Intervertebral Discs

Each IVD was dissected in order to obtain pieces of tissue enriched for EP, AF, and NP. The control IVDs and degenerative IVDs were dissected into EP, AF, and NP (Fig. 9). Each type of tissue was used separately for further analysis. For scoliotic IVDs, the first step of the dissection procedure was the separation of the concave and convex parts of each disc. Subsequently, these two parts were dissected into EP, AF, and NP (Fig. 10), in order to obtain tissues for comparative analysis of the concave and convex aspects of the scoliotic discs. Thus, six different types of tissue were obtained after the dissection of scoliotic IVDs, namely EP-concave, EP-convex, AF-concave, AF-convex, NP-concave, NP-convex.

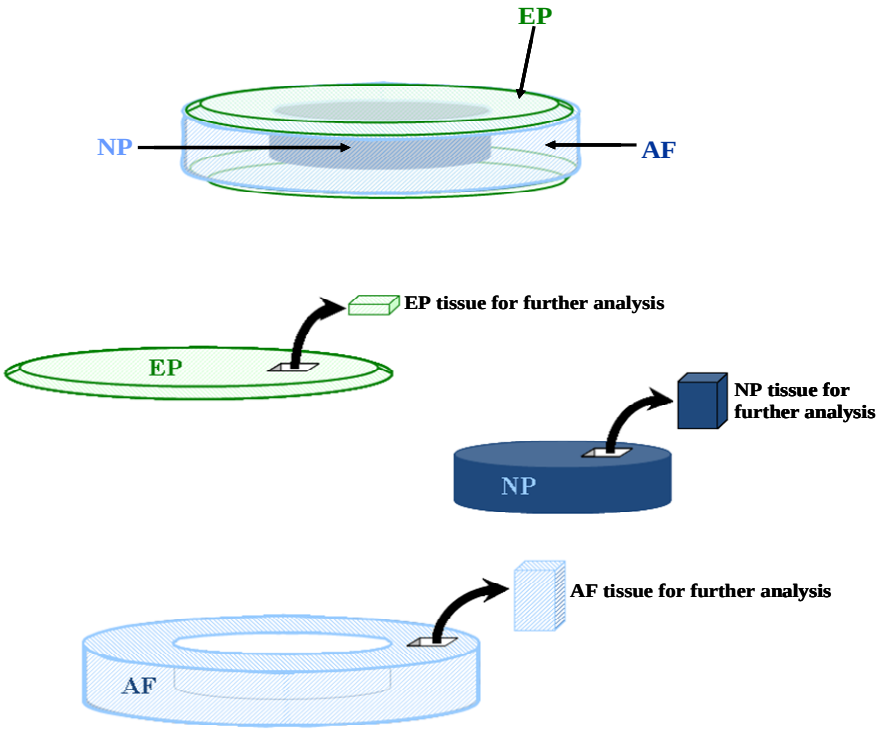

Figure 9: **Schematic representation of the dissection procedure for control and degenerative intervertebral discs**. EP: cartilage endplate; AF: annulus fibrosus; NP: nucleus pulposus.

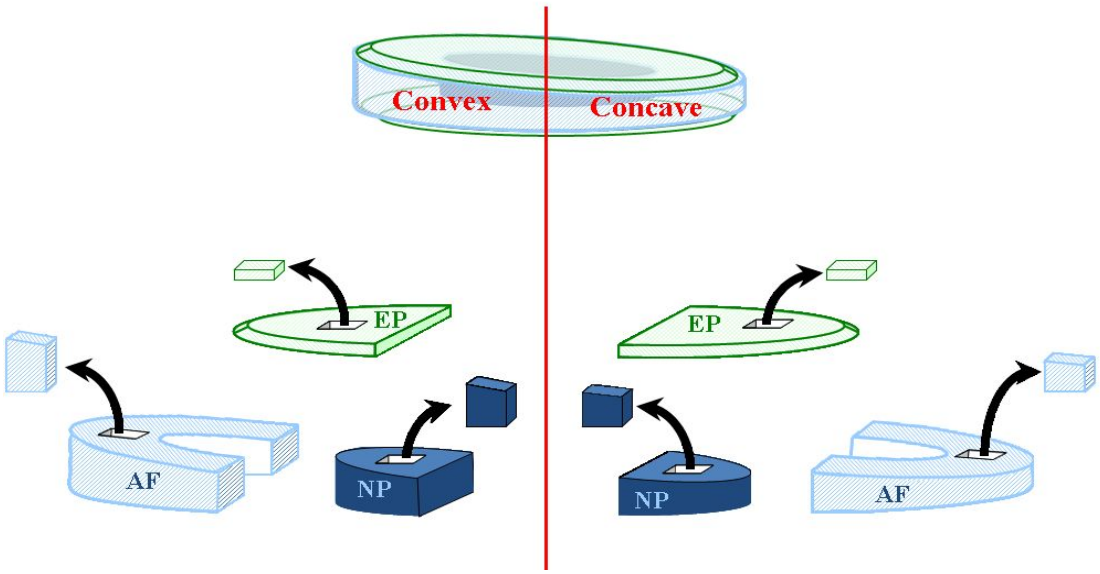

Figure 10: **Schematic representation of the dissection procedure for scoliotic intervertebral discs**. After the disc was initially dissected into its concave and convex parts. The EP, AF, and NP of each part were then separated and pieces are taken for further analysis. EP: cartilage endplate; AF: annulus fibrosus; NP: nucleus pulposus.

2.2. Processing of the Intervertebral Discs

The IVD tissues obtained after the dissection were processed in different manners depending on the different groups of experiments to be performed (Figure 11). Each type of tissue (EP, AF and NP) derived from the dissected IVDs was divided into three pieces. One piece was placed in Tris-$MgCl_2$ buffer for the purpose of analyzing it biochemically for alkaline phosphatase (ALP) activity, calcium, and inorganic phosphate (Pi) concentrations. The Tris-$MgCl_2$ buffer was composed of 10 mM Tris and 0.5 mM Magnesium Chloride in distilled water, with pH=8.6 which was the pH recommended by the manufacturer of the reagents used for the analysis of ALP activity (BioAssay Systems, Hayward, CA). Another piece was placed in Trizol in order to undergo Western blot analysis for type X collagen. The third piece of tissue was placed in 10% v/v neutral buffered formalin and processed for further histological and immunohistochemical analyses.

2.3. Biochemical Analysis of the Intervertebral Discs

IVD tissues placed in the Tris-$MgCl_2$ buffer were homogenized mechanically using a Polytron homogenizer, model PT–10–35, Kinematica, Germany (Fig. 11). The initial mechanical homogenization was necessary in order to extract the alkaline phosphatase from the tissue in its active state and analyze its enzymatic activity. Subsequently, the liquid phase (supernatant) of the homogenates was analyzed for ALP activity, calcium and Pi concentrations, using commercially available analytical kits from BioAssay Systems, Hayward, CA.

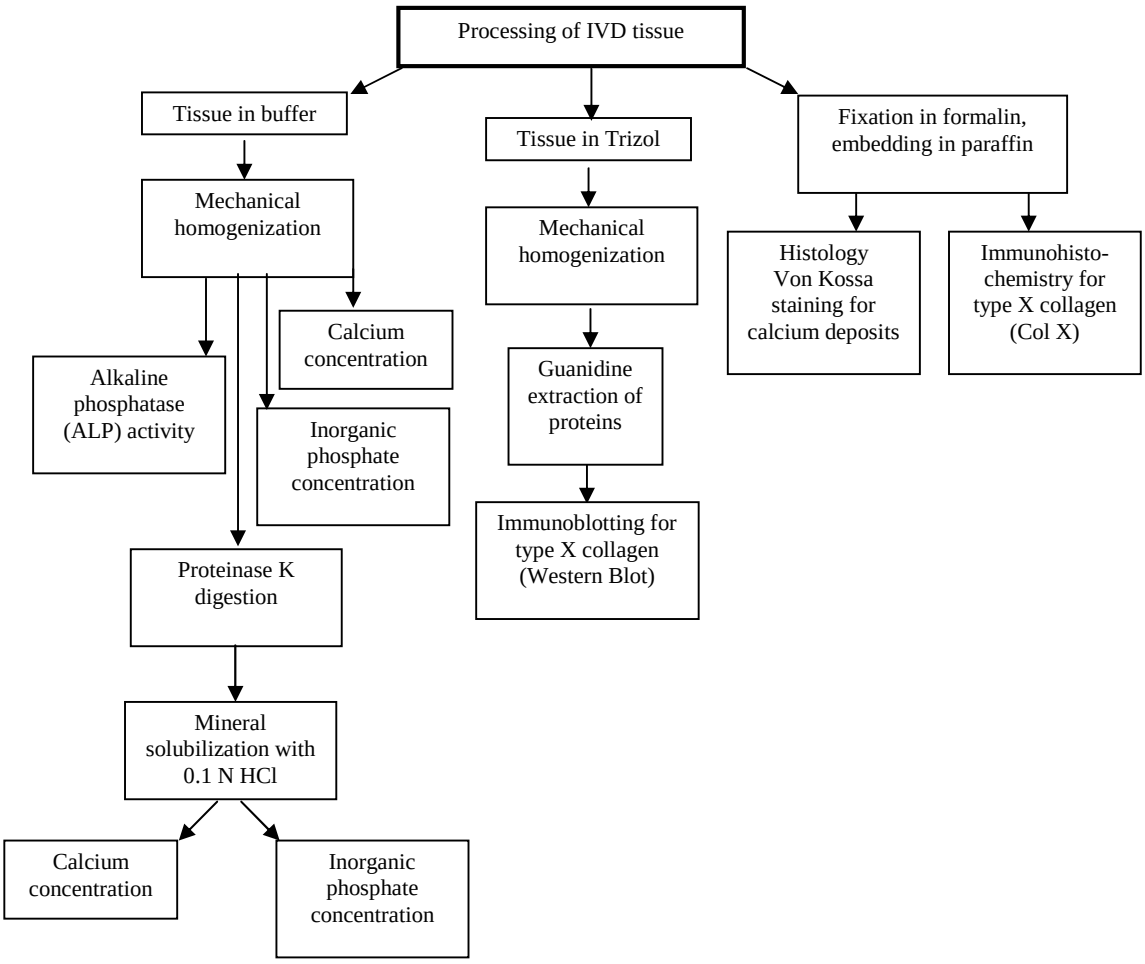

Figure 11: **Processing of intervertebral disc tissues**. Figure represents a schematic diagram of the steps undertaken in order to perform different analyses.

Results were normalized in function of the wet weight of the tissues and the concentration of proteins. Since both normalization methods yielded similar results, only normalization in function of the wet weight will be showed in the results section. The normalization against the wet weight of the samples is also well appropriate for the present study as it is a surrogate measure of the tissue volume. Thus, it can also be considered as a surrogate measure for the cell number in the sample (Ford & Downes, 2002; Roughley, 2004). The use of the dry weight of the samples for normalization was not applicable in this study since drying procedure affects ALP activity.

After the mechanical homogeneization, the remaining tissue was digested using Protienase K (1 mg/ml in 7.5 mM Tris) for 48 h at 56.5ºC. The insoluble minerals were then solubilized using 0.1 N hydrochloric acid (HCl) as previously described (Wu, et al., 1995). Calcium and Pi concentrations were analyzed again. The results for calcium and Pi concentrations are the sum of the concentrations after the mechanical extraction and after the complete solubilization of the tissues.

2.3.1. Biochemical Analysis of Alkaline Phosphatase Activity

ALP activity was analyzed using the pNPP Phosphatase Assay Kit from BioAssay Systems, Hayward, CA. The assay is based on the reaction between alkaline phosphatase and the para-nitrophenil phosphate from the kit. The reaction yields para-nitrophenol, which is a yellow soluble product, measurable at 405 nm on a spectrophotometer. The assay was performed following the protocol provided by the manufacturer of the analytical kit, in 96-well microtest plates (round bottom) purchased from Sarstedt Inc., Newton, North Carolina. The incubation time allowed for the reaction to develop was 30 minutes. Samples were analyzed in triplicates. The following formula was applied for the calculation of the enzyme activity of the alkaline phosphatase:

$$\text{Enzyme Activity (nmoles/min/µg)} = \frac{\text{Volume in the well (µL) x (OD of sample – OD of blank)}}{\varepsilon \text{ x incubation time (min) x Wet weight of the sample (g)}}$$

where:

Volume in the well = 150 µL

OD = optical density measured at 405 nm

$\varepsilon = 17.8\ M^{-1}.cm^{-1}$

2.3.2. Biochemical Analysis of Calcium Concentration

The calcium concentration in IVD tissues was analyzed using the QuantiChromTM Calcium Assay Kit (DICA – 500) of BioAssay Systems, Hayward, CA. The assay is based on the reaction between the phenolsulphonephtalein dye in the kit and the calcium in the sample, which yields a blue colored complex, measurable at 620 nm on a spectrophotometer. The assay was performed following the protocol provided by the manufacturer of the analytical kit, in 96-well microtest plates (round bottom) from Sarstedt Inc (Montreal, QC). Samples were analyzed in duplicates. Dilutions of the samples were applied when the optical density of the sample solution was higher than the optical density of the standard with the highest calcium concentration, in order to measure the calcium concentration in the linear range of the assay. The following formula was applied for the calculation of the calcium concentration:

$$\text{Calcium concentration (mg/g tissue)} = \frac{(OD_{Sample} - OD_{Blank}) \times \text{Dilution (if applied)}}{\text{Slope} \times \text{Wet weight of the sample (g)} \times 100}$$

where:

OD = optical density measured at 620 nm

Slope = slope of the standard curve (standards provided by the manufacturer)

2.3.3. Biochemical Analysis of Inorganic Phosphate Concentration

The Pi concentration in IVD tissues was analyzed using the QuantiChromTM Phosphate Assay Kit (DIPI–500) of BioAssay Systems (Hayward, CA). The reagents from the analytical kit form a green colored complex Pi in the sample, measurable at 620 nm on a spectrophotometer. The assay was performed following the protocol

provided by the manufacturer of the analytical kit, in 96-well microtest plates (round bottom) from Sarstedt Inc. When the optical density of the sample solution was higher than the optical density of the standard, dilutions of the samples were applied in order to adjust the Pi concentration in the linear range of the assay. The samples were analyzed in duplicates. The following formula was applied for the calculation of the Pi concentration:

$$\text{Pi concentration (mg/g tissue)} = 0.28 \times \frac{(OD_{Sample} - OD_{Blank}) \times \text{Dilution (if applied)}}{(OD_{Standard} - OD_{Blank}) \times \text{Wet weight (g)} \times 100}$$

where:

OD = optical density measured at 620 nm

$OD_{Standard}$ = optical density of the standard provided by the manufacturer

After the analysis of the liquid phase of the homogenized IVD tissues, the non-liquid phase was digested using Protienase K (Fig. 11). The digestion was performed for 48 h in 56.5º C temperature using a 1 mg/ml solution of Proteinase K in 7.5 mM Tris buffer.

2.4. Histological and Immunohistochemical Analyses of the Intervertebral Discs

Tissues were fixed in 10% v/v neutral buffered formalin for 18 h, embedded in paraffin, and sectioned in 4-µm thick sections. The sections were then deparaffinized (cleared) 3 times for 3 min in toluene and hydrated by a serial of 2-min incubations (2 times each) in 100%, 95%, 80%, and 70% ethanol. Finally, the sections were rinsed for 2 min in distilled water.

2.4.1. Von Kossa Staining for Calcium Deposits

The visualization of the mineral deposits in analyzed IVD tissues was achieved using Von Kossa staining. After the gradual deparaffinization, the sections were placed in 10% silver nitrate for 15 min in the dark. They were then exposed to strong light for 15 min for the visualization of the black Von Kossa stain. Subsequently, the sections were rinsed in distiller water and fixed in 3% sodium thiosulfate for 2 min and then rinsed again in distilled water and counterstained with Toluidine Blue. The microscopic examination of the IVD tissue was performed using a light (optical) microscope set at 200 times magnification. Calcium deposits appear as opaque black areas on the stained sections.

2.4.2. Immunohistochemical Analysis for Type X Collagen

After deparaffinization, the sections were treated for 60 min at 37ºC with 0.25 units/ml Chondroitinase in 0.1 M Tris-Acetate buffer (pH 7.3) in order to degrade the proteoglycan and to allow antibody penetration. The sections were then quenched in 0.3% H_2O_2 in methanol for 30 min at room temperature, washed in PBS for 15 min, and blocked with the blocking solution of the Vectastain Elite ABC analytical kit (Vector Laboratories, Burlingame, CA) for 20 min at room temperature. The blocking solution contained serum of the secondary antibody host (goat normal serum) and was prepared according to the instructions provided by the manufacturer. Sections were then incubated for 30 min at room temperature with 10 µg/ml of rabbit anti-type X collagen antibody (generously gift from Dr. E. Lee, Shriners Hospital for Children, Montreal, QC), washed for 10 min in PBS, and incubated for 30 min at room temperature with a biotinylated goat anti-rabbit IgG antibody coupled with streptavidin-horseradish peroxidase according to the manufacturer's instructions (Vectastain Elite ABC analytical kit, Vector Laboratories, Burlingame, CA). Sections

were then washed in PBS for 10 min, incubated for 30 min at room temperature with the Vectastain ABC reagent mix, washed in PBS for 10 min, and incubated with the DAB (3,3'-diaminobenzidine) substrate reagent for 5 min. Horseradish peroxidase, linked to the secondary antibody, catalyzes the oxidation of the DAB by hydrogen peroxide from the DAB substrate reagent. This reaction yielded the brown staining of type X collagen on the slide section. After the DAB reactions, sections were washed in water for 5 min, dried on a hot plate, counterstained with hematoxylin using the Vector Hematoxylin Nuclear Counterstain (Gill's formula), washed thoroughly in water, dried on a hot plate, and permanently mounted in non-aqueous mounting media. The microscopic examination of the immunostained IVD tissue was performed using a light (optical) microscope set at 200 times magnification.

2.5. Protein Extraction and Immunoblotting

2.5.1. Protein Extraction

Concave and convex parts of the EP, AF, and NP of the scoliotic IVDs, as well as a control sample from bovine fetal growth plate, were placed in Trizol. The bovine fetal growth plate presumably contains type X collagen and was used as positive control. The tissues in Trizol were homogenized mechanically using a Polytron homogenizer (model PT–10–35, Kinematica, Germany). The liquid phase of the homogenates was used as a sample for guanidine extraction of proteins. Chloroform was added to each sample in a volume proportion 1:5 (1 part chloroform **:** 5 parts sample). The next step was to vortex the mix and let it sit at room temperature for 2 – 3 min. Then the samples were centrifuged at 12000 x *g* for 15 min at 4º C temperature. This procedure induced a phase separation in the samples. The lowest organic phase which contained the proteins was further used in the Procedure of Guanidine extraction of proteins.

Proteins were then precipitated by centrifugation at 12,000 x g for 10 min at 4ºC in isopropyl alcohol, and washed 3 times for 20 min at room temperature in a solution of 0.3 M guanidine hydrochloride in 95% ethanol and once in 100% ethanol, followed by centrifugation at 7500 x g for 5 min at 4ºC. The protein pellets were dried and re-dissolve 1% sodium dodecyl sulfate (SDS) in water. The non-dissolved proteins were separated from the dissolved proteins by centrifugation at 10,000 x g for 10 min at 4ºC temperature.

Protein concentration of each sample was measured using the commercially available reagents of Bio-Rad DC Protein Assay. The analysis was performed according to the instructions and the protocol provided by the manufacturer using bovine serum albumin (BSA, Fraction V: EM Science, Gibbstown, NJ) (0.25, 0.5, 1.0, and 1.5 mg/ml) as standards. The reaction between the assay reagents and the proteins in the sample yields a blue colored complex, measurable at 750 nm on spectrophotometer. The intensity of the blue color is proportional to the concentration of proteins in the solution. In order to measure the protein concentration of the sample solution in the linear range of the assay, samples were diluted when their optical density was higher than the optical density of the standard with the highest protein concentration of 1.5 mg/ml. The following formula was applied for the calculation of the protein concentration:

$$\text{Protein concentration (mg/ml)} = \frac{(OD_{Sample} - OD_{Blank}) \text{ x Dilution (if applied)}}{\text{Slope}}$$

where:

OD = optical density measured at 620 nm

Slope = the slope of the standard curve, constructed by measuring of the optical density of the protein standards

2.5.2. Western Blot Analysis

The expression of type X collagen in scoliotic IVD tissues was measured by Western blot. Fifteen (15 μg) of denaturized total protein, as measured by the Bio-Rad DC Protein Assay were applied on acrylamide gels and separated by sodium dodecyl sulfate-polyacrylamide gel electrophoresis (SDS-PAGE). Due to the very low cellularity of the IVD tissue (Bibby, et al., 2002; Ford & Downes, 2002; Roberts, et al., 2006; Roughley, 2004), which renders difficult the use of housekeeping genes such as actin, tubulin, or GAPDH as of loading controls, total protein content was used for loading control.

Protein samples from the concave and convex parts of the EP, AF, and NP of scoliotic discs and proteins extracted from bovine fetal growth plate (used as a positive control for type X collagen) were mixed 1:1 with loading buffer (Tris-Glycine-SDS 2X buffer, Invitrogen), boiled for 3 min, chilled on ice and afterwards loaded on 4-20% acrylamide gels (Invitrogen). Gels were run for 2h at about 125 volts in electrophoresis buffer (25 mM Tris-Base, 200 mM Glycine, and 0.1 % SDS). Proteins were then transferred to 0.45 μm nitrocellulose membrane (Bio-Rad Canada) for 2h at 25 volts in transfer buffer (12.5 mM Tirs-Base, 100 mM Glycine, and 20% Methanol).

Nitrocellulose membranes were incubated overnight at 4º C in 1:1 Chemiblocker**:**TBS-Tween (1:1) to reduce non-specific binding of the antibldy. Chemiblocker was purchased from Millipore (Temecula, CA), while TBS-Tween contained 5% Tween-20 in TBS buffer (containing 6.05 g Tris-Base and 8.76 g Sodium Chloride per liter distilled water, pH=7.5). Membranes were then incubated for 1h at room temperature with a monoclonal anti-type X collagen antibody (IgM isotype, Sigma-Aldrich, Oakville, ON) as a primary antibody, diluted 1:1000 in

Chemiblocker**:**TBS-Tween (1:1), and subsequently washed 4 times for 15 minutes in TBS-Tween. As a next step, the nitrocellulose membrane were incubated for 1h at room temperature with horseradish peroxidase-conjugated goat anti-mouse IgM antibody (Invitrogen) as a secondary antibody, diluted 1:3000 in Chemiblocker**:**TBS-Tween (1:1), and washed again 4 times for 15 min in TBS-Tween.

Proteins were detected using the Western Lightning Chemiluminescence Reagent Plus kit (Perkin Elmer Laboratories, Vaudreuil-Dorion, QC). The horseradish peroxidase, linked to the secondary antibody, when reacting with the oxidizing reagent from the kit, releases oxygen, and thus activates the luminol, which is a chemiluminescent reporter that exhibits luminescence when activated with an oxidant. The chemiluminescent signal indicates the presence of type X collagen and the intensity of the signal is proportional to the amount of the type X collagen in the sample. The chemiluminescent signal was visualized using a Model 3000 Versa Doc Imaging System (Bio-Rad Laboratories) equipped with a cooled CCD 12 bit camera. Type X collagen was detected at approximately 59 kilodaltons (kDa) as previously described (Schmid & Linsenmayer, 1983). The image was further analyzed semi-quantitatively. The Versa Doc software was used to evaluate the relative amount of the chemiluminescent signal, indicating the presence of type X collagen. The intensity of the chemiluminescent signal was compared between the concave and convex aspect of the EP, AF and NP of each scoliotic IVD.

3. Statistical Analysis

Statistical analyses were performed using Stat View (SAS Institute Inc., Cary, NC). The statistical significance of the differences between degenerative and control IVDs, as well as between scoliotic and control IVDs, was assessed using the Non-parametric Mann-Whitney-Wilcoxon Rank Sum Test, which is considered to be an excellent tool for comparing of two independent groups, when the observations are not normally distributed or the variances are not equal (Beth Dawson & Trapp, 2004). The statistical significance of the differences between the concave and convex parts of each scoliotic IVD was assessed using the Non-parametric Wilcoxon Signed Rank Test, which is the most appropriate tool for paired analysis when the observations are not normally distributed (Beth Dawson & Trapp, 2004). A value of $p<0.05$ was considered as significant.

III. RESULTS

1. Mineral Deposition

The histological analysis using the Von Kossa staining was performed in order to detect the presence of mineral deposits in the analyzed tissue. The histological analysis of the degenerative discs was performed in comparison with the control discs (Fig. 12). The analysis of the scoliotic IVDs was also performed in comparison with the control IVDs (Fig. 13). The mineral deposits in the IVD tissue in both degenerative and scoliotic IVDs, visualized as black spots, were the evidence that a process of mineralization occurs in the damaged IVD tissue. Regardless whether the underlying reason of the tissue damage was degenerative disc disease or adolescent idiopathic scoliosis, similar mineral deposition in the IVDs was detectable. Furthermore, the mineral deposits were present in all morphological types of IVD tissue, EP, AF and NP, of both degenerative and scoliotic IVDs. The Von Kossa staining for mineral deposits was positive in both concave and convex parts of the scoliotic IVDs. In contrast, in the control non-diseased IVD tissue mineral deposits were not detected, which is shown by the absence of Von Kossa staining (black spots) in the EP, AF and NP of the control IVDs. The Von Kossa staining for mineral deposits also demonstrated the topo-morphological characteristics of the mineral deposits in IVD tissue. In tissue where the process of mineral deposition was not very advanced, the mineral deposits were be observed around the cellular constituents of the tissue. This was consistent with the fact that alkaline phosphatase, which is considered to be the enzyme that initiates the mineralization process, is produced by the cells of the tissue. However, in tissue where the mineral deposition was more abundant, the black spots of the Von Kossa staining were very intense and confluent.

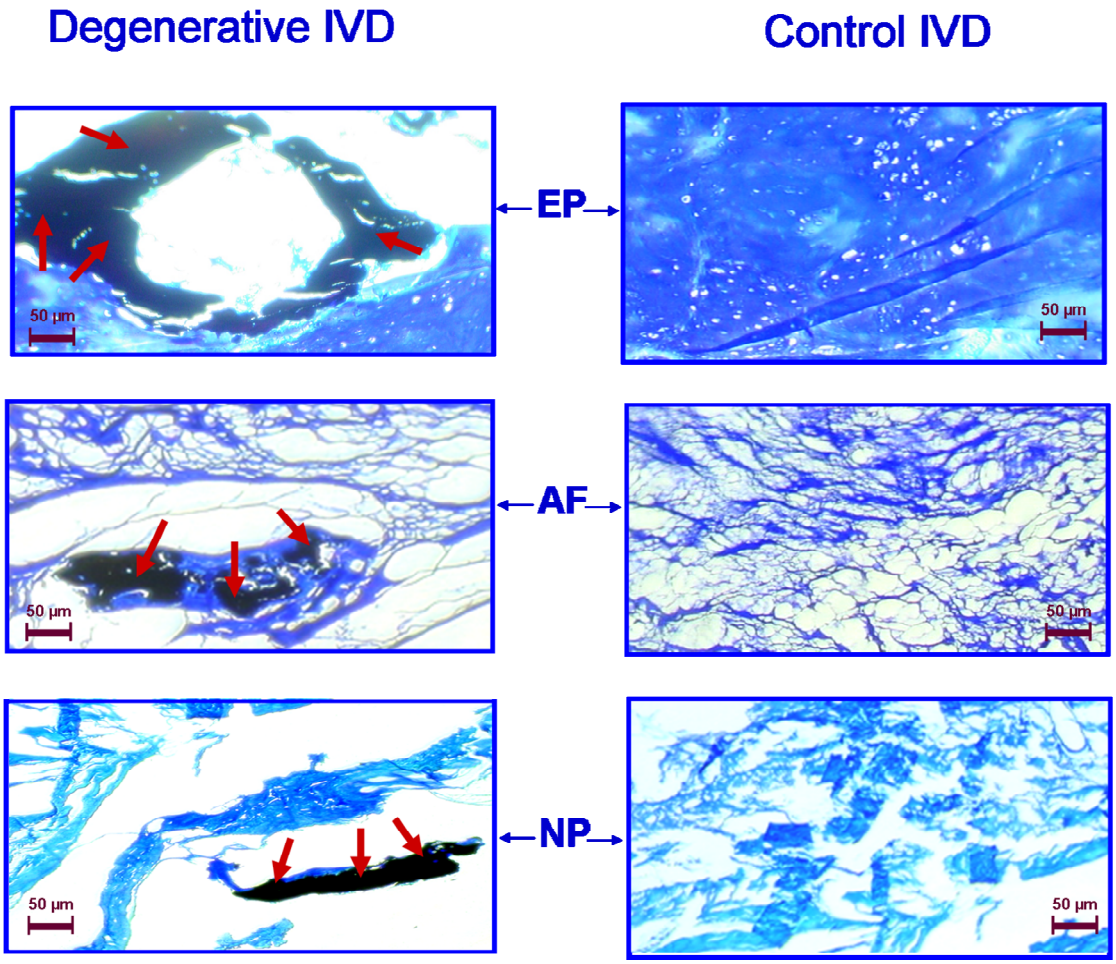

Figure 12: **Histological analysis for mineral deposits in degenerative intervertebral disc.** Figure represents typical images of Von Kossa staining for visualization of mineral depositions in degenerative compared to control intervertebral disc tissues. The black stain represents the mineral deposits (indicated by red arrows), whereas the toluidine blue used as counterstaining stains the proteoglycans. The microscopic magnification is 200 times. IVD: intervertebral disc; EP: cartilage endplate; AF: annulus fibrosus; NP: nucleus pulposus.

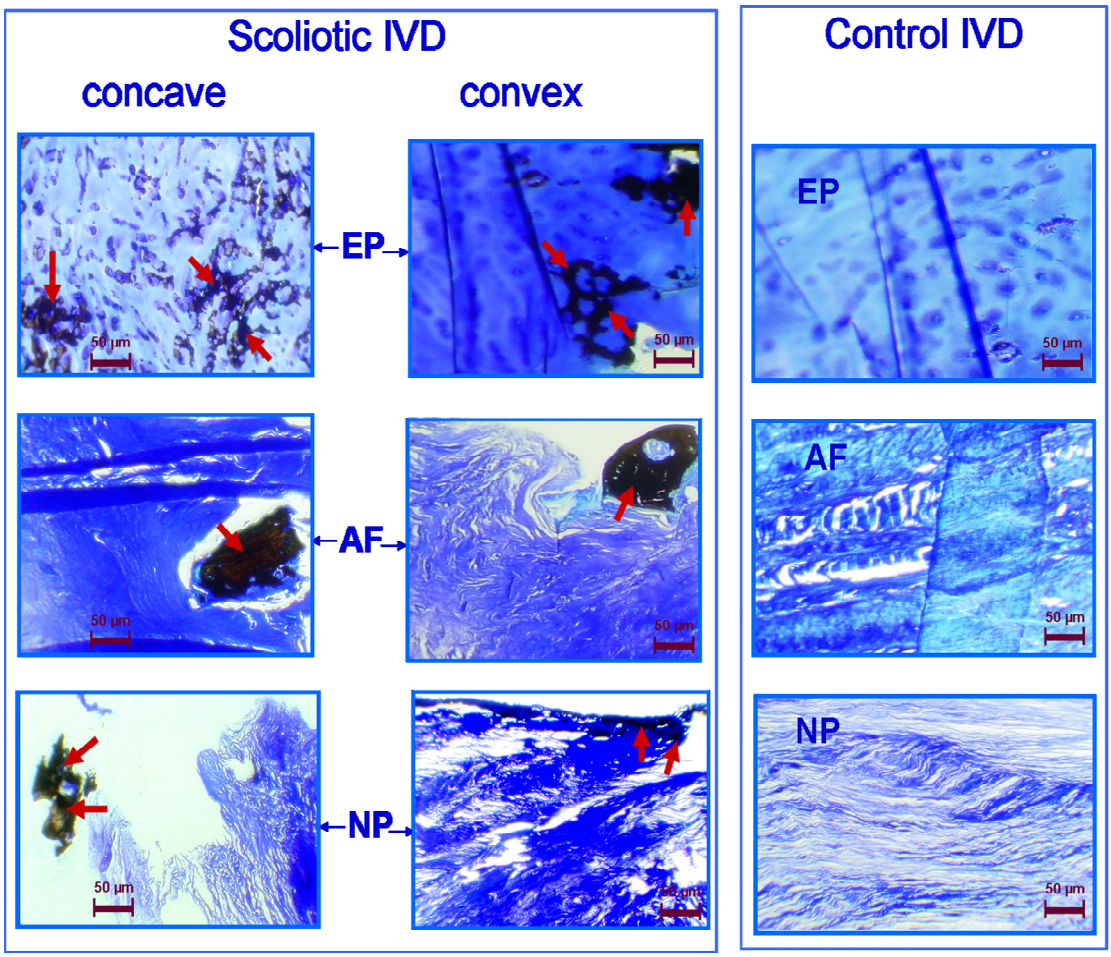

Figure 13: Histological analysis for mineral deposits in scoliotic intervertebral disc. Figure represents typical images of Von Kossa staining for visualization of mineral depositions in scoliotic compared to control intervertebral disc tissues. The concave and convex parts of scoliotic IVDs were processed and analyzed separately. The black stain represents the mineral deposits (indicated by red arrows), whereas the toluidine blue used as counterstaining stains the proteoglycans in the tissue. The microscopic magnification is 200 times. IVD: intervertebral disc; EP: cartilage endplate; AF: annulus fibrosus; NP: nucleus pulposus.

2. Assessment of the Calcification Markers

Whereas the visualization of the mineral deposits by Von Kossa staining demonstrated the final product of past mineralization process in the IVD tissue and thus proved the occurrence of this process in the past, it did not define the future mineralization potential of the analyzed tissue. For the purpose of assessing the calcification potential of the IVD tissue, a biochemical analysis of three calcification markers was performed, namely the analysis of the alkaline phosphatase (ALP) activity, calcium and inorganic phosphate (Pi) concentrations.

2.1. Calcification Markers in Degenerative Intervertebral Discs

The calcification markers in the EP, AF and NP of the degenerative discs were analyzed in comparison with the calcification markers in the EP, AF and NP of the control IVDs. For the purpose of detecting a possible impact of the age on the calcification markers, the measured values of the ALP activity and calcium and Pi concentrations in degenerative IVDs are represented in an ascending order according to the increasing age of the patients. The statistical analysis of the three markers of calcification process in all three types of IVD tissue (EP, AF, and NP) demonstrated a non-parametric type of distribution of the values of these markers in different IVDs and different patients.

2.1.1. Calcification Markers in the Endplate of Degenerative Discs

The analyses of the calcification markers in the EP of the degenerative discs compared to control IVDs are represented on Figure 14. The statistical analysis of results is represented on Table 4. The values of the mean and the median for ALP activity and calcium and Pi concentrations in the EP were considerably higher in

degenerative than in the control IVDs (Table 4). The range of the values of all three measured was much wider in the EP of degenerative than in the EP of control IVDs. Whereas the minimum value of the ALP activity in the EP of degenerative IVDs was comparable to the minimum value of ALP activity in the EP of control IVDs, the maximum value of this calcification marker was much higher in the EP of degenerative than in the EP of control IVDs. However, the minimum values of the calcium and Pi concentrations in the EP of degenerative IVDs were considerably higher than the minimum values of the calcium and Pi concentrations in the EP of control IVDs. The same correlation was present regarding the maximum values. The statistical analysis with the Non-parametric Mann-Whitney-Wilcoxon Rank Sum Test demonstrated that the detected higher levels of the ALP activity and calcium and Pi concentrations in the EP of degenerative IVDs were highly statistically significant, with p-values<0.0001 (Table 4).

The levels of the ALP activity in the EP (Fig. 14) of the youngest patient who was 23-year-old were comparable to the same levels in the EP of patients who were 30, 34 and 40-year-old (approximately 0.14 nmol/min/g tissue). The level of the ALP activity in the EP of the next patient who was 26-year-old was comparable to the one of the oldest patient analyzed who was 55-year-old. The lowest level of ALP activity was detected in the EP of degenerative IVD of a 34-year-old patient (0.027 nmol/min/g tissue). This level was comparable with the levels of the ALP activity in the control IVDs. It is also interesting to note that in the 38-year-old control donor the IVD of the disc level L5–S1, which is the lowest IVD level in the spine, demonstrated an ALP activity in the EP (0.161 nmol/min/g tissue) much higher than the other 15 control IVDs. During the IVD dissection this disc was graded at grade 2 on the Thompson grade for degeneration, which indicated an initial stage of disc

degeneration. This could probably be related to the position of this disc on the lowest level in the spine, which is associated with an increased mechanical loading.

Regarding the levels of the calcium concentration in the EP (Fig. 14), the youngest 23-year-old patient had approximately 0.3 milligrams calcium per gram tissue which was comparable to the same level of the calcium concentration in the EP of 30, 34, 40 and 45-year-old patients. In the oldest patient (55-year old), the level of calcium concentration in the EP (approximately 0.5 mg/g tissue) was comparable to the levels in 45 and 50-year old patients. The lowest level of calcium concentration (0.088 mg/g tissue) was detected in the EP of the 39-year old patient. The control IVDs demonstrated consistently and significantly lower values of the calcium concentration compared to the degenerative IVDs.

Pi concentration in the EP (Fig. 14) of the youngest 23-year-old patient was similar to the Pi concentration in the EP of 34, 40 and 42-years old patients. The highest values of Pi concentration (approximately 0.74 mg/g tissue) were detected in the EP of 26 and 40-year-old patients. The oldest patient (55-year-old) demonstrated a Pi concentration in the EP of 0.03 mg/g tissue, which was comparable to the value of one of the discs of the 30-year-old patient (0.026 mg/g tissue). Even the lowest value of Pi concentration in the EP in degenerative IVDs (0.006 mg/g tissue) was higher than the mean and the median of Pi concentrations in the EP in control IVDs (0.004 mg/g tissue and 0.002 mg/g tissue respectively). In general, Pi concentration in the EP of degenerative IVDs was significantly higher than in the control IVDs.

ALP activity and calcium and Pi concentrations in the EP of degenerative IVDs did not show a consistent trend of increase or decrease with the age of the patient.

A few of the patients with degenerative disc disease had undergone a surgical removal of more than one IVD, such as the 23-year-old, the 30-year old, one of the 34-year-olds and both 40-year old patients. This provided the possibility for analysis of the influence of IVD level in the spine on the calcification markers.

The ALP activity and the Pi concentration in the EP (Fig. 14) of the 30-year-old patient were higher in the higher L4–L5 disc level than in the lower L5–S1 level, whereas the values of the calcium concentration in the EP of the same discs were higher in the lower than in the higher IVD level. The same type of variation was observed between the two discs of the 34-year-old patient, where the ALP activity and the Pi concentration in the EP were higher in the higher L4–L5 disc level, whereas the calcium concentration was higher in the EP of the lower L5–S1 IVD level. The ALP activity and the Pi concentration in the EP of one of the 40-year-old patients did not show much variation. However, the calcium concentration was higher in the EP of the lower L5–S1 IVD level. In the EP of the other 40-year-old patient, the ALP activity and the calcium concentration were higher in the higher L4–L5 IVD level, whereas the Pi concentration was higher in the lower L5–S1 disc level. In summary, ALP activity and calcium and Pi concentrations in the EP degenerative discs did not demonstrate a trend related to the level of the IVD in the spine.

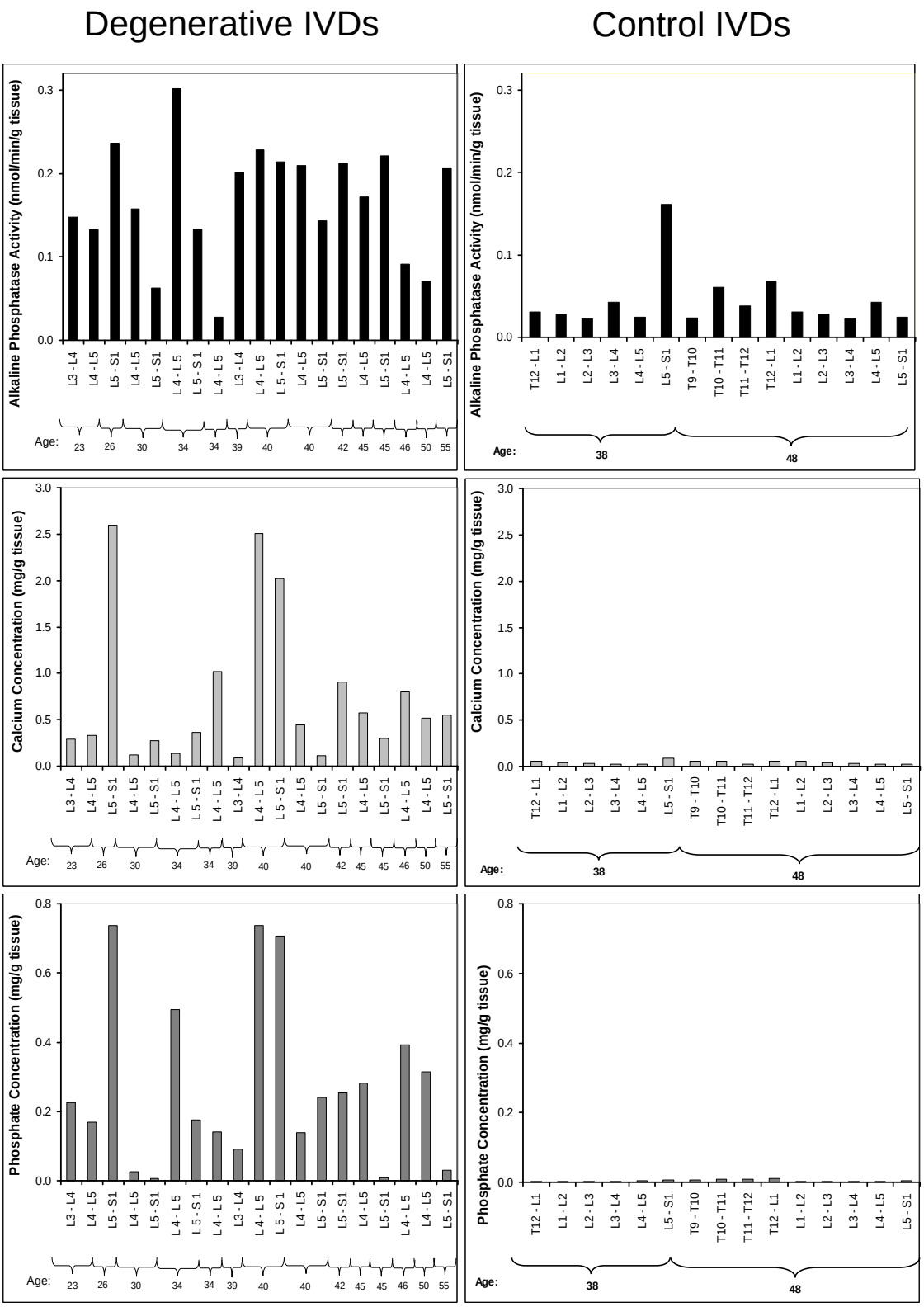

Figure 14: **Biochemical analysis of the calcification markers in the endplate of degenerative intervertebral disc**. Alkaline phosphatase activity and calcium and inorganic phosphate concentrations were measured as described in Methods.

Table 4. **Statistical analysis of alkaline phosphatase activity and calcium and inorganic phosphate concentrations in the endplate of degenerative discs.**

Endplate - Degenerative versus Control IVDs

Alkaline Phosphatase Activity

Descriptive Statistics

	Degenerative IVDs	Control IVDs
Mean	0.167	0.043
Standard Deviation	0.070	0.035
Minimum	0.027	0.023
Maximum	0.302	0.161
Range	0.274	0.139
Median	**0.173**	**0.031**

p - value calculated using the Non-parametric Mann-Whitney Wilcoxon Rank Sum Test

p<0.0001

Calcium Concentration

Descriptive Statistics

	Degenerative IVDs	Control IVDs
Mean	0.735	0.042
Standard Deviation	0.782	0.019
Minimum	0.088	0.022
Maximum	2.593	0.087
Range	2.506	0.065
Median	**0.449**	**0.037**

p - value calculated using the Non-parametric Mann-Whitney Wilcoxon Rank Sum Test

p<0.0001

Inorganic Phosphate Concentration

Descriptive Statistics

	Degenerative IVDs	Control IVDs
Mean	0.272	0.004
Standard Deviation	0.240	0.003
Minimum	0.006	0.001
Maximum	0.737	0.011
Range	0.731	0.009
Median	**0.225**	**0.002**

p - value calculated using the Non-parametric Mann-Whitney Wilcoxon Rank Sum Test

p<0.0001

2.1.2. Calcification Markers in the Annulus Fibrosus of Degenerative Discs

The statistical analysis of the levels of calcification markers in the AF demonstrated that the values of the mean and the median for the ALP activity, calcium, and Pi concentration were considerably higher in degenerative than in the control IVDs (Table 5). The range of the values of all three measured calcification markers was much wider in the AF of degenerative than in the AF of control IVDs. Similar to the minimum value of the ALP activity in the EP, the minimum value of the ALP activity in the AF of degenerative IVDs was comparable to the minimum value of the ALP activity in the AF of control IVDs. However, the maximum value of this calcification marker was much higher in the AF of degenerative than in the AF of control IVDs. The minimum value of the calcium concentration was slightly lower in the AF of degenerative IVDs (0.009 mg/g tissue) than in the AF of control IVDs (0.012 mg/g tissue). However, the maximum value was much higher in the AF of degenerative than in the AF of control IVDs (1.665 mg/g tissue versus 0.072 mg/g tissue respectively). Regarding Pi concentration, both the minimum and the maximum values were considerably higher in the AF of degenerative IVDs than in the AF of control IVDs. The Non-parametric Mann-Whitney-Wilcoxon Rank Sum Test showed a high statistical significance of the observed elevated levels of the calcification markers in the AF of degenerative IVDs compared to control IVDs. Regarding calcium concentration, the p-value was 0.003. Regarding ALP activity and Pi concentration, the p-values were found to be even lower ($p<0.0001$) (Table 5).

The levels of the ALP activity in the AF (Fig. 15) of the youngest patient (23-year-old) were low (0.035 nmol/min/g tissue and 0.040 nmol/min/g tissue) but comparable to the same levels in the AF of patients who were 42, 45 and 50-year-old (0.066, 0.063, and 0.062 nmol/min/g tissue, respectively) and even to the level of the

oldest 55-year-old patient (0.067 nmol/min/g tissue). The highest ALP activity was found in the AF of the L5–S1 IVD of one of the 40-year-old patients (0.48 nmol/min/g tissue). Although the highest value of the ALP activity in the AF of control IVDs (0.047 nmol/min/g tissue) exceeded the lowest value of the ALP activity in the AF of degenerative IVDs (0.017 nmol/min/g tissue), in general, the AF of degenerative discs demonstrated considerably higher ALP activity compared to control discs.

The lowest calcium concentration (Fig. 15) was found in the AF of the 42-year-old patient (0.009 mg/g tissue). The calcium concentration in the AF of the youngest patient (23-year-old) was very low compared to the other degenerative discs (approximately 0.02 mg/g tissue). The highest calcium concentration was found in the AF of one of the 45-year-old patients (1.665 mg/g tissue, disc level L5–S1), followed by the AF of the 26-year-old patient (1.292 mg/g tissue, disc level L5–S1). All other degenerative IVDs demonstrated moderate levels of the calcium concentration in the AF, usually between 0.1 and 0.2 mg/g tissue.

The highest value of Pi concentration (Fig. 15) was detected in the AF of the disc of the 26-year-old patient (0.284 mg/g tissue, disc level L5–S1), whereas the lowest value of was detected in the AF of the L4–L5 disc of the 30-year-old patient (0.003 mg/g tissue). The disc of the oldest 55-year-old patient also demonstrated low Pi concentration of approximately 0.01 mg/g tissue. All other degenerative IVDs showed moderate levels of the Pi concentration, between 0.02 mg/g tissue and 0.06 mg/g tissue. In general, Pi concentration in the AF of degenerative IVDs demonstrated significantly higher values compared to the control IVDs.

Similarly to the observations in the EP, ALP activity and calcium and Pi concentrations in the AF of degenerative IVDs did not demonstrate an obvious trend related to the increase in age of the patient.

Among the discs extracted from a single patient, the ALP activity in the AF (Fig. 15) did not vary considerably. It showed considerable variability only between the discs of one of the 40-year-old patients, where ALP activity was more than twice larger in the AF of the lower L5–S1 disc than in the AF of the upper L4–L5 disc. On the other hand, when looking at calcium concentration in the AF of the other 40-year-old patient, it was almost five times larger in the upper L4–L5 disc than in the lower L5–S1 disc. The other discs originating from one patient showed slight or no variability in calcium concentration in the AF. In the 23-year-old patient, the upper L3–L4 disc demonstrated three times higher Pi concentration in the AF compared to the lower L4–L5 disc. Similarly, the AF of the upper L4–L5 disc of one of the 40-year-old patients showed four times higher Pi concentration than the lower L5–S1 disc. However, in the AF of the 30-year-old patient, Pi concentration was higher in the lower L5–S1 disc than in the upper L4–L5 disc. Thus, there was no correlation between the levels of calcification markers in the AF and the disc level in the spine.

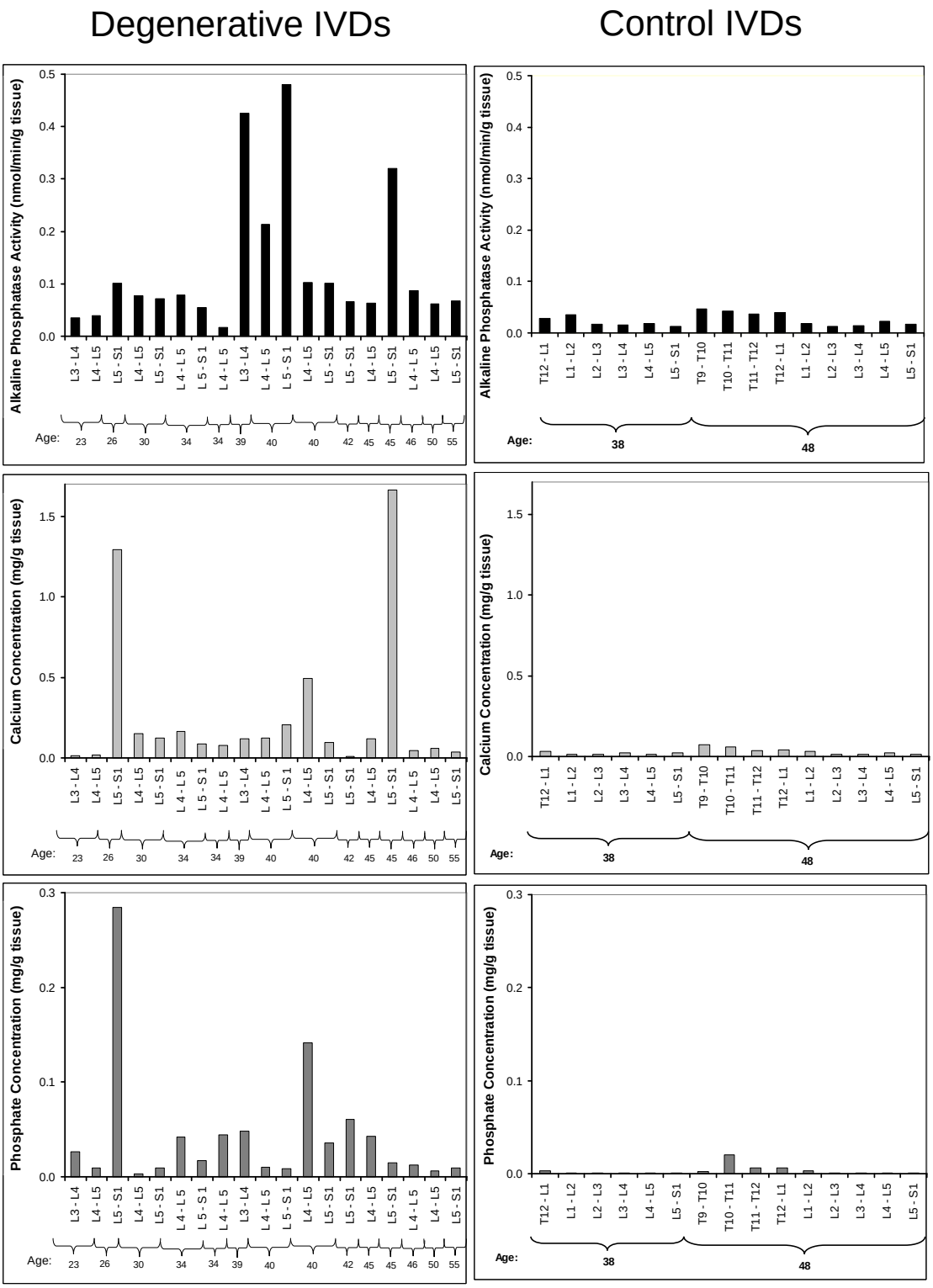

Figure 15: **Biochemical analysis of the calcification markers in the annulus fibrosus of degenerative intervertebral discs**. Alkaline phosphatase activity and calcium and inorganic phosphate concentrations were measured as described in Methods.

Table 5. Statistical analysis of alkaline phosphatase activity and calcium and inorganic phosphate concentrations in the annulus fibrosus of degenerative discs.

Annulus Fibrosus - Degenerative versus Control IVDs

Alkaline Phosphatase Activity

Descriptive Statistics

	Degenerative IVDs	Control IVDs
Mean	0.130	0.025
Standard Deviation	0.133	0.012
Minimum	0.017	0.013
Maximum	0.480	0.047
Range	0.463	0.034
Median	**0.077**	**0.019**

p - value calculated using the Non-parametric Mann-Whitney-Wilcoxon Rank Sum Test

p<0.0001

Calcium Concentration

Descriptive Statistics

	Degenerative IVDs	Control IVDs
Mean	0.258	0.028
Standard Deviation	0.447	0.018
Minimum	0.009	0.012
Maximum	1.665	0.072
Range	1.656	0.059
Median	**0.118**	**0.023**

p - value calculated using the Non-parametric Mann-Whitney-Wilcoxon Rank Sum Test

p=0.0003

Inorganic Phosphate Concentration

Descriptive Statistics

	Degenerative IVDs	Control IVDs
Mean	0.044	0.003
Standard Deviation	0.067	0.005
Minimum	0.003	0.001
Maximum	0.284	0.020
Range	0.281	0.020
Median	**0.017**	**0.001**

p - value calculated using the Non-parametric Mann-Whitney-Wilcoxon Rank Sum Test

p<0.0001

2.1.3. Calcification Markers in the Nucleus Pulposus of Degenerative Discs

The values of the mean and the median for ALP activity and calcium and Pi concentrations in the NP were considerably higher in degenerative than in the control IVDs (Table 6). The range of the values of all three measured calcification markers was much wider in the NP of degenerative than in the NP of control IVDs. The minimum values of the three calcification markers in the NP of degenerative IVDs were much higher than the corresponding minimum values in the NP of control IVDs. Also, the maximum values of the calcification markers in the NP of degenerative IVDs were considerably higher than the corresponding maximum values in the NP of control IVDs. The Non-parametric Mann-Whitney-Wilcoxon Rank Sum Test showed a high statistical significance of the observed elevation in the calcification markers in the NP of degenerative IVDs compared to control IVDs, with $p<0.0001$(Table 6).

The highest value of ALP activity (Fig. 16) was observed in the NP of the L4–L5 disc of one of the 40-year-old patients (1.296 nmol/min/g). The L4–L5 disc of the youngest 23-year-old patient, as well as the disc of the oldest patient (55 year-old) showed low ALP activities in the NP, between 0.1 nmol/min/g and 0.2 nmol/min/g. All other IVDs demonstrated moderated values of ALP activity in the NP, between 0.3 and 0.4 nmol/min/g. The highest calcium concentration was found in the NP of the L5–S1 disc of one of the 45-year-old patients (2.89 mg/g). The lowest value of calcium concentration was observed in the NP of the oldest patient (55-year-old) (0.03 mg/g). All other IVDs had calcium concentration in the NP between 0.1 mg/g and 0.4 mg/g. The highest value of the Pi concentration was detected in the NP of the L5–S1 disc of one of the 40-year-old patients (0.66 mg/g). The lowest value of the Pi concentration was detected in the NP of the L5–S1 disc of the 30-year-old patient (0.006 mg/g). Pi concentrations in the NP of the other IVDs varied between 0.01 mg/g

and 0.2 mg/g. Although the lowest values of the calcification markers in the NP of degenerative IVDs were below the highest values of the calcification markers in the NP of control IVDs, on average, degenerative IVDs demonstrated much higher levels of calcification markers than the control IVDs. ALP activity and calcium and Pi concentrations in the NP of degenerative IVDs, in accordance with the findings in the EP and AF, demonstrated considerable individual variation with no consistent trend related to the increase in age of the patient.

The comparison between different IVD levels in the same patient indicated that, in some discs, ALP activity in the NP did not show variability, whereas in others it varied, however, with no correlation with the disc level. ALP activity in the NP was higher in the upper discs of the 23 and the other 40-year-old patients, whereas in the 34-year-old patient it was higher in the lower disc level. Calcium concentration in NP varied slightly but with no consistent trend for higher values in the upper or lower disc levels. Similarly, Pi concentration in the NP of one of the 40-year-old patients was higher in the upper IVD, whereas in the NP of the other 40-year-old patient it was higher in the lower disc level. The variations of Pi concentration in the NP of the other IVDs originating from one patient were minimal. In general, in IVDs originating from one patient, the NP variability of all three calcification markers did not show a clear trend related to the level of the IVD in the spine.

In summary the EP, AF, and NP of the degenerative IVDs demonstrated the same trend of elevation in all three markers of the calcification process (Fig. 17). The magnitude of this elevation was highly variable, but the elevation in the ALP activity correlated more closely with Pi concentration than with calcium concentration. Consistent trends in calcification markers related to the age of the patient or the IVD level were not observed.

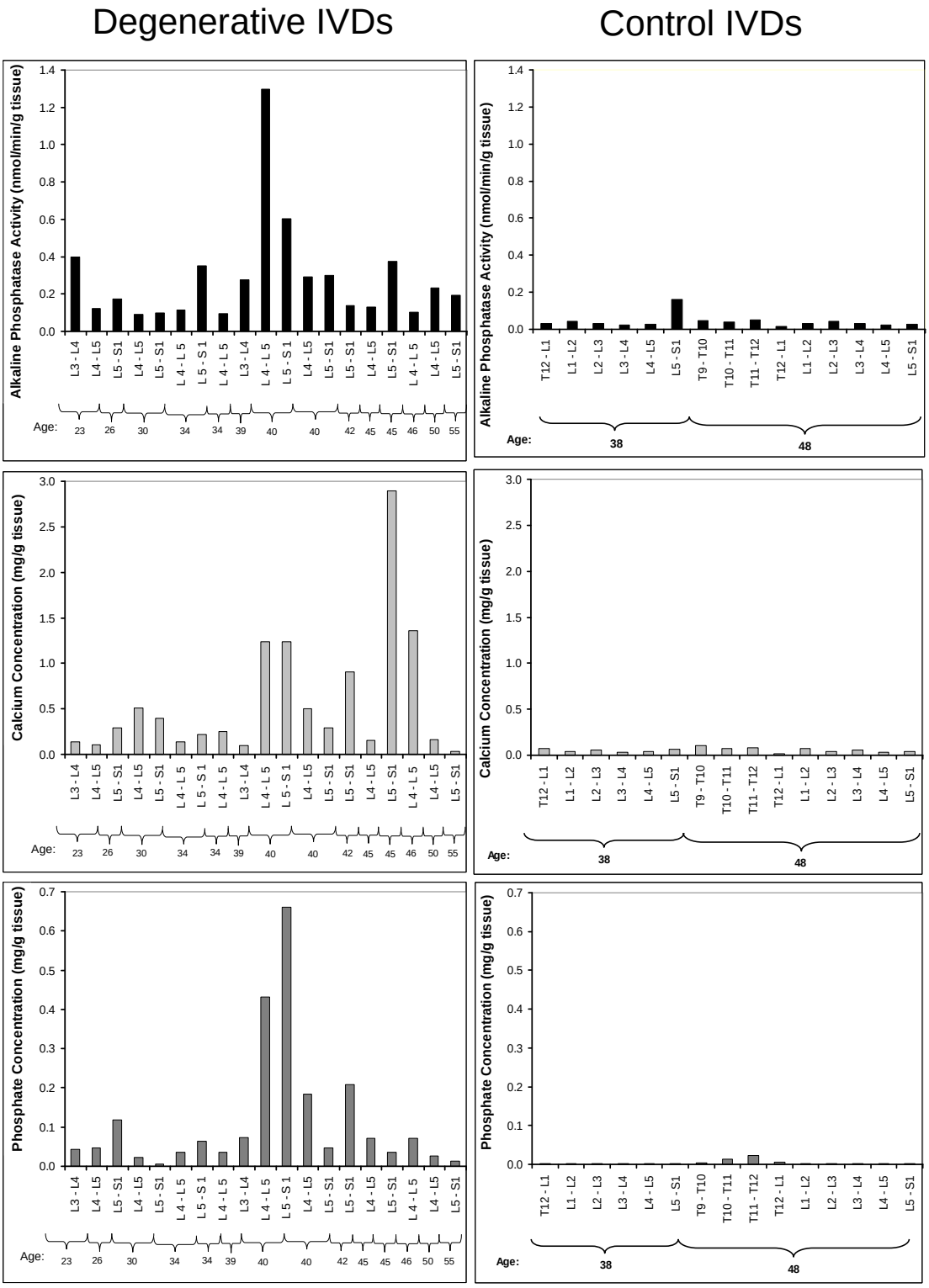

Figure 16: **Biochemical analysis of the calcification markers in the nucleus pulposus of degenerative intervertebral discs.** Alkaline phosphatase activity and calcium and inorganic phosphate concentrations were measured as described in Methods.

Table 6. Statistical analysis of alkaline phosphatase activity and calcium and inorganic phosphate concentrations in the nucleus pulposus of degenerative discs.

Nucleus Pulposus - Degenerative versus Control IVDs

Alkaline Phosphatase Activity

Descriptive Statistics	Degenerative IVDs	Control IVDs
Mean	0.283	0.042
Standard Deviation	0.281	0.034
Minimum	0.092	0.014
Maximum	1.296	0.160
Range	1.205	0.145
Median	**0.193**	**0.033**

p - value calculated using the Non-parametric Mann-Whitney-Wilcoxon Rank Sum Test: **p<0.0001**

Calcium Concentration

Descriptive Statistics	Degenerative IVDs	Control IVDs
Mean	0.575	0.055
Standard Deviation	0.702	0.025
Minimum	0.033	0.013
Maximum	2.892	0.109
Range	2.858	0.095
Median	**0.293**	**0.054**

p - value calculated using the Non-parametric Mann-Whitney-Wilcoxon Rank Sum Test: **p<0.0001**

Inorganic Phosphate Concentration

Descriptive Statistics	Degenerative IVDs	Control IVDs
Mean	0.116	0.004
Standard Deviation	0.165	0.006
Minimum	0.006	0.001
Maximum	0.661	0.022
Range	0.655	0.021
Median	**0.048**	**0.002**

p - value calculated using the Non-parametric Mann-Whitney-Wilcoxon Rank Sum Test: **p<0.0001**

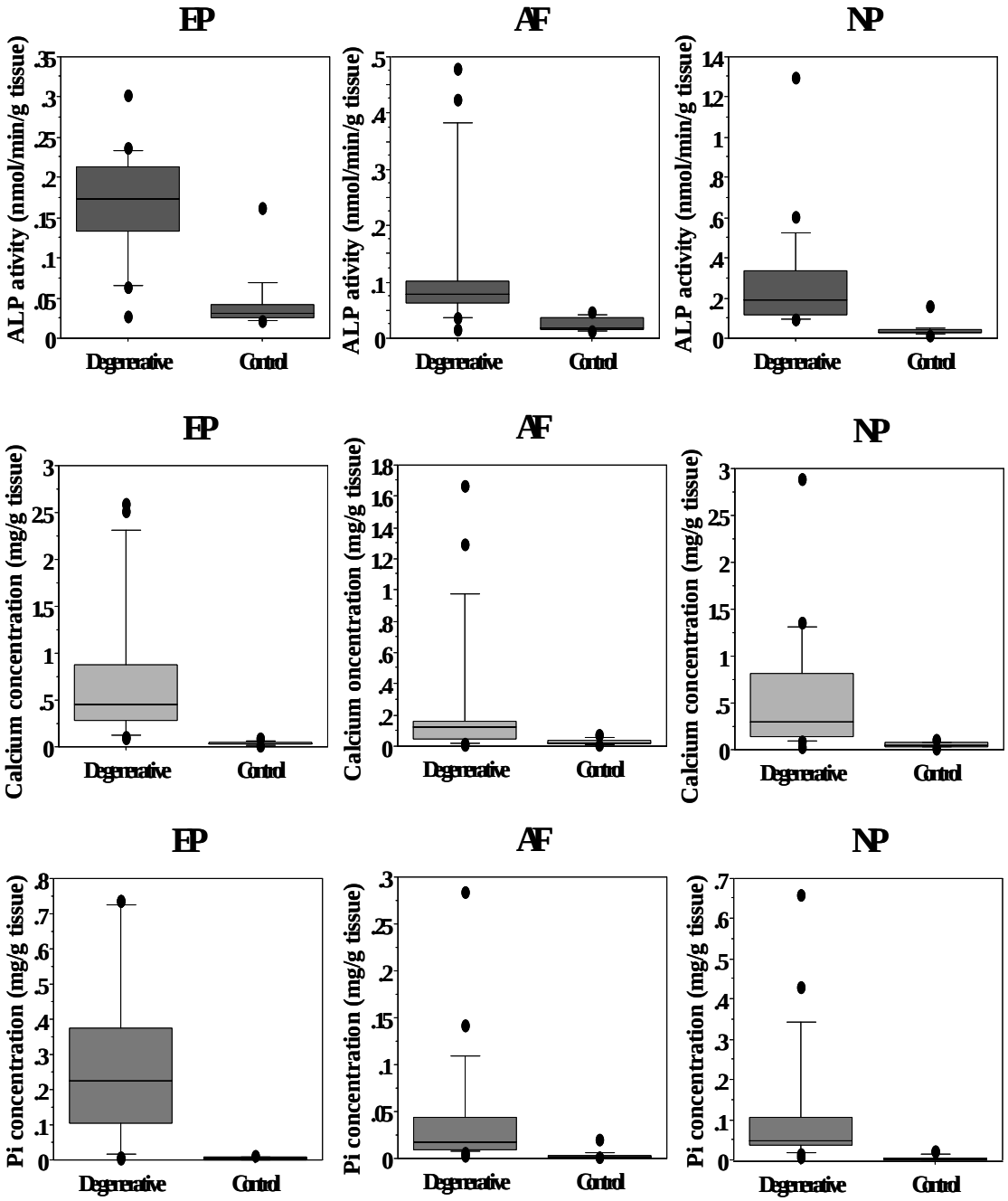

Figure 17: Calcification Markers in EP, AF, and NP of degenerative IVDs.

Figure represents a comparative analysis of alkaline phosphatase (ALP) activity and calcium and inorganic phosphate (Pi) concentrations in degenerative versus control intervertebral discs (IVDs). The box plots are used to represent the non-parametric distribution of the three makers of calcification process. The box displays the data lying within the interquartile range (between the 25^{th} and 75^{th} percentiles) containing 50% of the observations. The line within the box displays the median.

2.2. Calcification Markers in Scoliotic Intervertebral Discs

The calcification markers of the scoliotic IVDs were assessed in comparison with the calcification markers of the control IVDs. In order to detect a possible influence of the degree of scoliotic deformity on the levels of calcification markers, the values of ALP activity and calcium and Pi concentrations are represented in an ascending order according to the increase of the Cobb angle of the patient. Information about the IVD level that corresponds to the apex of scoliotic curve was not available. For this reason study data was not analyzed in relation to the apex of scoliotic curve. However, IVDs that are situated on lower levels in the spine experience increased mechanical loading due to the increased body mass they are bearing in standing body position. In order to find out whether the position of IVD in the spine had influenced the calcification markers, the study data was analyzed in relation to the level of IVD in the spine. Furthermore, in order to account for the impact of concavity and convexity of scoliotic curve on the calcification process, the three markers of calcification were assessed separately for the concave and convex parts of each scoliotic IVD. The markers of the calcification process of both concave and convex parts of the scoliotic IVDs demonstrated a non-parametric type of distribution of the values.

2.2.1. Calcification Markers in the Endplate of Scoliotic Discs

The levels of calcification markers in the EP of the degenerative IVDs are represented on Figure 18. The statistical analysis of the results is represented on Table 7. The values of the mean and the median for ALP activity and calcium and Pi concentrations in the concave and convex parts of the EP (Table 7) were higher in scoliotic than in the control IVDs. The range of the values of all three measured markers was wider in the EP of scoliotic IVDs (again both concave and convex parts)

than in the EP of control IVDs. The minimum values were variable, with no clear prevalence in either location. The maximum values in the EP of scoliotic IVDs (concave and convex), although variable, were higher than the corresponding maximum values in the EP of control IVDs. The Non-parametric Mann-Whitney-Wilcoxon Rank Sum Test demonstrated that only the elevation of Pi concentration in scoliotic IVDs was statistically significant, with a p-value of 0.0019, whereas the p-values for ALP activity and calcium concentration (0.1590) were higher than $p<0.05$, showing no statistical significance of the differences (Table 7).

The highest value of the ALP activity was observed in the EP of the patient with 61º Cobb angle (Fig. 18), in both concave and convex parts of the disc (0.75 and 0.65 nmol/min/g tissue, respectively). At the same time, the lowest values of the ALP activity were found in the IVDs of the patients with 66º and 78º Cobb angles (which was the largest Cobb angle in this study), as well as in some of the discs of the patients with 55º and 56º Cobb angles. These values were 10 to 15 times lower than the highest values observed. The other analyzed scoliotic IVDs demonstrated intermediate levels of ALP activity in the EP. The highest calcium concentration was found in the EP of the concave part of the T11–T12 disc of the patient with 55º Cobb angle (more than 10 mg/g tissue). However, calcium concentration in the convex part of the same scoliotic disc was more than 10 times lower (0.76 mg/g tissue). The patient with the highest Cobb angle (78º) had rather low calcium concentrations in the EP varying between 0.12 and 0.36 mg/g tissue. The highest value of Pi concentration was detected in the EP of the concave part of the T11–T12 disc of the patient with Cobb angle 56º (1.96 mg/g tissue), whereas Pi concentration in the convex part in the EP of the same disc was more than six times lower (0.3 mg/g tissue). The patient with the highest Cobb angle (78º) had moderate levels of Pi concentration in the EP

varying between 0.05 and 0.3 mg/g tissue. Thus, ALP activity and calcium and Pi concentrations in the EP of concave and convex parts of scoliotic IVDs did not demonstrate consistent trend related to the increase in Cobb angle of the patient.

Many of the patients with AIS had undergone surgical removal of more than one IVD. This provided the possibility to analyze the data for a possible trend related to the level of IVD in the spine. The analysis of the variations between the discs extracted from one patient (Fig. 18) showed that the patients with Cobb angles 52º, 55º and 56º had higher levels of ALP activity in the EP of the upper disc levels, whereas the patients with Cobb angles 58º and 66º had higher levels of the ALP activity in the EP of the lower disc levels. At the same time, the patient with the highest Cobb angle (78º) did not show any considerable variability in the ALP activity in the EP.

Regarding calcium concentration, the patient with the 52º Cobb angle had higher values in the lower disc levels, whereas the patient with the 56º Cobb angle had higher values in the upper disc levels. The patients with Cobb angles 55º, 58º, 66º and 78º did not show much variability related to the IVD level.

Similarly, regarding Pi concentration, some patients showed higher values in the lower disc levels (patient with the 52º Cobb angle), others demonstrated higher values in the upper disc levels (patients with the 55º and 56º Cobb angles), whereas the patients with Cobb angles 58º, 66º, and 78º did not show much variability related to the level of the IVD in the spine.

Thus, the EP variations of the calcification markers between the discs originating from one patient did not demonstrate any consistent trend related to the level of the disc in the spine.

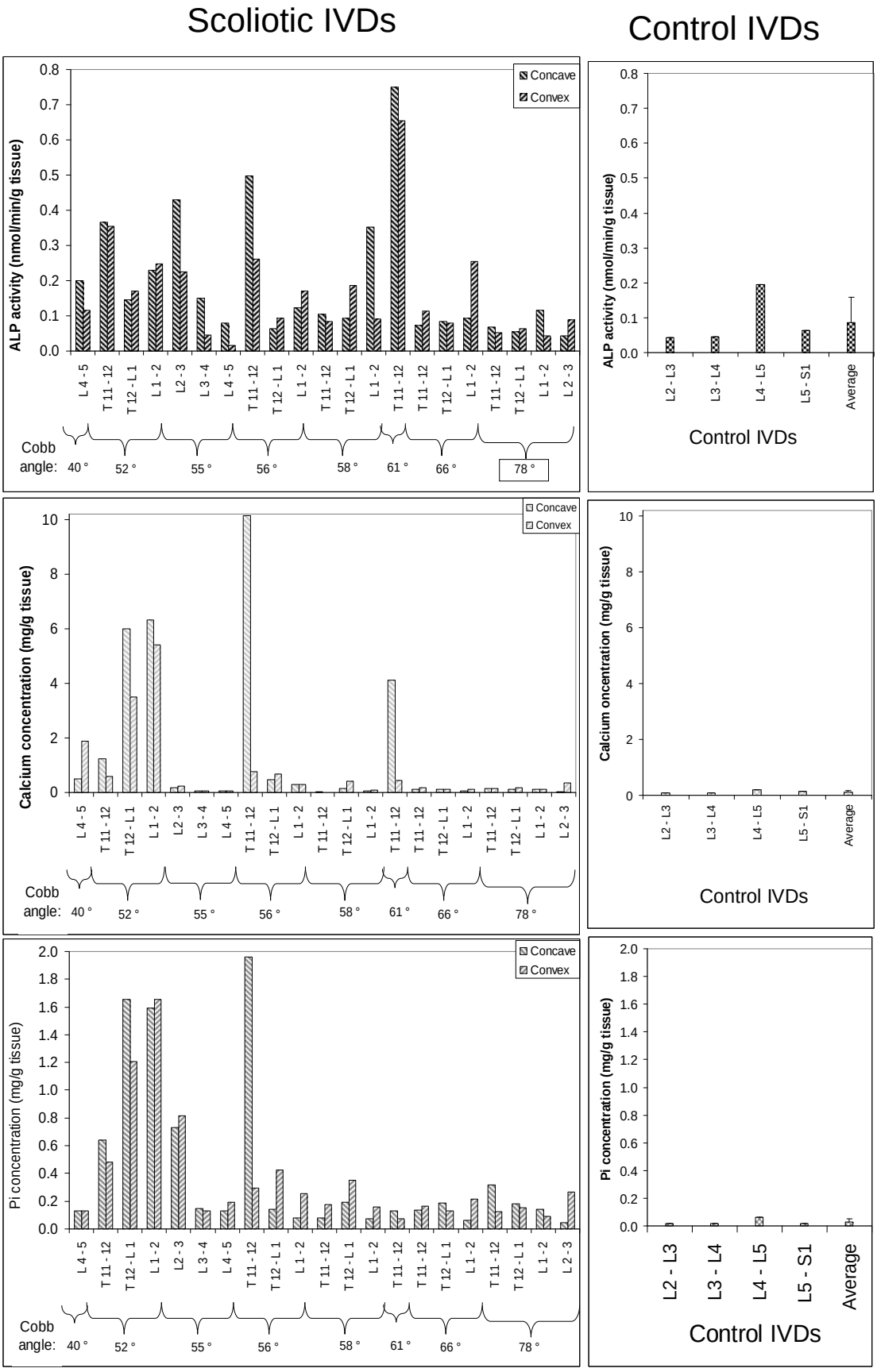

Figure 18: **Biochemical analysis of the calcification markers in the endplate of scoliotic intervertebral discs**. Alkaline phosphatase activity and calcium and inorganic phosphate concentrations were measured as described in Methods.

Table 7. Statistical analysis of alkaline phosphatase activity and calcium and inorganic phosphate concentrations in the endplate of scoliotic discs.

Endplate - Scoliotic versus Control IVDs

Alkaline Phosphatase Activity

Descriptive Statistics

	Scoliotic IVDs Concave	Scoliotic IVDs Convex	Control IVDs
Mean	0.196	0.162	0.087
Standard Deviation	0.183	0.144	0.072
Minimum	0.044	0.016	0.044
Maximum	0.750	0.654	0.195
Range	0.706	0.638	0.151
Median	**0.115**	**0.113**	**0.054**

p - value calculated using the Non-parametric Mann-Whitney-Wilcoxon Rank Sum Test

p=0.1590

Calcium Concentration

Descriptive Statistics

	Scoliotic IVDs Concave	Scoliotic IVDs Convex	Control IVDs
Mean	1.443	0.743	0.114
Standard Deviation	2.776	1.336	0.056
Minimum	0.017	0.014	0.071
Maximum	10.133	5.417	0.187
Range	10.116	5.403	0.117
Median	**0.139**	**0.235**	**0.099**

p - value calculated using the Non-parametric Mann-Whitney-Wilcoxon Rank Sum Test

p=0.1590

Inorganic Phosphate Concentration

Descriptive Statistics

	Scoliotic IVDs Concave	Scoliotic IVDs Convex	Control IVDs
Mean	0.417	0.357	0.009
Standard Deviation	0.582	0.401	0.004
Minimum	0.047	0.072	0.005
Maximum	1.961	1.656	0.014
Range	1.914	1.583	0.009
Median	**0.144**	**0.190**	**0.009**

p - value calculated using the Non-parametric Mann-Whitney-Wilcoxon Rank Sum Test

p=0.0019

(p<0.05)

2.2.2. Calcification Markers in the Annulus Fibrosus of Scoliotic Discs

Statistical analysis indicated that the values of the mean and the median for ALP activity and calcium and Pi concentrations in the concave and convex parts of the AF, although highly variable, were higher in scoliotic than in control IVDs (Table 8). The mean and the median of the Pi concentration in both concave and convex parts of scoliotic IVDs were considerably higher than the corresponding values in control IVDs. The range of the values of all three calcification markers was wider in the AF of scoliotic IVDs (in both concave and convex parts) than in the AF of control IVDs. The minimum values of all three calcification markers in the concave AF were higher than in the control AF. However, in the convex AF they were not higher than in the control. For all three calcification markers, the maximum values were variable but considerably higher in the AF of scoliotic IVDs (both concave and convex) than the maximum values in the AF of control IVDs. The Non-parametric Mann-Whitney-Wilcoxon Rank Sum Test demonstrated that the elevation in both ALP activity and Pi concentration in the AF of scoliotic IVDs were statistically significant, with p-values of 0.0144 and 0.0049, respectively. The p-value for the calcium concentration was 0.2662, which indicates no statistical significance (Table 8).

The highest value of the ALP activity (Fig. 19) was observed in the concave AF of the L2–L3 disc of the patient with 55º Cobb angle (1.15 nmol/min/g). However, the convex AF of the same disc showed almost three times lower value of the ALP activity (0.4 nmol/min/g). The lowest value of the ALP activity was detected in the convex AF of the L4–L5 disc of the same patient (0.01 nmol/min/g). The patient with the lowest Cobb angle (40º) demonstrated rather low values of ALP activity in both concave and convex AF parts (about 0.15 nmol/min/g). The patient with the highest Cobb angle (78º) also demonstrated rather low values of ALP activity. The highest

calcium concentration was found in the convex AF of the patient with the lowest Cobb angle (40º) (4.2 mg/g). However, calcium concentration in the concave AF of the same disc was almost 10 times lower (0.42 mg/g). The patient with the highest Cobb angle (78º) showed rather low values of calcium concentration, with highest value of 0.14 mg/g tissue and lowest value of 0.016 mg/g. The lowest value of the calcium concentration was detected in the convex AF of the L1-L2 disc of the patient with 58º Cobb angle (0.07 mg/g). The highest values of Pi concentration were found in the AF of the patient with Cobb angle of 52º. The lowest value of the Pi concentration was found in the convex AF of the disc of the patient with the lowest 40º Cobb angle (0.001 mg/g). The patient with the highest Cobb angle (78º) demonstrated rather low levels of Pi concentration in the AF, with values between 0.033 and 0.13 mg/g. This pattern of variation indicates that ALP activity and calcium and Pi concentrations in the AF of concave and convex parts of scoliotic IVDs did not show a clear trend related to the increase in Cobb angle of the patient. In the discs extracted from one patient, the patients with Cobb angles of 52º, 55º, 56º and 78º had higher values of the ALP activity in the AF of the upper than in the lower disc levels. The values of the calcium concentration in the patients with 52º and 78º Cobb angles were also higher in the upper IVD levels. At the same time, however, the patients with Cobb angles of 55º, 56º, 58º and 66º did not show consistent variability between the different IVD levels. Pi concentration also did not demonstrate a consistent trend related to the IVD level in the spine. The patients with Cobb angles of 52º, 56º, 58º and 78º had higher Pi concentrations in the AF of the lower disc levels, whereas the patients with Cobb angles of 55º and 66º had higher Pi concentrations in the upper levels. Thus, the variations of the calcification markers in AF between the discs extracted from a single patient did not demonstrate clear trends.

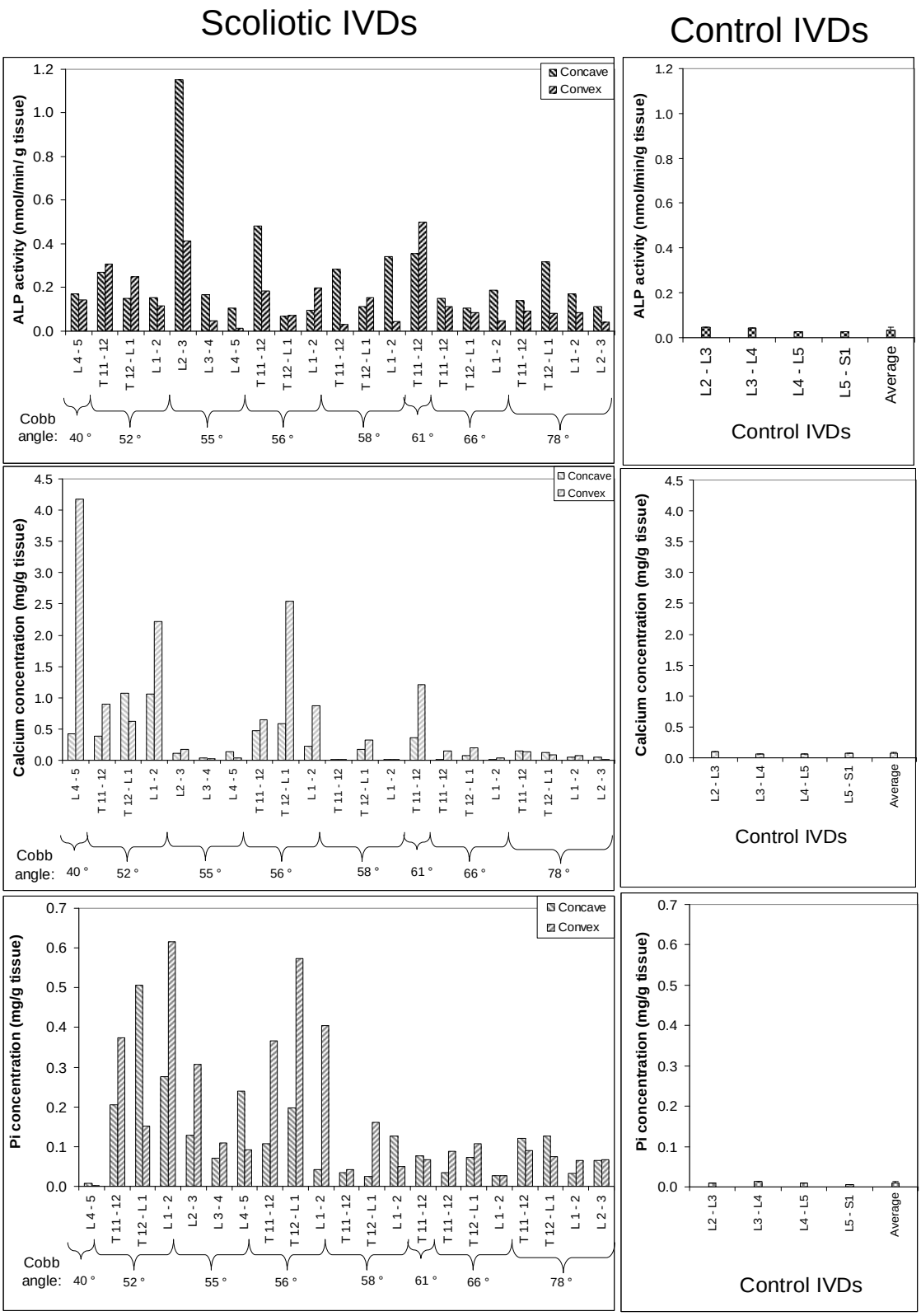

Figure 19: **Biochemical analysis of the calcification markers in the annulus fibrosus of scoliotic intervertebral discs**. Alkaline phosphatase activity and calcium and inorganic phosphate concentrations were measured as described in chapter Methods.

Table 8. Statistical analysis of alkaline phosphatase activity and calcium and inorganic phosphate concentrations in the annulus fibrosus of scoliotic discs.

Annulus Fibrosus - Scoliotic versus Control IVDs

Alkaline Phosphatase Activity

Descriptive Statistics				p - value calculated using the Non-parametric Mann-Whitney-Wilcoxon Rank Sum Test
	Scoliotic IVDs Concave	Scoliotic IVDs Convex	Control IVDs	**p=0.0144**
Mean	0.243	0.144	0.035	
Standard Deviation	0.234	0.129	0.010	**(p<0.05)**
Minimum	0.070	0.012	0.025	
Maximum	1.153	0.498	0.046	
Range	1.083	0.486	0.020	
Median	**0.167**	**0.094**	**0.035**	

Calcium Concentration

Descriptive Statistics				p - value calculated using the Non-parametric Mann-Whitney-Wilcoxon Rank Sum Test
	Scoliotic IVDs Concave	Scoliotic IVDs Convex	Control IVDs	**p=0.2662**
Mean	0.264	0.690	0.074	
Standard Deviation	0.314	1.070	0.018	
Minimum	0.015	0.007	0.057	
Maximum	1.070	4.172	0.098	
Range	1.055	4.164	0.042	
Median	**0.132**	**0.175**	**0.070**	

Inorganic Phosphate Concentration

Descriptive Statistics				p - value calculated using the Non-parametric Mann-Whitney-Wilcoxon Rank Sum Test
	Scoliotic IVDs Concave	Scoliotic IVDs Convex	Control IVDs	**p=0.0049**
Mean	0.120	0.182	0.009	
Standard Deviation	0.118	0.182	0.004	**(p<0.05)**
Minimum	0.008	0.001	0.005	
Maximum	0.507	0.616	0.014	
Range	0.499	0.615	0.009	
Median	**0.078**	**0.091**	**0.009**	

2.2.3. Calcification Markers in the Nucleus Pulposus of Scoliotic Discs

The values of ALP activity and calcium and Pi concentrations in the NP of the scoliotic IVDs are represented according to the increase of the Cobb angle of the patient (Fig. 20). ALP activity and calcium and Pi concentrations in the NP of both concave and convex parts of the scoliotic IVDs demonstrated a non-parametric type of distribution of the values (Table 9). The values of the mean were higher in both concave and convex parts of the NP of scoliotic IVDs compared to control IVDs. The median for the ALP activity and Pi concentration was also higher in both concave and convex parts of the NP of scoliotic IVDs. However, the median for the calcium concentration was higher in the NP of control IVDs than in the both concave and convex parts of the NP of scoliotic IVDs. The range of the values of all three calcification markers was wider in the NP of scoliotic IVDs (in both concave and convex parts) than in the NP of control IVDs. The minimum values of ALP activity in the concave and convex NP of the scoliotic IVDs, as well as in the NP of control IVDs, were very similar. However, the corresponding maximum values were much higher in the scoliotic IVDs (in both concave and convex parts) than in the control IVDs. Regarding Pi concentration, the lowest minimum value was observed in the concave NP of the scoliotic IVDs. The maximum values of the Pi concentration in both concave NP and convex NP were higher than the maximum value in the NP of control IVDs. The Non-parametric Mann-Whitney-Wilcoxon Rank Sum Test did not show a statistical significance of the findings in either marker of the calcification process in the NP. The p-values for the ALP activity (0.0639) and Pi concentration (0.0539) were slightly above the level of statistical significance. The p-value for the calcium concentration (0.2994) also did not demonstrate statistical significance of the findings (Table 9).

ALP activity in the NP of concave and convex parts of scoliotic IVDs did not show a consistent trend related to the increase in Cobb angle of the patient (Fig. 20). The highest values of the ALP activity of about 1.2 nmol/min/g tissue were observed in both concave and convex NP of the L2–L3 disc of the patient with 55º Cobb angle. At the same time, the lowest values of the ALP activity were observed in the same patient, in the concave and convex NP of the L4–L5 disc (values about 0.04 nmol/min/g tissue). The patient with the lowest Cobb angle (40º) demonstrated rather low values of ALP activity (about 0.2 nmol/min/g tissue) compared to the values in the other scoliotic IVDs. The patient with the highest Cobb angle (78º) demonstrated moderate values of ALP in the NP.

Regarding calcium concentration in the NP, the patient with the lowest Cobb angle (40º) demonstrated the highest values (5.6 mg/g tissue in the concave NP and 2.7 mg/g tissue in the convex NP of the disc). The patient with the highest Cobb angle (78º) had very low values of the calcium concentration in the NP. However, these values were comparable to the values of the patients with 55º, 58º, and 66º Cobb angles.

The lowest value of the Pi concentration was observed in the concave NP of the patient with the lowest Cobb angle (40º) (0.008 mg/g tissue). The highest value was observed in the concave NP of the T11–T12 disc of the patient with the 52º Cobb angle (0.8 mg/g tissue). The patient with the highest Cobb angle (78º) had rather low values of Pi concentration (about 0.06 mg/g tissue), which were, however, comparable to the values of the patients with 58º, 61º and 66º Cobb angles.

Thus, the variations in the ALP activity and calcium and Pi concentrations in the NP of scoliotic IVDs, similarly to the observations in the EP and AF, did not show a clear trend related to the Cobb angle of the patient.

The comparison of the discs extracted from one patient showed that the patients with 52º, 55º, and 56º Cobb angles had higher levels of the ALP activity in the NP of the upper than in the lower IVD levels. However, the patients with 58º, 66º, and 78º Cobb angles did not show much variability of the ALP activity between the different disc levels. Regarding the calcium concentration, the patient with 52º Cobb angle had higher values in the upper than in the lower disc levels, however, most of the patients did not show much variability between the different levels of the IVD. In terms of Pi concentration, some patients had higher values in the upper IVD levels (52º, 55º, and 56º Cobb angles), whereas others did not demonstrate a correlation between the variability in Pi concentration and the disc level in the spine (58º, 66º and 78º Cobb angles).

The analysis of the variability of calcification markers in the NP of discs extracted from one patient did not show a consistent trend for changes related to the IVD level in the spine.

The analysis of the three markers of calcification process demonstrated that their values were usually higher in scoliotic IVDs compared to control IVDs (Fig. 21). However, this prevalence was not always statistically significant (Tables 7, 8, and 9). All the three markers of calcification process in scoliotic IVDs demonstrated wide variations, with no consistent trends related to the Cobb angle of the patient or the level of the disc in the spine.

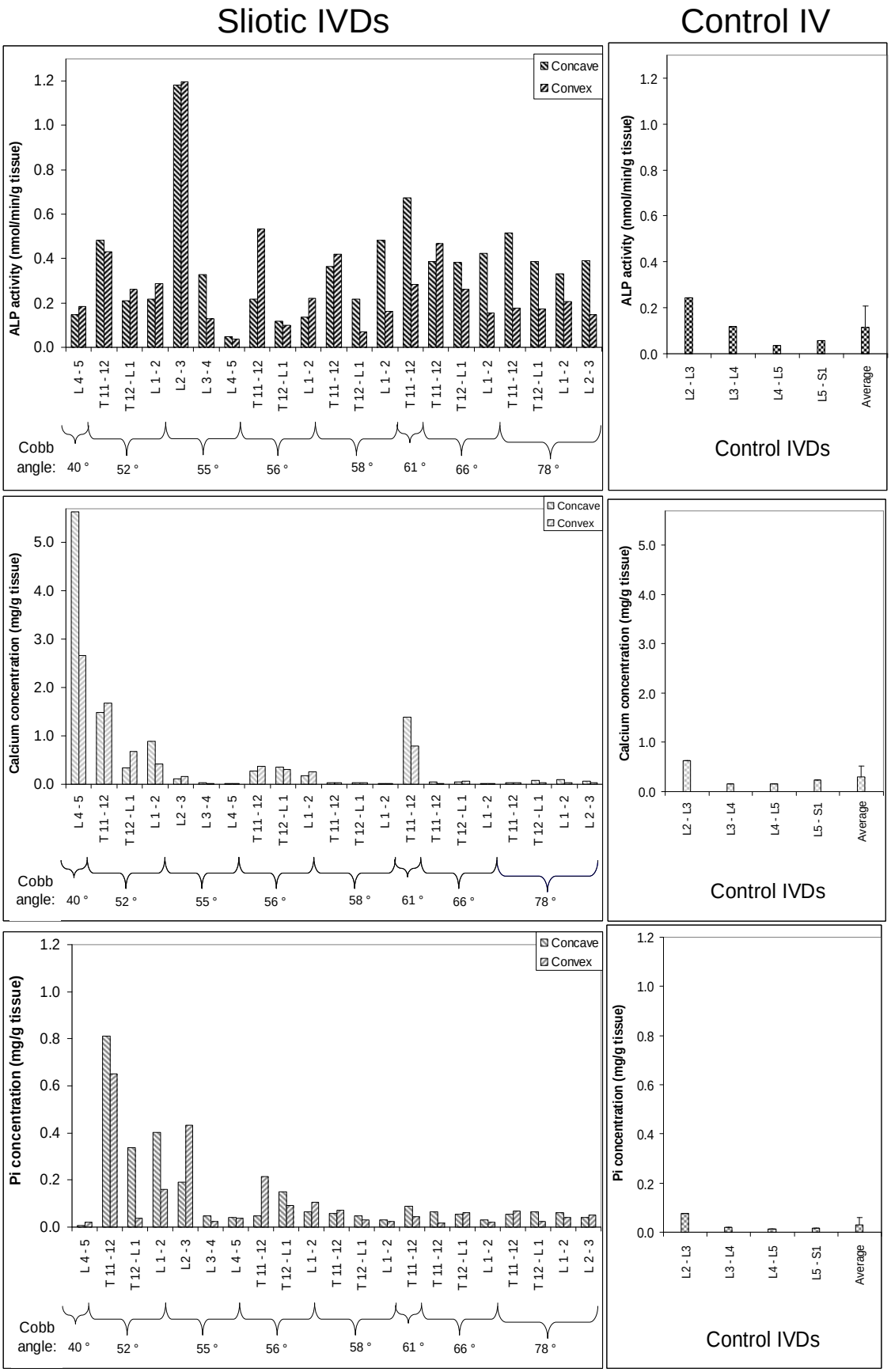

Figure 20: **Biochemical analysis of the calcification markers in the nucleus pulposus of scoliotic intervertebral discs**. Alkaline phosphatase activity and calcium and inorganic phosphate concentrations were measured as described in Methods.

Table 9. Statistical analysis of alkaline phosphatase activity and calcium and inorganic phosphate concentrations in the nucleus pulposus of scoliotic discs.

Nucleus Pulposus - Scoliotic versus Control IVDs

Alkaline Phosphatase Activity

Descriptive Statistics	Scoliotic IVDs Concave	Scoliotic IVDs Convex	Control IVDs
Mean	0.364	0.281	0.114
Standard Deviation	0.242	0.246	0.092
Minimum	0.049	0.036	0.037
Maximum	1.184	1.199	0.242
Range	1.134	1.163	0.206
Median	**0.363**	**0.206**	**0.088**

p - value calculated using the Non-parametric Mann-Whitney-Wilcoxon Rank Sum Test

p=0.0639

Calcium Concentration

Descriptive Statistics	Scoliotic IVDs Concave	Scoliotic IVDs Convex	Control IVDs
Mean	0.533	0.365	0.297
Standard Deviation	1.247	0.660	0.221
Minimum	0.018	0.018	0.159
Maximum	5.632	2.659	0.623
Range	5.614	2.642	0.464
Median	**0.087**	**0.035**	**0.203**

p - value calculated using the Non-parametric Mann-Whitney-Wilcoxon Rank Sum Test

p=0.2994

Inorganic Phosphate Concentration

Descriptive Statistics	Scoliotic IVDs Concave	Scoliotic IVDs Convex	Control IVDs
Mean	0.129	0.106	0.031
Standard Deviation	0.186	0.157	0.030
Minimum	0.008	0.018	0.013
Maximum	0.810	0.650	0.076
Range	0.803	0.632	0.063
Median	**0.058**	**0.044**	**0.017**

p - value calculated using the Non-parametric Mann-Whitney-Wilcoxon Rank Sum Test

p=0.0539

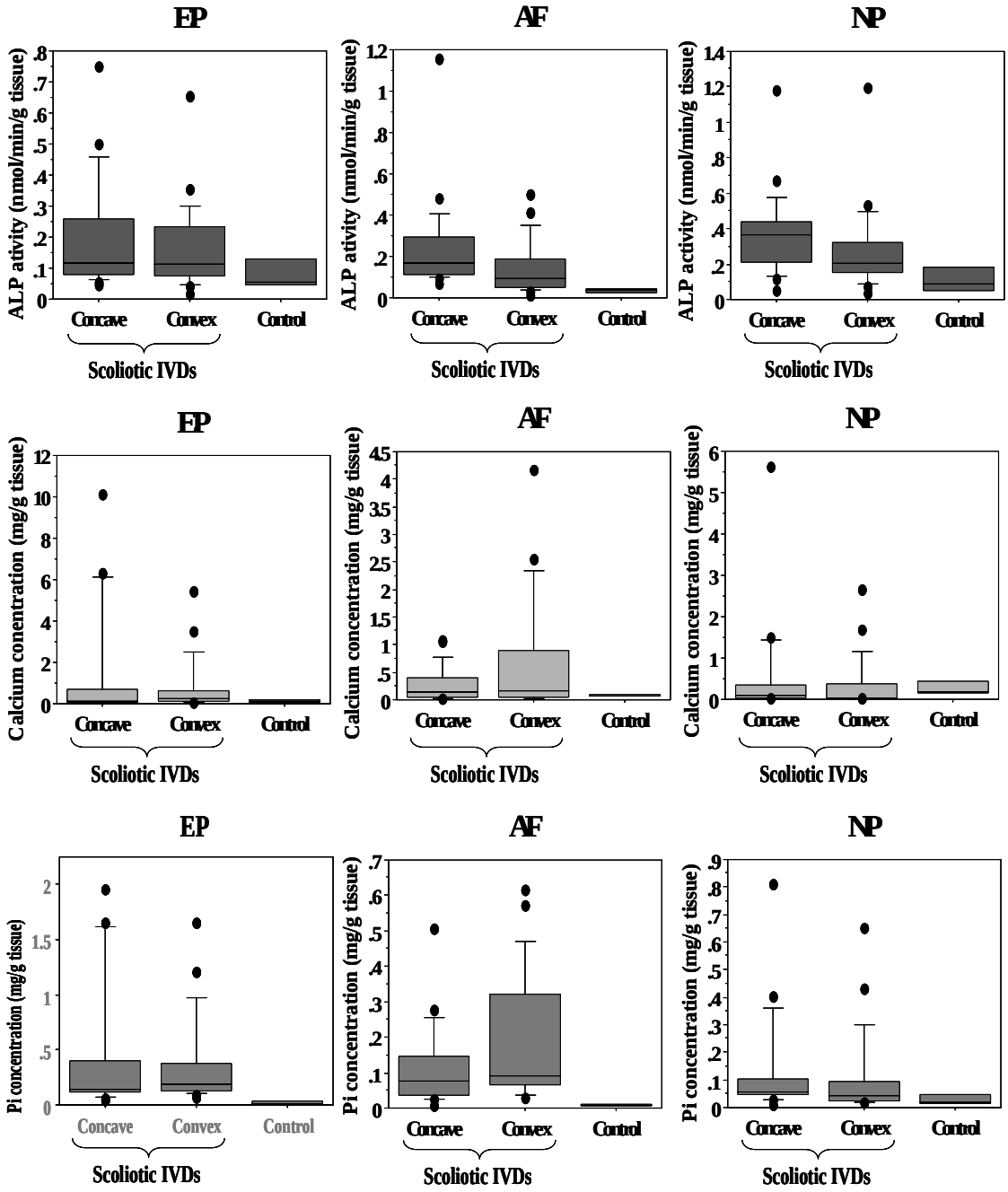

Figure 21: Calcification markers in EP, AF, and NP of scoliotic IVDs.

Figure represents a comparative analysis of alkaline phosphatase (ALP) activity and calcium and inorganic phosphate (Pi) concentrations in scoliotic versus control intervertebral discs (IVDs). The box plots are used to represent the non-parametric distribution of the three makers of calcification process. The box displays the data lying within the interquartile range (between the 25^{th} and 75^{th} percentiles) containing 50% of the observations. The line within the box displays the median.

2.3. Comparative Analysis of Calcification Markers in the Concave and Convex Parts of Scoliotic Intervertebral Discs

In order to facilitate the comparative analysis of the calcification markers between the concave and convex parts of the scoliotic IVDs, the experimental results for the three calcification markers are represented as ratios of the values found in the concave part versus the values found in the convex part of each scoliotic disc. Thus, a ratio above 1.2 demonstrates a prevalence of the concave part; a ratio below 0.8 shows a prevalence of the convex part, whereas the ratios between 0.8 and 1.2 indicate no prevalence in either part of the disc. For the purpose of detecting a possible influence of the degree of scoliotic deformity, all the ratios are arranged in an order reflecting the increase of the Cobb angle of the patient.

ALP activity in the EP, AF, and NP of the scoliotic IVDs, represented as ratios of the concave versus convex parts of each IVD, is shown on the Figure 22. The ratio showing the highest prevalence of the concave versus the convex part of the disc was found in the EP of the L4–L5 disc of the patient with Cobb angle 55º. The ratio showing the highest prevalence of the convex part over the concave part was found in the L1–L2 disc of the patient with the 66º Cobb angle. The patient with the lowest Cobb angle (40º) demonstrated a slight prevalence of the ALP activity in the concave over the convex EP. Two discs of the patient with the highest Cobb angle (78º) also showed a slight prevalence of the ALP activity in the concave EP, whereas the other two discs of the same patient demonstrated a slight prevalence of the ALP activity in the convex EP.

In the AF, the patient with the lowest Cobb angle (40º) had slight prevalence of the ALP activity in the concave AF. The patient with the highest Cobb angle (78º)

showed moderate prevalence of the ALP activity in the concave AF in all four analyzed IVDs.

In the NP, higher prevalence of the ALP activity in the convex aspect was found in the patient with the lowest Cobb angle (40º), as well as in seven other analyzed IVDs. However, most of the analyzed IVDs (13 out of 21) demonstrated prevalence of ALP activity in the concave part of the NP, including all four discs of the patient with 78º Cobb angle. The variations in the ALP activity ratios in the EP, AF, and NP were not statistically correlated to the variations of the Cobb angle of the patients.

The comparison between the discs extracted from one patient showed that in the EP, the ALP activity was more prevalent in the concave parts of the discs extracted from the patient with the 52º Cobb angle, whereas in the discs extracted from the patient with 55º Cobb angle, it was more prevalent in the convex part. In most of the discs extracted from one patient, a consistent prevalence of either part of the discs was not observed. In the AF, ALP activity was prevalent in the concave aspect of the discs of the patients with Cobb angles of 55º, 66º and 78º, whereas in the discs of the patients with Cobb angles of 52º, 56º, and 58º there was no consistent trend of prevalence of either aspect of the IVD. In the NP, ALP activity was more prevalent in the concave aspect of the IVDs from the patient with the highest Cobb angle (78º). However, in the rest of the discs a consistent trend was not observed.

The average values of the ratios for the ALP activity in the EP, AF, and NP were higher than 1.2, however, the error bars were large, reflecting the existing large variability. This suggests the absence of clear trend towards prevalence of the concave over the convex aspect of the IVDs. The Non-parametric Wilcoxon Signed Rank Test did not detect statistical significance of these findings.

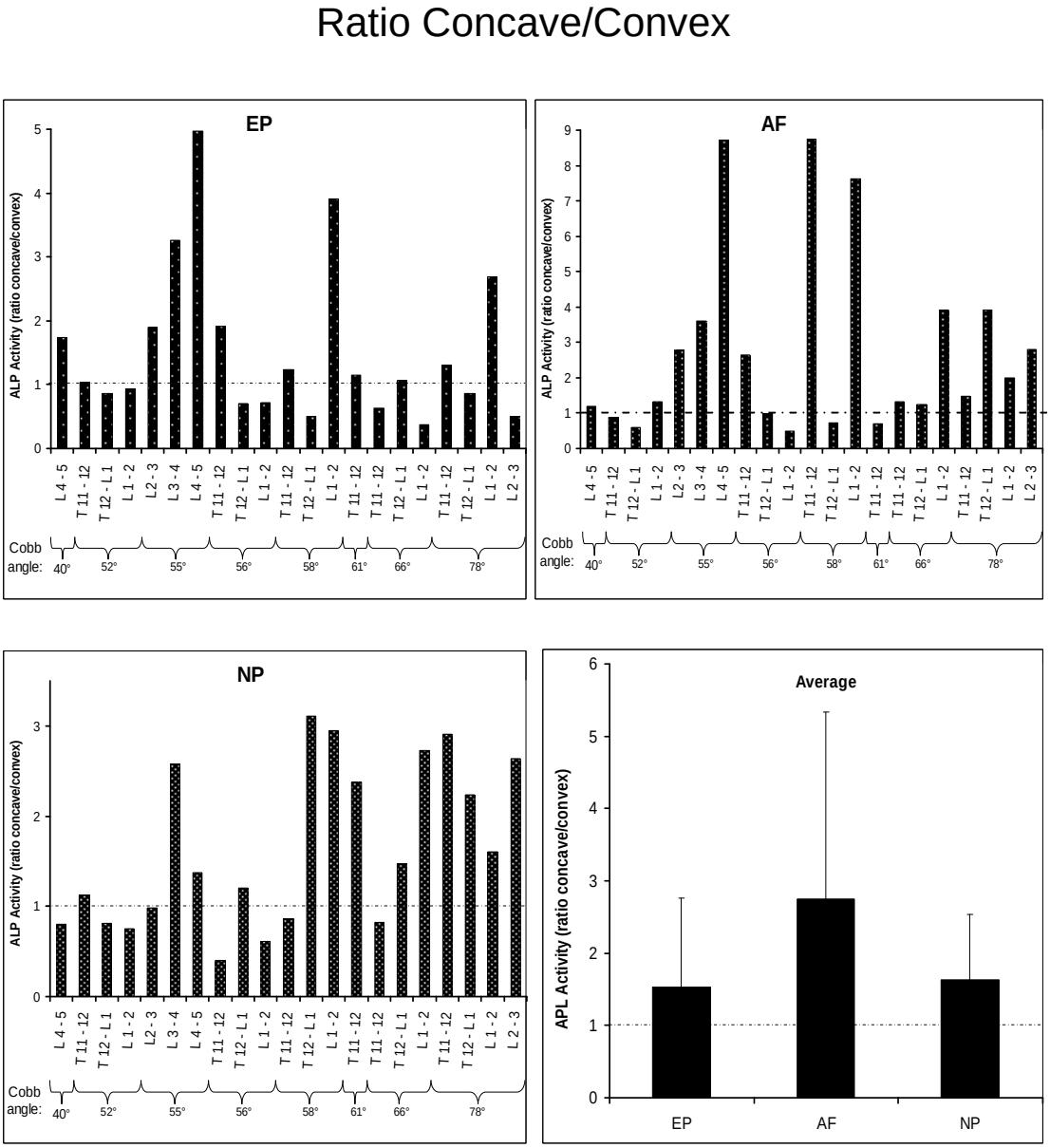

Figure 22: **Biochemical analysis of the alkaline phosphatase activity in scoliotic intervertebral discs – ratios in concave versus convex sides**. Figure represents the alkaline phosphatase (ALP) activity in scoliotic intervertebral discs (IVDs) in ratios of concave versus convex side of the disc. The four graphs represent the ratios in the endplate (EP), annulus fibrosus (AF), nucleus pulposus (NP), and averaged in the three types of IVD tissue.

The ratios related to the calcium concentration (Fig. 23) showed the highest concave prevalence in the EP in the T11–T12 disc of the patient with the 56º Cobb angle. The highest convex prevalence was detected in the L2–L3 disc of the patient with the largest Cobb angle (78º), followed by the disc of the patients with the smallest Cobb angle (40º). In the AF, the highest concave prevalence in the calcium concentration was found in the L2–L3 disc of the patient with 78º Cobb angle and in the L4–L5 disc of the patient with 55º Cobb angle. The highest convex prevalence was detected in the T11–T12 disc of the patient with 66º Cobb angle and in the patient with the smallest Cobb angle (40º). In the NP, concave prevalence in the calcium concentration is observed in the patients with the smallest (40º) and with the largest (78º) Cobb angles. The variations in the calcium concentration ratios in the EP, AF and NP were not clearly correlated to the variations of the Cobb angle of the patients. The analysis of the variability between the discs extracted from one patient showed no consistent trends related to the disc level. In the EP, the discs of the patient with the largest Cobb angle (78º) had convex prevalence in the calcium concentration. However, in the discs from the other patients, there was no consistency pattern of variations. In the AF, the discs of the patient with 56º Cobb angle had convex prevalence in the calcium concentration, which more pronounced in the lower IVD levels of the spine. However, in the discs of the patient with 66º Cobb angle which also had convex prevalence, it was more pronounced in the higher IVD levels in the spine. In the NP, although the discs of the patient with the largest Cobb angle (78º) demonstrated prevalence of the calcium concentration in the concave aspect, in the other patients this trend was not observed. The graph with the averaged ratios suggested a slight concave prevalence in EP and NP. However, the statistical test did not detect a significant trend, due to the large variability reflected by the large error bars.

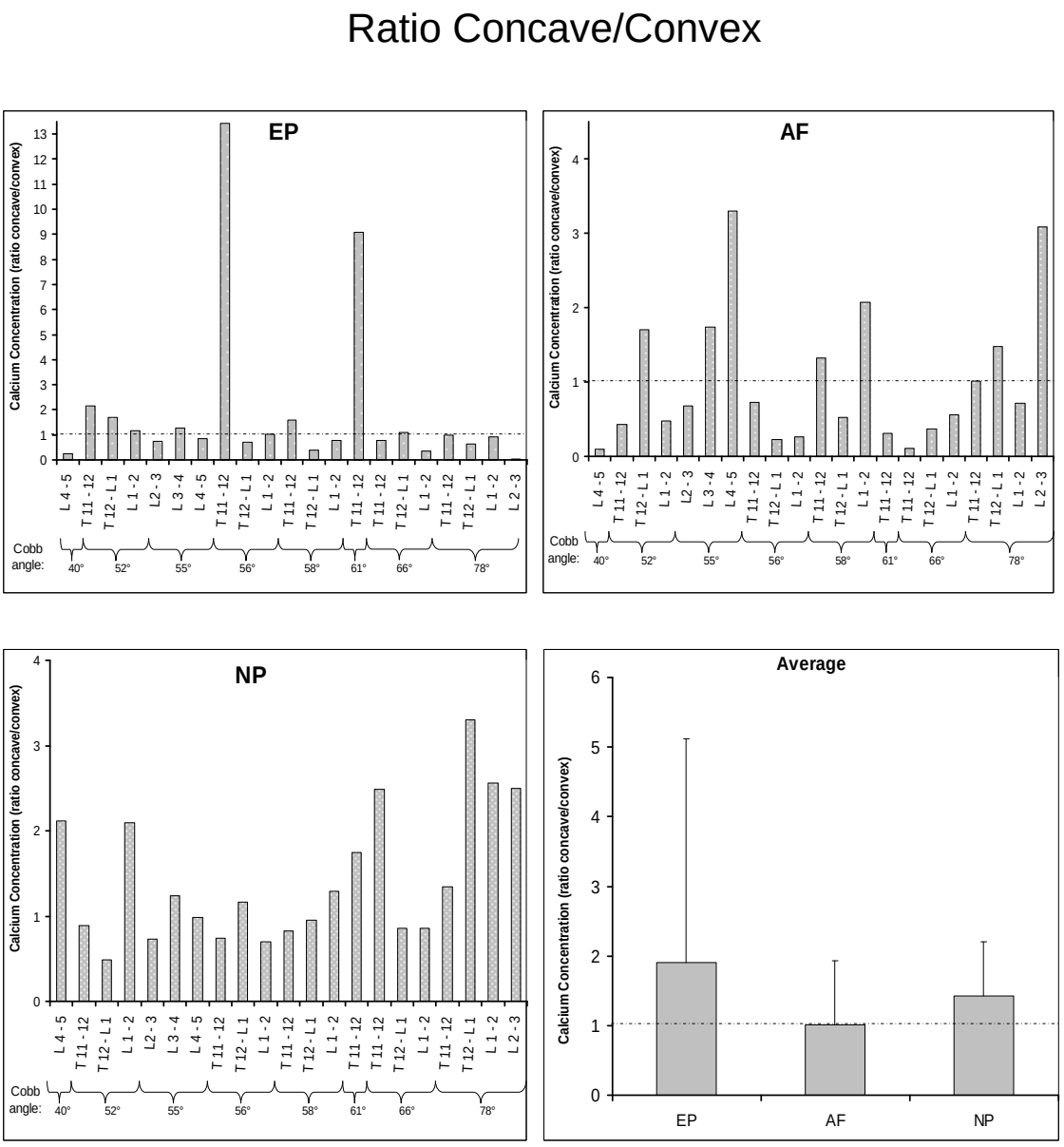

Figure 23: **Biochemical analysis of the calcium concentration in scoliotic intervertebral discs – ratios in concave versus convex sides**. Figure represents the calcium concentration in scoliotic intervertebral discs (IVDs) in ratios of concave versus convex side of the disc. The four graphs represent the ratios in the endplate (EP), annulus fibrosus (AF), nucleus pulposus (NP), and averaged in the three types of IVD tissue.

The ratios reflecting Pi concentration in scoliotic IVDs (Fig. 24) showed the highest concave prevalence in the EP in the T11–T12 disc of the patient with 56º Cobb angle, whereas the highest convex prevalence was found in the L2–L3 disc of the patient with the largest Cobb angle (78º). In the patient with the smallest Cobb angle (40º) no prevalence in either part was observed. In the AF, the highest concave prevalence was found in the disc of the patient with the smallest Cobb angle (40º), as well as in the T12–L1 disc of the patient with 52º Cobb angle. The highest convex prevalence in the Pi concentration was detected in the L1– L2 disc of the patient with 56º Cobb angle and in the T12–L1 disc of the patient with 58º Cobb angle. In the NP, the highest concave prevalence was found in the T12–L1 disc of the patient with 52º Cobb angle, whereas the highest convex prevalence was detected in the T11–T12 disc of the patient with 56º Cobb angle, as well as in the disc of the patient with the smallest Cobb angle (40º). Thus, the variations in the Pi concentration ratios in the EP, AF and NP were not clearly correlated to the variations in the Cobb angle of the patients. The analysis of the variations in Pi concentration in the discs extracted from one patient did not show a consistent trend of correlation with the disc level. In the EP, the discs of the patient with 58º Cobb angle demonstrated a tendency of convex prevalence, however, in all other patients there was no clear pattern of prevalence. In the AF, the discs of the patients with 56º Cobb angle demonstrated convex prevalence. The discs of the patient with 66º Cobb angle showed convex prevalence with a decreasing magnitude in the lower IVD levels. In NP there was no obvious pattern of variation. The average values of the ratios for the EP, AF and NP of the scloiotic IVDs suggested a possible trend towards concave prevalence in the Pi concentration. However, the error bars were large, reflecting the large individual variability, and statistical analysis did not detect any significant trend.

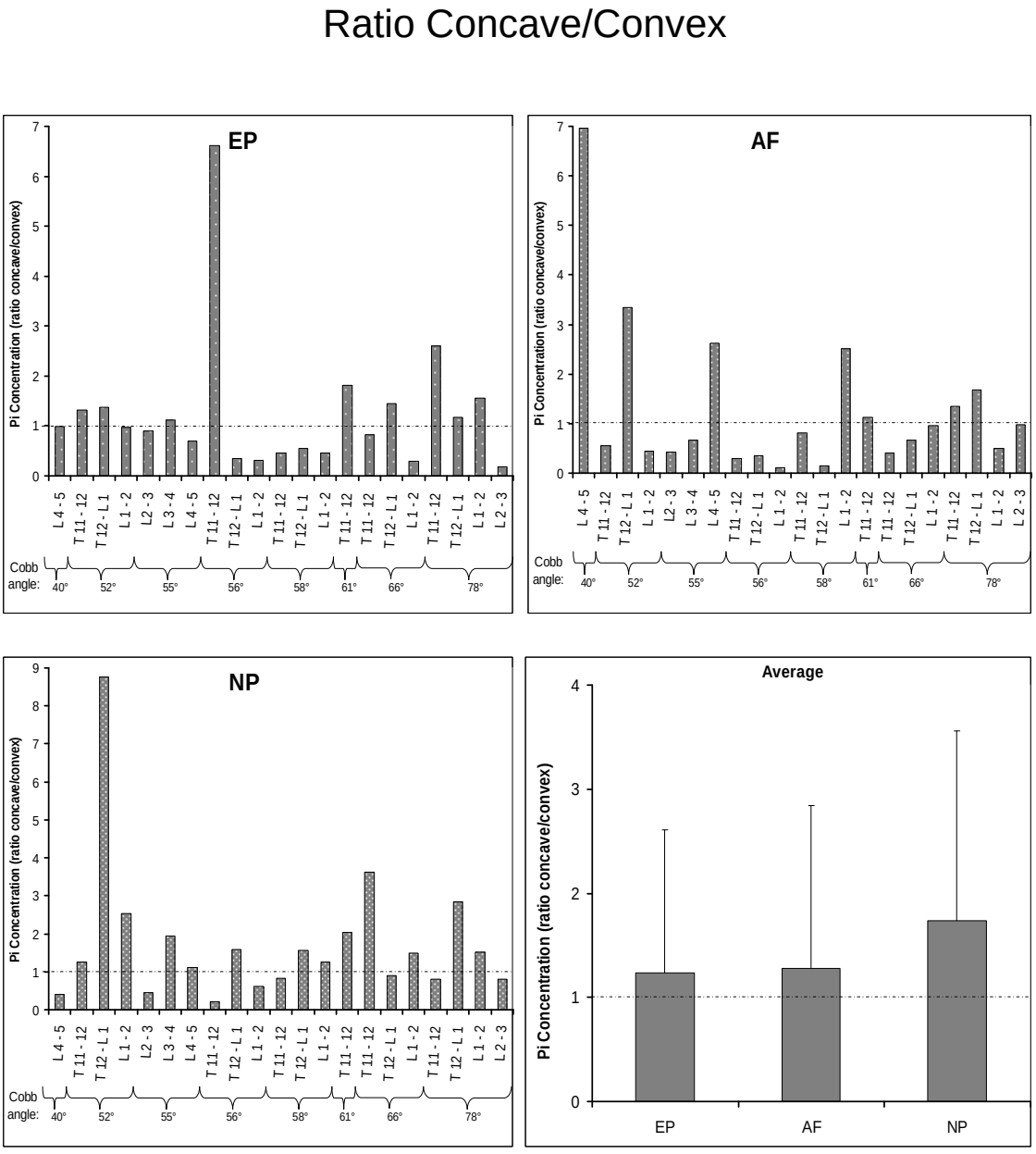

Figure 24: **Biochemical analysis of the Pi concentration in scoliotic intervertebral discs – ratios in concave versus convex sides**. Figure represents the inorganic phosphate (Pi) concentration in scoliotic intervertebral discs (IVDs) in ratios of concave versus convex side of the disc. The four graphs represent the ratios in the endplate (EP), annulus fibrosus (AF), nucleus pulposus (NP), and averaged in the three types of IVD tissue.

3. Visualization of Type X Collagen

The type X collagen has been associated with the calcification during the process of endochondral ossification. For this reason, an immunohistochemical analysis of all IVDs was performed in order to test whether the type X collagen can be detected and visualized in the calcifying IVD tissue.

The immunohistochemical analysis of the degenerative discs was performed in comparison with the control discs (Figure 25). The immunohistochemical analysis of the scoliotic IVDs was also performed in comparison with the control IVDs (Figure 26). The type X collagen in the IVD tissues in both degenerative and scoliotic IVDs was visualized as brown staining.

The staining for type X collagen in degenerative IVDs was present in all three morphological types of IVD tissue – EP, AF and NP. However, in the control non-diseased IVD tissue the staining for type X collagen was not detected at any site in the IVD tissue (EP, AF and NP). In scoliotic IVDs, the staining for type X collagen was also present in all three morphological types of IVD tissue (EP, AF and NP). The staining for type X collagen was positive in both concave and convex parts of the scoliotic IVDs. In the control non-diseased IVD tissue the staining for type X collagen was not detected.

The immunostaining for type X collagen also demonstrated the histo-morphological location of the type X collagen in the IVD tissue. The intensity of staining was highest around the cellular constituents of the tissue, which are presumably the source of type X collagen synthesis. In the tissue zones that are more remote from the cells, the intensity of the staining for type X collagen was lower.

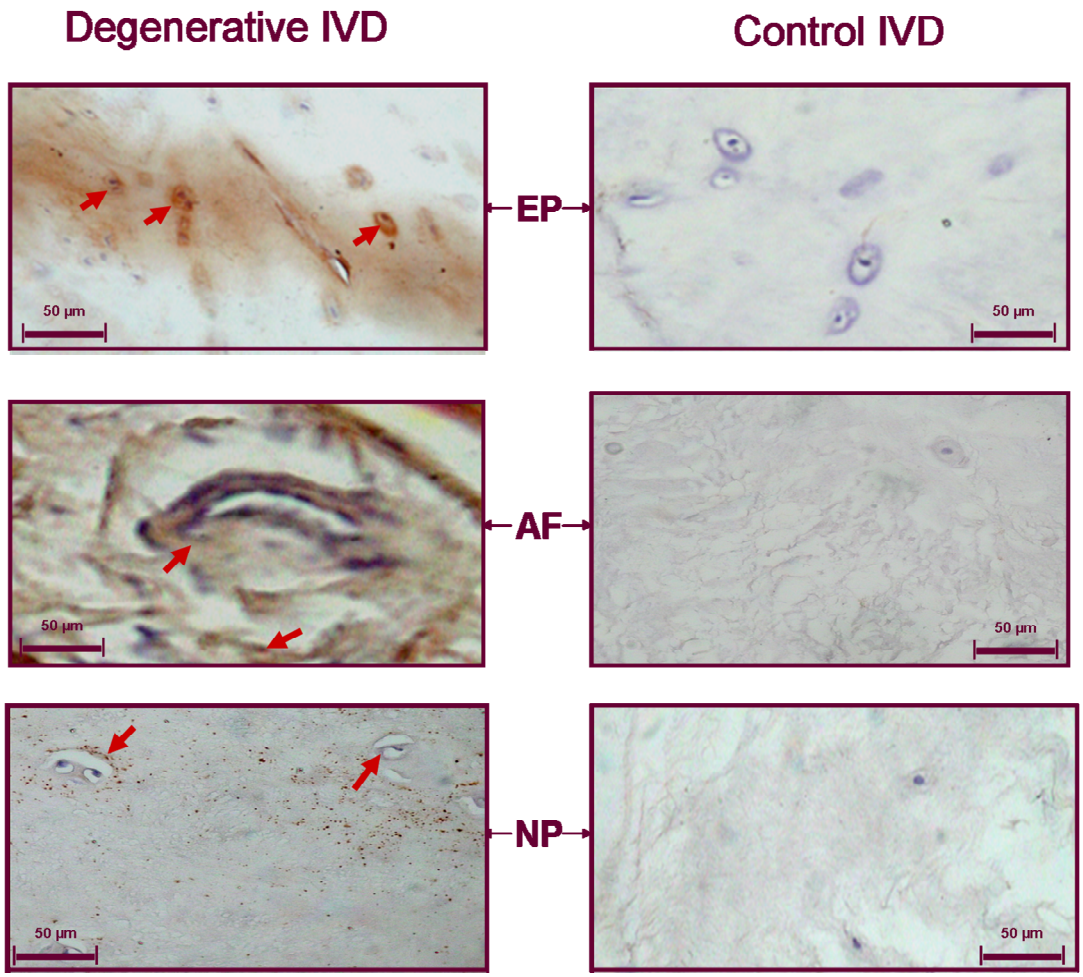

Figure 25: **Immunohistochemical analysis of type X collagen expression in degenerative intervertebral discs**. Figure represents typical images of immunohistochemical analysis for type X collagen in degenerative compared to control intervertebral disc tissues. The brown stain represents the type X collagen, which was detected predominantly in the pericellular space (indicated by res arrows), whereas the purple stain achieved by hematoxylin represents nuclei of the cells and other basophilic tissue constituents. The microscopic magnification is 200 times. IVD: intervertebral disc; EP: cartilage endplate; AF: annulus fibrosus; NP: nucleus pulposus.

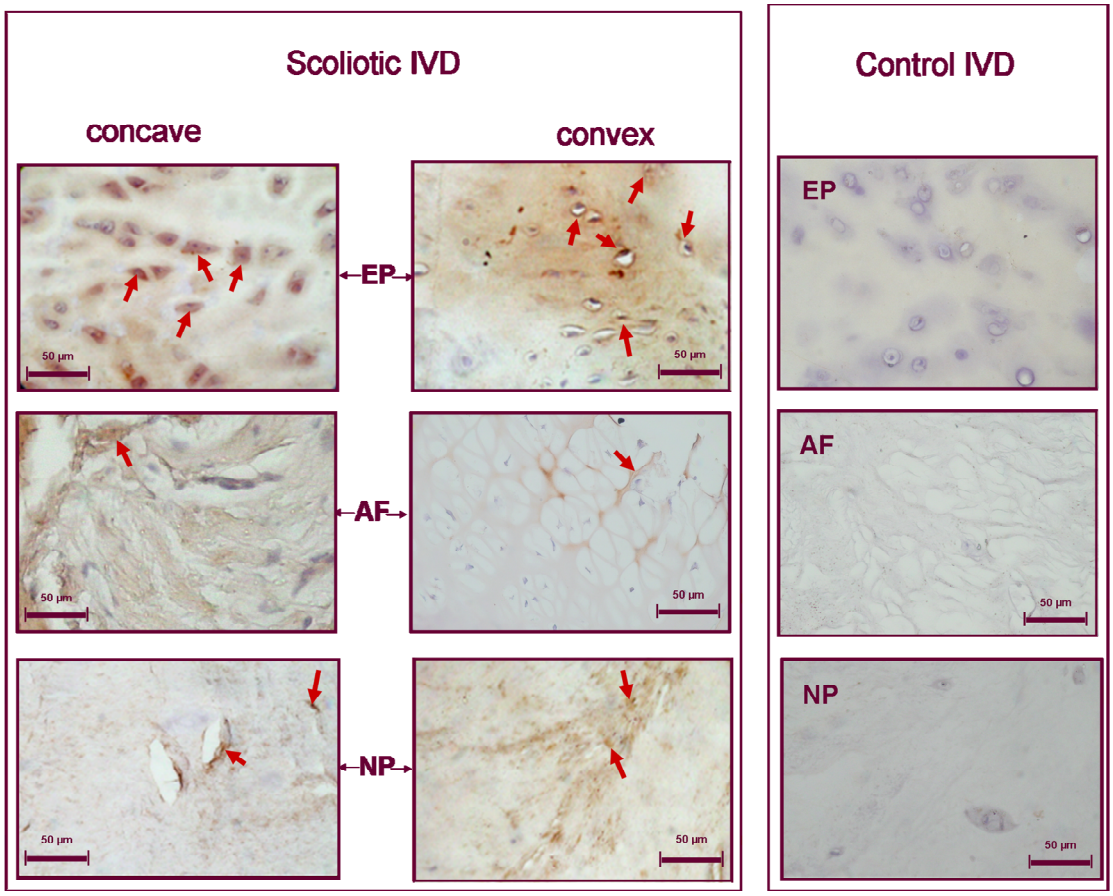

Figure 26: **Immunohistochemical analysis of type X collagen expression in scoliotic intervertebral discs**. Figure represents typical images of immunohistochemical analysis for visualization of type X collagen in scoliotic compared to control intervertebral disc tissues. The brown stain represents the type X collagen, which was detected predominantly in the pericellular space (indicated by res arrows), whereas the purple stain achieved by hematoxylin represents nuclei of the cells and other basophilic tissue constituents. The microscopic magnification is 200 times. IVD: intervertebral disc; EP: cartilage endplate; AF: annulus fibrosus; NP: nucleus pulposus.

4. Comparative Analysis of the Type X Collagen Expression in the Concave and Convex Parts of the Scoliotic Intervertebral Discs

In order to compare the level of type X collagen expression in the concave and convex aspects of the scoliotic IVDs, the results obtained from the immunoblotting experiments are represented as ratios of the concave versus the convex part of the disc (Figure 27). The ratios above 1.25 demonstrate a prevalence of the concave part, the ratios below 0.75 show a prevalence of the convex part, whereas the ratios between 0.75 and 1.25 indicate no prevalence in type X collagen expression in either concave or convex aspects of the scoliotic IVDs. In order to detect a possible influence of the degree of the scoliotic deformity, the concave/convex ratios in the EP, AF and NP of the scoliotic IVDs are arranged according to the patient's Cobb angle.

In the EP, the highest concave prevalence of the type X collagen was found in the L2–L3 disc of the patient with 55º Cobb angle and in the T11–T12 disc of the patient with 58º Cobb angle. The highest prevalence of the type X collagen in the convex part of the EP was found in the L2–L3 disc of the patient with the largest Cobb angle (78º), followed by the disc T12– L1 of the same patient and the disc T11–T12 of the patient with 56º Cobb angle. The patient with the smallest Cobb angle (40º) showed no prevalence of the type X collagen expression in either part of the disc. In the AF, the highest concave prevalence of type X collagen was found in the disc of the patient with the smallest Cobb angle (40º). The L1-L2 disc of patient with the largest Cobb angle (78º) demonstrated a pronounced convex prevalence, as well as discs T11-T12 and L1-L2 of the patients with 52º and 58º Cobb angles, respectively. In the NP, the highest concave prevalence of type X collagen was detected in the T11–T12 disc of the patient with 52º Cobb angle. The highest convex prevalence was found in all discs of the patient with 55º Cobb angle. The patient with the smallest Cobb angle

(40º) showed no prevalence in type X collagen in either aspect of the disc, whereas the NP of the patient with the largest Cobb angle (78º) had predominantly convex prevalence of type X collagen (except of the L2–L3 disc). These observations suggested that the variations in the concave/convex ratios for type X collagen in the EP, AF and NP were not clearly correlated to the variations of the patient's Cobb angle.

In the EP, the analysis of the concave/convex ratios of the discs extracted from one patient showed wide variability and no consistent trends towards concave or convex prevalence of type X collagen. In the AF, the discs of the patients with 56º and 66º Cobb angles demonstrated concave prevalence, whereas the discs of the patients with the largest Cobb angle (78º) showed predominantly convex prevalence of type X collagen. In the NP, the discs of the patient with 58º Cobb angle demonstrated a concave prevalence of type X collagen, whereas the discs of the patients with 55º and 56º Cobb angles had convex prevalence of type X collagen. In the patient with the largest Cobb angle (78º) the three upper discs also demonstrated a convex prevalence of type X collagen, with a decreasing magnitude towards the lower IVD levels in the spine. Thus, the analysis of the variability in type X collagen expression between the IVDs extracted from one patient did not show consistent trends towards either concave or convex prevalence. Also, an obvious influence of the IVD level in the spine was not detected.

The average values of type X collagen ratios in the EP and AF of scoliotic IVDs suggested a possible tendency towards concave prevalence, with a higher magnitude in the AF, whereas in the NP no prevalence was observed. The error bars in all three graphs were large, reflecting the large individual variability. The Non-parametric Wilcoxon Signed Rank Test did not detect statistical significance of any possible trend.

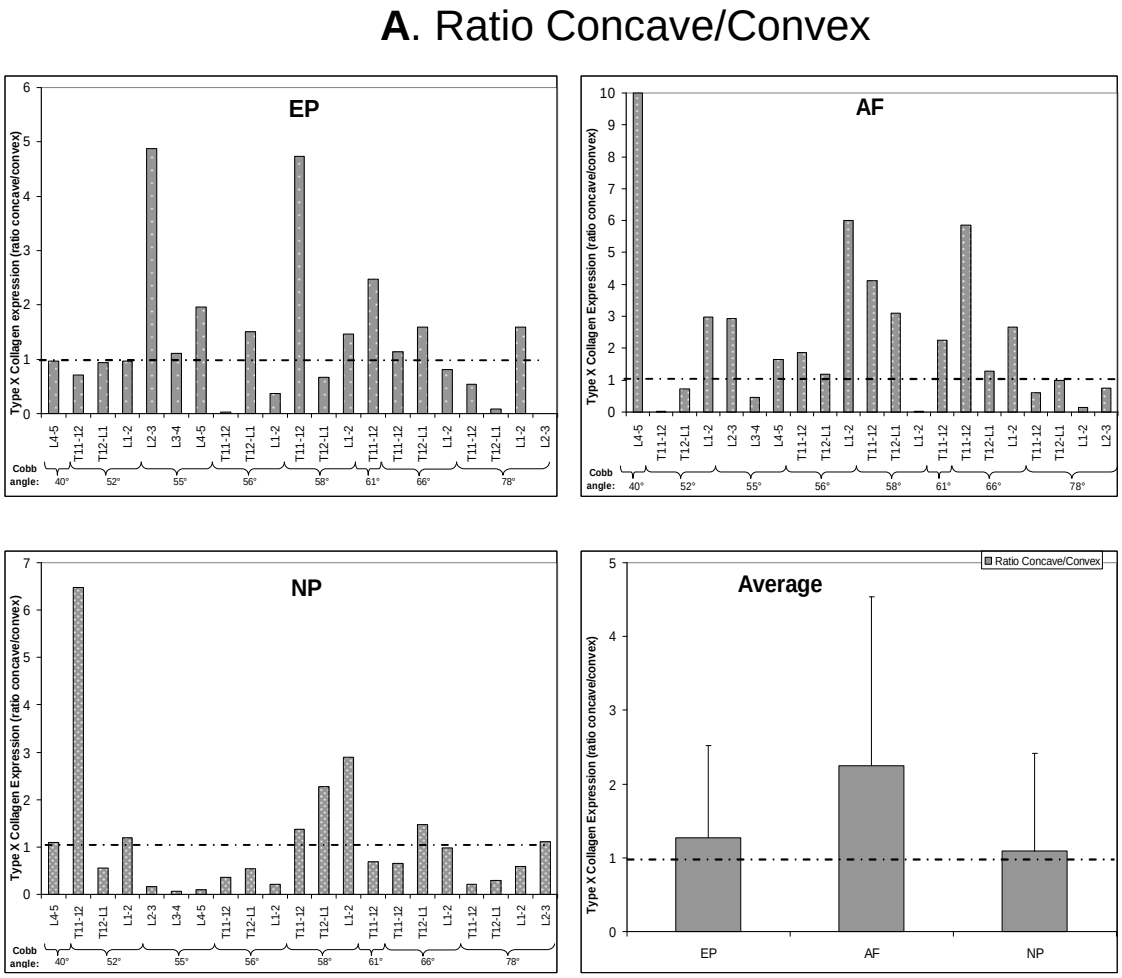

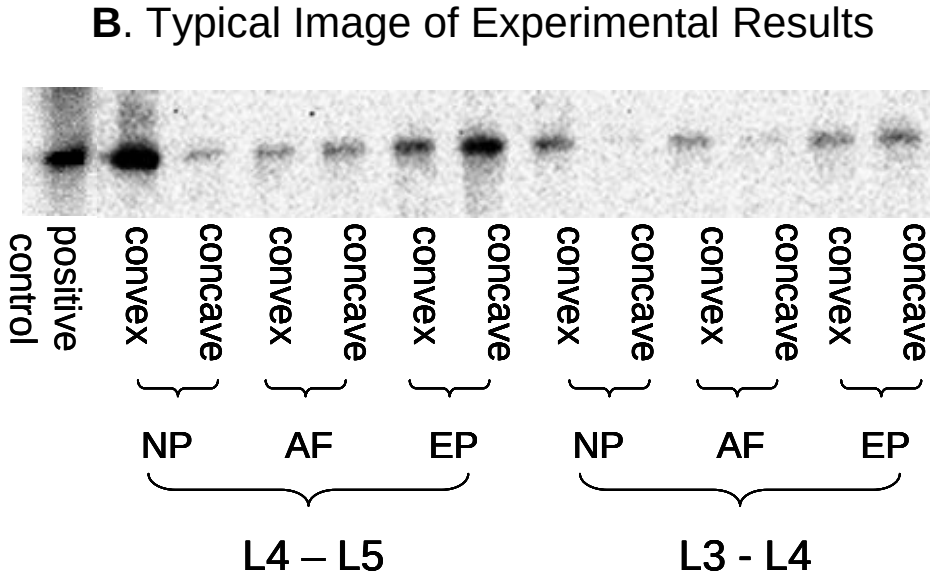

Figure 27: **Immunoblotting for type X collagen in scoliotic intervertebral discs**: **A.)** Ratios in the concave versus convex parts of the discs; **B.)** Typical image of experimental results (discs L3 – L4 and L4 – L5 of the patient with 55º Cobb angle).

IV. DISCUSSION

1. Calcification – Cause or Consequence of Intervertebral Disc Damage

In terms of studying the calcification process the components involved in apatite formation, such as the ALP, calcium and Pi, are of a particular interest. Their levels in tissues can be used as markers of the calcification process.

The importance of ALP activity for efficient endochondral ossification is emphasized in several studies (H. C. Anderson, 1995; H. C. Anderson, Garimella, & Tague, 2005). For instance, in a study of cartilage and bone mineralization in alkaline phosphatase-deficient mice (H. C. Anderson, et al., 2004), the mineral density in newly formed bone and growth plate cartilage matrix was significantly decreased. Within the matrix vesicles (MVs) of the growth plate the mineral crystals were initiated, however, their proliferation was insufficient to ensure mineral nucleation and growth beyond the vesicle membrane. This phenomenon was related to the excess of PPi found in the extracellular fluid around MVs as a result of the compromised ALP activity. The diseased condition in alkaline phosphatase-deficient mice was found to be very similar to the one in human hypophosphatasia, which is a heritable disease characterized by ALP deficiency (Mumm, Jones, Finnegan, & Whyte, 2001) resulting in severe hypomineralization of growth plates and bones (H. C. Anderson, Hsu, Morris, Fedde, & Whyte, 1997).

1.1. Calcification and Intervertebral Disc Damage in Degenerative Disc Disease

The question whether calcification observed in different types of IVD tissue (EP, AF and NP) is a cause or a consequence of the disc degeneration is widely discussed in the scientific literature.

In a study of degenerative diseases of vertebral column, the IVD calcification is considered to be a complication resulting from the disc degeneration process and a first step towards a subsequent IVD ossification (Resnick, 1985). In another study of the distribution of phagocytic cells in normal and degenerated IVDs, the presence of phagocytic cells in the tissue of degenerative human IVDs has been found to be most abundant in the NP tissue (Nerlich, Weiler, Zipperer, Narozny, & Boos, 2002). This study also confirmed that these phagocytic cells were derived from the disc cells via transformation and were involved in the phagocytosis of the disc's extracellular matrix (ECM), thus promoting the disc degeneration. A correlation between the abundance of phagocytic cells and enhanced ECM calcification was observed particularly in the EP.

Many other published studies, however, consider the ECM calcification to be causative or at least promoting the process of IVD degeneration. For instance, a study of the disc nutrition in relation to its degeneration emphasizes that disc cells depend on diffusion for their nutrient supply and metabolic waste removal (J. P. Urban, et al., 2004). This diffusion can be disturbed by EP calcification which subsequently leads to impaired cell viability, disturbed ECM production, increased ECM degradation, and thus to disc degeneration. A study of the relationship between cartilage end-plate calcification and disc degeneration has concluded that the EP calcification promotes disc degeneration in an experimental model of cervical disc degeneration in rabbits, and found a positive correlation between the magnitude of EP calcification and the degree of IVD degeneration (Peng, Shi, Shen, Wang, & Jia, 1999). A study of disc calcification in ageing sheep considers that calcification may be associated with proteoglycan degradation and suggests that IVD calcification may be a preceding or predisposing factor to disc degeneration (Melrose, et al., 2009).

In general, there is no scientific consensus on the question whether the calcification observed in degenerative IVDs is a cause or a consequence of disc degeneration. Many studies simply state that calcification and disc degeneration are associated and can be observed concomitantly (Gruber, et al., 2005). Whether the EP calcification causes disc degeneration by disturbing the disc metabolism, or alternatively whether degenerative changes in IVD tissue cause alterations in its physical and mechanical environment and lead to mineral deposition in the ECM, is still not clear (J. P. Urban, et al., 2004).

1.2. Calcification and Intervertebral Disc Damage in Adolescent Idiopathic Scoliosis

Abnormal mechanical loading is a characteristic of scoliotic IVDs and is a result of the scoliotic deformity. Its role in the IVD calcification process observed in scoliotic discs has been studied most extensively in the EP of scoliotic discs, which have been shown to be the most heavily calcified zone of the IVD. A study of the calcification of growth plate cartilage as a result of compressive force has demonstrated that calcification can be induced by abnormal loads in growth cartilages (Klein-Nulend, Veldhuijzen, & Burger, 1986). Another study of the histology and pathology of the human IVD has detected the consistent presence of mineral deposits in the cartilage EP of scoliotic IVDs and in some cases in the disc itself (Roberts, et al., 2006). The EP calcification has been described to occur at the edges of the cells and subsequently to spread around the whole cell and beyond into the ECM (Roberts, et al., 1993). The same study also detected reduced proteoglycan and as a result decreased water content in scoliotic IVDs compared to control IVDs from autopsy specimens. The decrease was more pronounced toward the concavity of the scoliotic

curve. This observation gives rise to the expectation for a difference in calcification markers between concave and convex parts of scoliotic discs, as the decrease in water content would relatively increase the concentration of calcium and Pi ions, thus providing better conditions for their precipitation and mineral formation. In such a case the concave part of the scoliotic IVDs would be expected to exhibit higher levels of calcification markers. On the other hand, another study has stated that the proteoglycan molecules and particularly their chondroitin sulfate chains are able to bind calcium ions, thus increasing the local concentration of calcium which presumably would enhance mineral formation (Poole, Matsui, Hinek, & Lee, 1989). In such a case the convex part of the scoliotic IVDs would be expected to show higher levels of calcification markers, given that the reduction in proteoglycan content is less pronounced in the convex aspect of the scoliotic curve. Consistent with this expectation, a study of the transport into scoliotic IVDs has demonstrated that the calcification pattern in scoliotic discs is asymmetric with little endplate calcification on the concave side of the disc and extensive calcification on the convexity. The same study also has detected a similarly altered pattern of the nutrient transport in scoliotic discs and have concluded that the reduction in solute transport, resulting from the increased endplate calcification, is secondary to the scoliotic deformity and probably arises as a consequence of the altered mechanical loading of the scoliotic disc (M. R. Urban, Fairbank, Etherington, et al., 2001). Thus, there is no generally accepted scientific consensus on whether the concave or convex part of scoliotic discs should be expected to be prevalent in terms of calcification marker levels. The present study also did not detect a consistent trend for increased levels of the calcification markers in either part of the scoliotic IVDs.

A study of the IVD composition in neuromuscular scoliosis emphasizes the importance of the magnitude of abnormal mechanical loading on scoliotic IVDs. The study reports that transport into the disc is most reduced at the apex of the curve, which is the most deformed and the most heavily loaded (M. R. Urban, Fairbank, Bibby, & Urban, 2001). This gives rise to the expectation that the severity of scoliotic deformity would have an impact on the extent of calcification process. Therefore, the Cobb angle which reflects the degree of scoliotic deformity should be associated with the magnitude of calcification marker levels. However, the present study did not detect a consistent correlation between the Cobb angle and the levels of calcification markers.

The elevation of the ALP activity, calcium, and Pi concentration observed in the present study is of similar magnitude in the discs of patients with DDD and AIS. This suggests the possibility of occurrence and development of a premature degenerative process in scoliotic IVDs. Such a possibility is supported by previous observations on EP calcification, which has been frequently observed in scoliotic IVDs. Many studies state that the EP calcification may be partly responsible for limiting solute diffusion through the disc and thus may contribute to the low number of viable cells in scoliotic IVDs and may eventually lead to cell death and possibly premature degeneration (Bibby, et al., 2002; Roberts, et al., 1996; J. P. Urban, et al., 2004; M. R. Urban, Fairbank, Etherington, et al., 2001). Other studies consider that the altered mechanical environment of the disc tissue is the primary cause of the premature degeneration observed in scoliotic discs. For instance, in a study of IVD degeneration in scoliosis versus physiological ageing, morphologic disc degeneration was observed approximately two decades earlier in scoliosis than in physiological ageing, and this phenomenon was related to the abnormal mechanical loading in

scoliotic IVDs (Bertram, et al., 2006). Other investigators also consider that abnormal loading especially in the concavity of scoliotic curves may accelerate disc degeneration (Buttermann & Beaubien, 2008). Another study based on magnetic resonance imaging in scoliosis patients suggests that degeneration of the deformed scoliotic discs may be similar to that in nondeformity patients (Buttermann & Mullin, 2008). A study of IVD changes in a rat model representing altered mechanics in scoliosis considers that impaired mobility may be a factor in disc degeneration in scoliosis (Stokes, McBride, & Aronsson, 2008). It has also been suggested that both, decreased EP permeability and abnormal physical loads may play a role in disease progression and degenerative changes in scoliotic discs (Bibby, Jones, Lee, Yu, & Urban, 2001). The investigators emphasize that disturbance in the supply of essential nutrients, such as oxygen and glucose, to the disc cells, as well as the inappropriate physical environment, inhibit the ability of the disc cells to synthesise and maintain the ECM. Thus, the impaired cellular activity and disturbed matrix turnover can lead to disc degeneration in scoliotic patients.

Regardless of the primary reason of degenerative changes, decreased cell viability is a common feature in both degenerative and scoliotic IVDs. In a study of the cellularity of annulus tissue of different pathologies, very little cellular activity in degenerate and scoliotic tissue is observed (Ford & Downes, 2002). The investigators suggested that cells in scoliotic and degenerate tissue are quiescent and remain in the G0 phase of the cell cycle for long periods of time. A study of the occurrence and regional distribution of apoptosis in scoliotic discs also draws a parallel between IVD degeneration and scoliosis, and considered that apoptotic mechanisms are involved in both pathologic conditions. The investigators observed an increased numbers of apoptotic cells in scoliotic IVDs, most prominent in the NP and the apex disc (Chen,

Fellenberg, Wang, Carstens, & Richter, 2005). A study of the disc morphology in health and disease also emphasizes that increased cell death, whether by necrosis or apoptosis, may be detected in degenerate discs and deformed discs in scoliosis (Roberts, 2002).

Similarities between disc degeneration and scoliosis can be also observed in the ECM. Proteoglycan and water contents are reduced (Roberts, et al., 1993), and matrix metalloproteinases 2 and 9 increased in both degenerative and scoliotic IVDs (Crean, Roberts, Jaffray, Eisenstein, & Duance, 1997). The grade of degenerative disc disease had a positive correlation with the increased levels of matrix metalloproteinases 2 and 9. In scoliosis, the levels of these enzymes demonstrated a differential expression across the scoliotic disc, with higher levels in the convex aspect of the disc.

In summary, it is very probable that the pathology in AIS is associated with premature IVD degeneration. What component of this complex pathology can be considered to play a primary causative role in the development of this degeneration still remains unclear. On the other hand, scoliotic deformity caused by advanced disc degeneration has been also described. It is often termed ‘‘de novo’’ scoliosis or type II scoliosis. This condition develops after skeletal maturity has been reached, and its proposed etiology involves accelerated IVD degeneration of the spine in middle age (Oskouian & Shaffrey, 2006).

It is important to mention that control discs used in the present study were extracted post mortem from a small group of age-matched donors. The control discs used in the analysis of degenerative IVDs were extracted from two donors and the control discs used in the analysis of scoliotic IVDs were extracted only from one donor. An increase in the number of control IVD donors may influence the study

findings. It may confirm detected tendencies and even potentiate the study power to uncover other trends that were not found when control discs from low number of individuals were used. On the other hand, an increase in the number of control IVD donors may possibly change the significance of present findings, rendering them more or less significant, or even change the study outcomes.

2. The Role of Type X Collagen in Intervertebral Disc Calcification

Type X collagen is a homotrimeric short-chain ECM molecule synthesized by hypertrophic chondrocytes in tissues undergoing endochondral ossification, such as growth plates. Genetic disorders affecting the gene encoding for human type X collagen, such as frameshift and missense mutations have been associated with the Schmid metaphyseal chondrodysplasia, which is an autosomal dominant skeletal disorder (Dharmavaram, et al., 1994; McIntosh, Abbott, Warman, Olsen, & Francomano, 1994; Wallis, et al., 1994; Warman, et al., 1993). Transgenic mice expressing mutant type X collagen are characterized by a disrupted hexagonal lattice collagen network in the pericellular space of hypertrophic chondrocytes, abnormal glycosaminoglycan and proteoglycan distribution, altered mineral deposition and skeletal deformities, suggesting that the intact type X collagen molecules are required for normal skeletal morphogenesis (Jacenko, et al., 2001; Jacenko, LuValle, & Olsen, 1993). However, the type X collagen-null mice do not demonstrate obvious skeletal abnormalities, suggesting that only the abnormal type X collagen molecules, but not the absence of type X collagen, can cause impairment in skeletal growth and development (Rosati, et al., 1994).

The precise function of type X collagen is yet unknown. It is widely accepted that spatial and temporal correlations exist between the synthesis of type X collagen

and the occurrence of endochondral ossification. Some investigators consider that type X collagen facilitates endochondral ossification by regulating matrix mineralization and compartmentalizing matrix components (Shen, 2005). Others suggest that matrix vesicle and alkaline phosphatase secretion are dependent on the type X collagen synthesis (Habuchi, Conrad, & Glaser, 1985). A study of the collagen expression, ultra-structural assembly, and mineralization in cultures of chicken embryo osteoblasts has shown that in chondrocyte cultures undergoing calcification the production of type X collagen increases concomitant with that of alkaline phosphatase, both of which immediately precede calcification (Gerstenfeld, et al., 1988). In a study of the interaction between collagen-binding proteins and different types of collagen, the investigators suggest that in growth plate cartilage the cartilage-specific collagens, such as type II and X collagens, bind to and cosediment with MVs. Alkaline phosphatase binds with high affinity to the native type X collagen, ensuring the interaction between the MVs and ECM and thus promoting the MV-mediated mineralization (Wu, et al., 1991). In a study of type X collagen supramolecular assembly and calcification, the investigators describe an existing correlation between the deposition of type X collagen within hypertrophic cartilage matrix and its subsequent calcification (Schmid, et al., 1990). Type II collagen fibrils in the hypertrophic matrix are described to be coated with type X before the tissue begins to calcify. The type X collagen distribution, however, extends beyond the classification front into the uncalcified cartilage. Similar distributions of type X have been observed by other investigators (Gibson, Bearman, & Flint, 1986; Grant, Sussman, & Balian, 1985; Kwan, Freemont, & Grant, 1986). A study of the cartilage macromolecules and the calcification of cartilage matrix describes that the type II collagen fibrils are

closely associated with type X collagen molecules and they remain associated at the time when the endochondral ossification occurs (Poole, et al., 1989).

In a study of the variation with age in the pattern of type X collagen expression in normal and scoliotic human IVDs the investigators describe type X collagen as a marker of hypertrophic chondrocytes, which has the property to bind calcium and thus is involved in the process of cartilage mineralization (Aigner, et al., 1998). On the other hand, in another study of hypertrophy, type X collagen synthesis and matrix calcification, an increase of type X collagen synthesis and calcium phosphate deposition has been observed, which occurs in response of increasing the calcium chloride concentration in chondrocyte cultures. Furthermore, the addition of calcium chloride to chondrocyte cultures increased the synthesis of type X collagen in a dose- and time-dependent manner (Schmid, Bonen, Luchene, & Linsenmayer, 1991). Thus, it is still unclear whether type X collagen is necessary for the occurrence of endochondral ossification or its synthesis simply coincides or is even promoted by the mineralization process.

The analysis of the ultrastructural morphology of the calcifying ECM in cartilage and bone has demonstrated that in the initial stage of the mineralization process the mineral is associated with the collagen fibrils (Bonucci, 1992). In the hypertrophic zone of growth plate cartilage, which is the zone of mineralization during the endochondral ossification, the type X collagen lattice constitute a considerable part of the collagen content. However, the nature of the interaction between the collagen fibrils and the mineral is not yet clarified. On the other hand, a study of calcification in ovine IVDs, which is a naturally occurring animal model of disc calcification, has demonstrated that in the ovine model of hydroxyapatite

deposition disease, there is no evidence that the IVD calcification in ageing sheep occurs by an endochondral ossification-like process (Melrose, et al., 2009).

2.1. The Role of Type X Collagen in Degenerative Disc Disease

Given that the cartilage EP of the IVD acts as a growth plate during the childhood and adolescence, it is logical to expect that type X collagen is expressed in the EP of children and adolescents before reaching the skeletal maturity. The first evidence for the occurrence of type X collagen in adult IVDs was provided by a study of the immunolocalization of type X collagen in human lumbar IVDs during ageing and degeneration (Boos, Nerlich, Wiest, von der Mark, & Aebi, 1997). The study has demonstrated that type X collagen is present more frequently in senile discs from individuals of more than seventy years of age with advanced stages of disc degeneration. A positive immunostaining for type X collagen has been detected in the NP of most of the mature IVDs and in the AF of a few discs from the same age group, as well as in EP, predominantly in samples with extensive cleft formation. The investigators suggest that type X collagen is re-expressed in late stages of IVD degeneration. These findings have been confirmed in another study of the age-related changes in human lumbar IVDs, which states that the NP chondrocytes express type X collagen in association with advanced age and degenerative disc lesions (Nerlich, Schleicher, & Boos, 1997). A study of the gene expression of types IX and X collagen in the lumbar disc has found a focal expressions of type X collagen in severe degenerated discs from adults (Xi, et al., 2004). This study associated the type X collagen expression with terminal stages of disc degeneration.

The type X collagen expression has been also studied in animal IVDs. A study of the type X collagen expression in chondrodystrophoid dog IVDs emphasizes type X collagen as one of the key molecules in ECM calcification (Itoh, et al., 2008). The

same study detected the presence of degeneration and calcification in the NP of the chondrodystrophoid dog. In this regard the investigators stated that the type X collagen might contribute to the development of the observed NP degeneration and calcification. Another study explored the role of prolonged upright posture in inducing degenerative changes in IVDs in rat lumbar spine (Liang, et al., 2008). In this study, immunostaining demonstrated a decreased level of type II collagen and an increased expression of type X collagen in both calcified and non-calcified zones of the EP in experimental compared to control animals. Another study of IVD degeneration during rat aging detected less collagen type II expression and more collagen type X expression in the calcified layer of the EP and in the NP of old than young rats (Zhang, et al., 2009). Thus, the increased type X collagen expression in IVD appears to correlate positively with the advancement of ageing and disc degeneration, even if the nature of this relationship is not yet clear.

2.2. The Role of Type X Collagen in Adolescent Idiopathic Scoliosis

The studies of type X collagen in EP are justified by the fact that in humans it functions as an epiphyseal growth plate and thus is associated with the growth and progression of the scoliotic curve (Roberts, et al., 1993). A study of the variation with age in the pattern of type X collagen expression in normal and scoliotic human IVDs demonstrated that type X collagen can be produced by the IVD cells, particularly the cells of the inner AF and the NP (Aigner, et al., 1998). The study indicated that with age or in scoliosis, some cells from the inner AF or from the NP of the disc can differentiate to the hypertrophic chondrocyte phenotype and produce type X collagen as component of the disc ECM. The investigators emphasized that type X collagen can be found at a far younger age in scoliotic than normal discs and suggested that the

type X collagen production might be the initiating event for the abnormal calcification described in aged and scoliotic IVDs. A similar idea has been inferred in a study of the patho-physiology of the IVD, where the investigators indicate that an increase in type X collagen is associated with calcification and particularly with abnormal EP calcification, which reduces its permeability and decreases nutrient supply (Bibby, et al., 2001).

A study of the type X collagen gene expression in the apical disc of idiopathic scoliosis demonstrates that the type X collagen mRNA levels in scoliotic IVDs are significantly higher than those of the normal IVDs (He, et al., 2004). The same study indicates that type X collagen is mainly distributed around the hypertrophic chondrocyte in the EP cartilage and the chondrocyte-like cells in the NP. The investigators also infer that the observed higher type X collagen gene expression in scoliotic patients might be a consequence of long term abnormal stress, which causes calcification of EP cartilage. In another study of type X collagen gene expression in the IVD of idiopathic scoliosis patients, the investigators observed significantly higher expression of type X collagen in the concave side of the apical disc than in its convex side (Lin, et al., 2004). This observation justifies the expectation that a difference in type X collagen levels might be found between the concave and convex parts of the IVDs analyzed in the present study.

In accordance with the previously conducted studies, the present study confirmed the presence of type X collagen in the different parts of the degenerative and scoliotic IVDs, whereas in the control non-diseased IVDs it was not detected. Whether a causal relationship exists between the pathology and the type X collagen expression and if so, what is the mechanism of this relationship, these questions still remain unclear. In the EP of scoliotic IVDs the presence of type X collagen can be

explained by the fact that in adolescents the EP cartilage possesses the function and the characteristics of a growth plate cartilage. However, regarding the AF and NP of scoliotic IVDs, as well as all the three analyzed parts of degenerative IVDs (EP, AF, and NP) such an explanation cannot be applied.

The semi-quantitative immunoblotting analysis of type X collagen in the concave and convex parts of scoliotic IVDs did not support the expectation of a significant difference in type X collagen abundance between the two sides of the scoliotic IVDs.

The comparison between the Von Kossa based histological analysis for mineral deposits and the immunohistochemical analysis for type X collagen did not indicate the existence of parallel between hypertrophic mineralization, which involves the presence of type X collagen, and degenerative disc mineralization. In general, data collected and analyzed in the present study did not find convincing evidence that degenerative IVD mineralization occurs under the pattern of hypertrophic mineralization and endochondral ossification.

The histological method used in the present study for visualization of mineralization process involved Von Kossa staining for mineral deposits. It should be mentioned that this type of staining generates black precipitates with phosphate ions and therefore is not specific for calcium ions. The biochemical analysis for calcium ions and phosphate ions in tissue extracts demonstrated a wide variety of calcium-to-phosphate ratios in different tissue samples. Some of these ratios considerably differed from the calcium-to-phosphate ratio in hydroxyapatite (HA), thus suggesting the presence of a mineralization process which might be quite different from the process of crystal HA formation. Certain discrepancies also exist between the staining patterns in the Western Blot analysis for type X collagen and the immunohistological images.

These discrepancies can be explained with the study design which involves the selection of a small tissue sample to represent the entire tissue mass (EP, AF or NP) of the whole IVD. However, it should be pointed out that IVD has heterogeneous structure even within each particular tissue type. Thus, the EP, AF and NP are not uniform throughout the whole IVD. Therefore, during the sampling process in a particular IVD the areas with the most pronounced pathological changes might have been selected for one type of analysis, while for another type of analysis the sample might consist of a less damaged piece of tissue. Also, while in some IVDs the areas with the most advanced pathologies might have been sampled in others they might have been missed.

In conclusion, it is important to mention that IVD mineralization is a focal process and therefore EP, AF and NP calcification of one disc is not homogenous. For the purposes of this study, different parts of IVD were used for different types of analyses. Thus, a few different pieces from each part were generated and used for different analyses. Given that IVD mineralization is not uniform and the analyses performed in the present study did not use entire IVDs, it is possible that the large heterogeneity observed in the study is due to sampling variation. While this may limit the relevance of the absolute values of mineralization markers, it does not negate the overall conclusions linking elevated levels of mineralization markers to both DDD and AIS.

3. Future Directions

Elucidation of the mechanisms of calcification in disc degeneration and scoliosis has possible implications in the development of future strategies for the prevention and treatment of DDD and AIS. In this regard some questions concerning

IVD mineralization that still remain without scientifically proven answers should be further addressed and clarified. For instance, calcification and degeneration are observed simultaneously in IVDs of patients with DDD. This suggests the possibility of an existing causal relationship between IVD calcification and degeneration. However, which of these two phenomena is the cause and which one is the consequence remains to be answered. While many studies suggest that EP calcification might cause degenerative changes in the disc by disturbing its nutrition, it is still possible that in AF and NP tissue calcification develops as a consequence of already initiated and progressing disc degeneration. Similarly, the possibility that IVD calcification in AIS may promote a process of premature disc degeneration should be further explored and confirmed. Also, the role of type X collagen in the process of disc mineralization and its relevance to DDD and AIS should be further studied, as it is not clear whether type X collagen is involved in the pathogenesis of these diseases, or is merely an indication of altered cell metabolism.

REFERENCES:

Adams, M. A., & Roughley, P. J. (2006). What is intervertebral disc degeneration, and what causes it? *Spine, 31*(18), 2151-2161.

Aigner, T., Gresk-otter, K. R., Fairbank, J. C., von der Mark, K., & Urban, J. P. (1998). Variation with age in the pattern of type X collagen expression in normal and scoliotic human intervertebral discs. *Calcif Tissue Int, 63*(3), 263-268.

Akeson, W. H., Woo, S. L., Taylor, T. K., Ghosh, P., & Bushell, G. R. (1977). Biomechanics and biochemistry of the intervertebral disks: the need for correlation studies. *Clin Orthop Relat Res*(129), 133-140.

Ali, S. Y., Sajdera, S. W., & Anderson, H. C. (1970). Isolation and characterization of calcifying matrix vesicles from epiphyseal cartilage. *Proc Natl Acad Sci U S A, 67*(3), 1513-1520.

Anderson, D. G., Li, X., & Balian, G. (2005). A fibronectin fragment alters the metabolism by rabbit intervertebral disc cells in vitro. *Spine, 30*(11), 1242-1246.

Anderson, H. C. (1989). Mechanism of mineral formation in bone. *Lab Invest, 60*(3), 320-330.

Anderson, H. C. (1995). Molecular biology of matrix vesicles. *Clin Orthop Relat Res*(314), 266-280.

Anderson, H. C., Garimella, R., & Tague, S. E. (2005). The role of matrix vesicles in growth plate development and biomineralization. *Front Biosci, 10*, 822-837.

Anderson, H. C., Hsu, H. H., Morris, D. C., Fedde, K. N., & Whyte, M. P. (1997). Matrix vesicles in osteomalacic hypophosphatasia bone contain apatite-like mineral crystals. *Am J Pathol, 151*(6), 1555-1561.

Anderson, H. C., Sipe, J. B., Hessle, L., Dhanyamraju, R., Atti, E., Camacho, N. P., et al. (2004). Impaired calcification around matrix vesicles of growth plate and bone in alkaline phosphatase-deficient mice. *Am J Pathol, 164*(3), 841-847.

Antoniou, J., Goudsouzian, N. M., Heathfield, T. F., Winterbottom, N., Steffen, T., Poole, A. R., et al. (1996). The human lumbar endplate. Evidence of changes in biosynthesis and denaturation of the extracellular matrix with growth, maturation, aging, and degeneration. *Spine, 21*(10), 1153-1161.

Balcerzak, M., Hamade, E., Zhang, L., Pikula, S., Azzar, G., Radisson, J., et al. (2003). The roles of annexins and alkaline phosphatase in mineralization process. *Acta Biochim Pol, 50*(4), 1019-1038.

Bernick, S., & Cailliet, R. (1982). Vertebral end-plate changes with aging of human vertebrae. *Spine (Phila Pa 1976), 7*(2), 97-102.

Bertram, H., Steck, E., Zimmerman, G., Chen, B., Carstens, C., Nerlich, A., et al. (2006). Accelerated intervertebral disc degeneration in scoliosis versus physiological ageing develops against a background of enhanced anabolic gene expression. *Biochem Biophys Res Commun, 342*(3), 963-972.

Beth Dawson, & Trapp, R. (2004). *Basic and Clinical Biostatistics* (Fourth Edition ed.): McGraw-Hill Medical Publisher.

Bibby, S. R., Fairbank, J. C., Urban, M. R., & Urban, J. P. (2002). Cell viability in scoliotic discs in relation to disc deformity and nutrient levels. *Spine, 27*(20), 2220-2228; discussion 2227-2228.

Bibby, S. R., Jones, D. A., Lee, R. B., Yu, J., & Urban, J. P. G. (2001). The pathophysiology of the intervertebral disc. *Joint Bone Spine, 68*(6), 537-542.

Bonucci, E. (1992). Comments on the ultrastructural morphology of the calcification process: an attempt to reconcile matrix vesicles, collagen fibrils, and crystal ghosts. *Bone Miner, 17*(2), 219-222.

Boos, N., Nerlich, A. G., Wiest, I., von der Mark, K., & Aebi, M. (1997). Immunolocalization of type X collagen in human lumbar intervertebral discs during ageing and degeneration. *Histochem Cell Biol, 108*(6), 471-480.

Boos, N., Weissbach, S., Rohrbach, H., Weiler, C., Spratt, K. F., & Nerlich, A. G. (2002). Classification of age-related changes in lumbar intervertebral discs: 2002 Volvo Award in basic science. *Spine, 27*(23), 2631-2644.

Borg, T. K., Runyan, R. B., & Wuthier, R. E. (1978). Correlation of freeze-fracture and scanning electron microscopy of epiphyseal chondrocytes. *Calcif Tissue Res, 26*(3), 237-241.

Borras, T., & Comes, N. (2009). Evidence for a calcification process in the trabecular meshwork. *Exp Eye Res, 88*(4), 738-746.

Buckwalter, J. A. (1995). Aging and degeneration of the human intervertebral disc. *Spine, 20*(11), 1307-1314.

Buttermann, G. R., & Beaubien, B. P. (2008). In vitro disc pressure profiles below scoliosis fusion constructs. *Spine (Phila Pa 1976), 33*(20), 2134-2142.

Buttermann, G. R., & Mullin, W. J. (2008). Pain and disability correlated with disc degeneration via magnetic resonance imaging in scoliosis patients. *Eur Spine J, 17*(2), 240-249.

Castelein, R. M., van Dieen, J. H., & Smit, T. H. (2005). The role of dorsal shear forces in the pathogenesis of adolescent idiopathic scoliosis--a hypothesis. *Med Hypotheses, 65*(3), 501-508.

Chanchairujira, K., Chung, C. B., Kim, J. Y., Papakonstantinou, O., Lee, M. H., Clopton, P., et al. (2004). Intervertebral disk calcification of the spine in an elderly population: radiographic prevalence, location, and distribution and correlation with spinal degeneration. *Radiology, 230*(2), 499-503.

Chen, B., Fellenberg, J., Wang, H., Carstens, C., & Richter, W. (2005). Occurrence and regional distribution of apoptosis in scoliotic discs. *Spine (Phila Pa 1976), 30*(5), 519-524.

Christoffersen, J., & Landis, W. J. (1991). A contribution with review to the description of mineralization of bone and other calcified tissues in vivo. *Anat Rec, 230*(4), 435-450.

Crean, J. K., Roberts, S., Jaffray, D. C., Eisenstein, S. M., & Duance, V. C. (1997). Matrix metalloproteinases in the human intervertebral disc: role in disc degeneration and scoliosis. *Spine (Phila Pa 1976), 22*(24), 2877-2884.

Dharmavaram, R. M., Elberson, M. A., Peng, M., Kirson, L. A., Kelley, T. E., & Jimenez, S. A. (1994). Identification of a mutation in type X collagen in a family with Schmid metaphyseal chondrodysplasia. *Hum Mol Genet, 3*(3), 507-509.

Duance, V. C., Crean, J. K., Sims, T. J., Avery, N., Smith, S., Menage, J., et al. (1998). Changes in collagen cross-linking in degenerative disc disease and scoliosis. *Spine, 23*(23), 2545-2551.

Feng, H., Danfelter, M., Stromqvist, B., & Heinegard, D. (2006). Extracellular matrix in disc degeneration. *J Bone Joint Surg Am, 88 Suppl 2*, 25-29.

Ferguson, S. J., Ito, K., & Nolte, L. P. (2004). Fluid flow and convective transport of solutes within the intervertebral disc. *J Biomech, 37*(2), 213-221.

Ford, J. L., & Downes, S. (2002). Cellularity of human annulus tissue: an investigation into the cellularity of tissue of different pathologies. *Histopathology, 41*(6), 531-537.

Gebhard, S., Poschl, E., Riemer, S., Bauer, E., Hattori, T., Eberspaecher, H., et al. (2004). A highly conserved enhancer in mammalian type X collagen genes drives high levels of tissue-specific expression in hypertrophic cartilage in vitro and in vivo. *Matrix Biol, 23*(5), 309-322.

Gerstenfeld, L. C., Chipman, S. D., Kelly, C. M., Hodgens, K. J., Lee, D. D., & Landis, W. J. (1988). Collagen expression, ultrastructural assembly, and mineralization in cultures of chicken embryo osteoblasts. *J Cell Biol, 106*(3), 979-989.

Gibson, G. J., Bearman, C. H., & Flint, M. H. (1986). The immunoperoxidase localization of type X collagen in chick cartilage and lung. *Coll Relat Res, 6*(2), 163-184.

Girodias, J. B., Azouz, E. M., & Marton, D. (1991). Intervertebral disk space calcification. A report of 51 children with a review of the literature. *Pediatr Radiol, 21*(8), 541-546.

Grant, W. T., Sussman, M. D., & Balian, G. (1985). A disulfide-bonded short chain collagen synthesized by degenerative and calcifying zones of bovine growth plate cartilage. *J Biol Chem, 260*(6), 3798-3803.

Gruber, H. E., Ashraf, N., Kilburn, J., Williams, C., Norton, H. J., Gordon, B. E., et al. (2005). Vertebral endplate architecture and vascularization: application of micro-computerized tomography, a vascular tracer, and immunocytochemistry in analyses of disc degeneration in the aging sand rat. *Spine (Phila Pa 1976), 30*(23), 2593-2600.

Gruber, H. E., Gordon, B., Williams, C., Norton, H. J., & Hanley, E. N., Jr. (2007). Vertebral endplate and disc changes in the aging sand rat lumbar spine: cross-sectional analyses of a large male and female population. *Spine (Phila Pa 1976), 32*(23), 2529-2536.

Gruber, H. E., Johnson, T., Norton, H. J., & Hanley, E. N., Jr. (2002). The sand rat model for disc degeneration: radiologic characterization of age-related changes: cross-sectional and prospective analyses. *Spine (Phila Pa 1976), 27*(3), 230-234.

Habuchi, H., Conrad, H. E., & Glaser, J. H. (1985). Coordinate regulation of collagen and alkaline phosphatase levels in chick embryo chondrocytes. *J Biol Chem, 260*(24), 13029-13034.

Harrington, D., Anker, S. D., Chua, T. P., Webb-Peploe, K. M., Ponikowski, P. P., Poole-Wilson, P. A., et al. (1997). Skeletal muscle function and its relation to exercise tolerance in chronic heart failure. *J Am Coll Cardiol, 30*(7), 1758-1764.

Harrison, G., Shapiro, I. M., & Golub, E. E. (1995). The phosphatidylinositol-glycolipid anchor on alkaline phosphatase facilitates mineralization initiation in vitro. *J Bone Miner Res, 10*(4), 568-573.

Hayes, A. J., Benjamin, M., & Ralphs, J. R. (2001). Extracellular matrix in development of the intervertebral disc. *Matrix Biol, 20*(2), 107-121.

He, H. L., Wu, Z. H., Zhang, J. G., Wang, Y. P., Zhou, Y., Xu, Y. Q., et al. (2004). [Primary study on collagen X gene expression in the apical disc of idiopathic scoliosis]. *Zhonghua Yi Xue Za Zhi, 84*(20), 1681-1685.

Hsu, H. H. (1994). Mechanisms of initiating calcification. ATP-stimulated Ca- and Pi-depositing activity of isolated matrix vesicles. *Int J Biochem, 26*(12), 1351-1356.

Iatridis, J. C., MacLean, J. J., Roughley, P. J., & Alini, M. (2006). Effects of mechanical loading on intervertebral disc metabolism in vivo. *J Bone Joint Surg Am, 88 Suppl 2*, 41-46.

Itoh, H., Asou, Y., Hara, Y., Haro, H., Shinomiya, K., & Tagawa, M. (2008). Enhanced type X collagen expression in the extruded nucleus pulposus of the chondrodystrophoid dog. *J Vet Med Sci, 70*(1), 37-42.

Jacenko, O., Chan, D., Franklin, A., Ito, S., Underhill, C. B., Bateman, J. F., et al. (2001). A dominant interference collagen X mutation disrupts hypertrophic chondrocyte pericellular matrix and glycosaminoglycan and proteoglycan distribution in transgenic mice. *Am J Pathol, 159*(6), 2257-2269.

Jacenko, O., LuValle, P. A., & Olsen, B. R. (1993). Spondylometaphyseal dysplasia in mice carrying a dominant negative mutation in a matrix protein specific for cartilage-to-bone transition. *Nature, 365*(6441), 56-61.

Ketteler, M., & Floege, J. (2006). Calcification and the usual suspect phosphate: still guilty but there are other guys behind the scenes. *Nephrol Dial Transplant, 21*(1), 33-35.

Klein-Nulend, J., Veldhuijzen, J. P., & Burger, E. H. (1986). Increased calcification of growth plate cartilage as a result of compressive force in vitro. *Arthritis Rheum, 29*(8), 1002-1009.

Kopylov, P., Jonsson, K., Thorngren, K. G., & Aspenberg, P. (1996). Injectable calcium phosphate in the treatment of distal radial fractures. *J Hand Surg Br, 21*(6), 768-771.

Kwan, A. P., Freemont, A. J., & Grant, M. E. (1986). Immunoperoxidase localization of type X collagen in chick tibiae. *Biosci Rep, 6*(2), 155-162.

LeGeros, R. Z. (2002). Properties of osteoconductive biomaterials: calcium phosphates. *Clin Orthop Relat Res*(395), 81-98.

Liang, Q. Q., Zhou, Q., Zhang, M., Hou, W., Cui, X. J., Li, C. G., et al. (2008). Prolonged upright posture induces degenerative changes in intervertebral discs in rat lumbar spine. *Spine (Phila Pa 1976), 33*(19), 2052-2058.

Lin, Q., Wu, Z. H., Liu, Y., Wang, Y. P., Weng, X. S., Lin, J., et al. (2004). [Gene expression of type X collagen in the intervertebral disc of idiopathic scoliosis patients]. *Zhongguo Yi Xue Ke Xue Yuan Xue Bao, 26*(6), 696-699.

Matsuzawa, T., & Anderson, H. C. (1971). Phosphatases of epiphyseal cartilage studied by electron microscopic cytochemical methods. *J Histochem Cytochem, 19*(12), 801-808.

McIntosh, I., Abbott, M. H., Warman, M. L., Olsen, B. R., & Francomano, C. A. (1994). Additional mutations of type X collagen confirm COL10A1 as the Schmid metaphyseal chondrodysplasia locus. *Hum Mol Genet, 3*(2), 303-307.

Meakin, J. R., & Hukins, D. W. (2000). Effect of removing the nucleus pulposus on the deformation of the annulus fibrosus during compression of the intervertebral disc. *J Biomech, 33*(5), 575-580.

Meir, A. R., Fairbank, J. C., Jones, D. A., McNally, D. S., & Urban, J. P. (2007). High pressures and asymmetrical stresses in the scoliotic disc in the absence of muscle loading. *Scoliosis, 2*, 4.

Melrose, J., Burkhardt, D., Taylor, T. K., Dillon, C. T., Read, R., Cake, M., et al. (2009). Calcification in the ovine intervertebral disc: a model of hydroxyapatite deposition disease. *Eur Spine J, 18*(4), 479-489.

Miller, G. J., & DeMarzo, A. M. (1988). Ultrastructural localization of matrix vesicles and alkaline phosphatase in the Swarm rat chondrosarcoma: their role in cartilage calcification. *Bone, 9*(4), 235-241.

Mumm, S., Jones, J., Finnegan, P., & Whyte, M. P. (2001). Hypophosphatasia: molecular diagnosis of Rathbun's original case. *J Bone Miner Res, 16*(9), 1724-1727.

Mwale, F., Tchetina, E., Wu, C. W., & Poole, A. R. (2002). The assembly and remodeling of the extracellular matrix in the growth plate in relationship to mineral deposition and cellular hypertrophy: an in situ study of collagens II and IX and proteoglycan. *J Bone Miner Res, 17*(2), 275-283.

Narisawa, S., Frohlander, N., & Millan, J. L. (1997). Inactivation of two mouse alkaline phosphatase genes and establishment of a model of infantile hypophosphatasia. *Dev Dyn, 208*(3), 432-446.

Nerlich, A. G., Schleicher, E. D., & Boos, N. (1997). 1997 Volvo Award winner in basic science studies. Immunohistologic markers for age-related changes of human lumbar intervertebral discs. *Spine (Phila Pa 1976), 22*(24), 2781-2795.

Nerlich, A. G., Weiler, C., Zipperer, J., Narozny, M., & Boos, N. (2002). Immunolocalization of phagocytic cells in normal and degenerated intervertebral discs. *Spine (Phila Pa 1976), 27*(22), 2484-2490.

Noltenius, H., & Prescher, W. (1977). [Morphology of histological subgroups of Hodgkin's disease (author's transl)]. *Med Klin, 72*(39), 1579-1585.

Ornoy, A., & Langer, Y. (1978). Scanning electron microscopy studies on the origin and structure of matrix vesicles in epiphyseal cartilage from young rats. *Isr J Med Sci, 14*(7), 745-752.

Oskouian, R. J., Jr., & Shaffrey, C. I. (2006). Degenerative lumbar scoliosis. *Neurosurg Clin N Am, 17*(3), 299-315, vii.

Peng, B., Shi, Q., Shen, P., Wang, Y., & Jia, L. (1999). [The relationship between cartilage end-plate calcification and disc degeneration: an experimental study]. *Zhonghua Wai Ke Za Zhi, 37*(10), 613-616.

Ponseti, I. V., Pedrini, V., Wynne-Davies, R., & Duval-Beaupere, G. (1976). Pathogenesis of scoliosis. *Clin Orthop Relat Res*(120), 268-280.

Poole, A. R., Matsui, Y., Hinek, A., & Lee, E. R. (1989). Cartilage macromolecules and the calcification of cartilage matrix. *Anat Rec, 224*(2), 167-179.

Resnick, D. (1985). Degenerative diseases of the vertebral column. *Radiology, 156*(1), 3-14.

Roberts, S. (2002). Disc morphology in health and disease. *Biochem Soc Trans, 30*(Pt 6), 864-869.

Roberts, S., Evans, H., Trivedi, J., & Menage, J. (2006). Histology and pathology of the human intervertebral disc. *J Bone Joint Surg Am, 88 Suppl 2*, 10-14.

Roberts, S., Menage, J., Duance, V., Wotton, S., & Ayad, S. (1991). 1991 Volvo Award in basic sciences. Collagen types around the cells of the intervertebral disc and cartilage end plate: an immunolocalization study. *Spine, 16*(9), 1030-1038.

Roberts, S., Menage, J., & Eisenstein, S. M. (1993). The cartilage end-plate and intervertebral disc in scoliosis: calcification and other sequelae. *J Orthop Res, 11*(5), 747-757.

Roberts, S., Urban, J. P., Evans, H., & Eisenstein, S. M. (1996). Transport properties of the human cartilage endplate in relation to its composition and calcification. *Spine (Phila Pa 1976), 21*(4), 415-420.

Rosati, R., Horan, G. S., Pinero, G. J., Garofalo, S., Keene, D. R., Horton, W. A., et al. (1994). Normal long bone growth and development in type X collagen-null mice. *Nat Genet, 8*(2), 129-135.

Roughley, P. J. (2004). Biology of intervertebral disc aging and degeneration: involvement of the extracellular matrix. *Spine, 29*(23), 2691-2699.

Schmid, T. M., Bonen, D. K., Luchene, L., & Linsenmayer, T. F. (1991). Late events in chondrocyte differentiation: hypertrophy, type X collagen synthesis and matrix calcification. *In Vivo, 5*(5), 533-540.

Schmid, T. M., & Linsenmayer, T. F. (1983). A short chain (pro)collagen from aged endochondral chondrocytes. Biochemical characterization. *J Biol Chem, 258*(15), 9504-9509.

Schmid, T. M., Popp, R. G., & Linsenmayer, T. F. (1990). Hypertrophic cartilage matrix. Type X collagen, supramolecular assembly, and calcification. *Ann N Y Acad Sci, 580*, 64-73.

Setton, L. A., & Chen, J. (2006). Mechanobiology of the intervertebral disc and relevance to disc degeneration. *J Bone Joint Surg Am, 88 Suppl 2*, 52-57.

Shen, G. (2005). The role of type X collagen in facilitating and regulating endochondral ossification of articular cartilage. *Orthod Craniofac Res, 8*(1), 11-17.

Skinner, H. B. (Ed.). (2005). *Current diagnosis and treatment in orthopedics*: McGraw-Hill Medical Publisher.

Standring, S. (Ed.). (2008). *Gray's Anatomy: The Anatomical Basis of Clinical Practice, Expert Consult* Churchill Livingstone.

Stokes, I. A., Burwell, R. G., & Dangerfield, P. H. (2006). Biomechanical spinal growth modulation and progressive adolescent scoliosis--a test of the 'vicious

cycle' pathogenetic hypothesis: summary of an electronic focus group debate of the IBSE. *Scoliosis, 1*, 16.

Stokes, I. A., Clark, K. C., Farnum, C. E., & Aronsson, D. D. (2007). Alterations in the growth plate associated with growth modulation by sustained compression or distraction. *Bone, 41*(2), 197-205.

Stokes, I. A., McBride, C. A., & Aronsson, D. D. (2008). Intervertebral disc changes in an animal model representing altered mechanics in scoliosis. *Stud Health Technol Inform, 140*, 273-277.

Takahashi, S., Suzuki, N., Asazuma, T., Kono, K., Ono, T., & Toyama, Y. (2007). Factors of thoracic cage deformity that affect pulmonary function in adolescent idiopathic thoracic scoliosis. *Spine, 32*(1), 106-112.

Thompson, J. P., Pearce, R. H., Schechter, M. T., Adams, M. E., Tsang, I. K., & Bishop, P. B. (1990). Preliminary evaluation of a scheme for grading the gross morphology of the human intervertebral disc. *Spine, 15*(5), 411-415.

Urban, J. P., & Roberts, S. (2003). Degeneration of the intervertebral disc. *Arthritis Res Ther, 5*(3), 120-130.

Urban, J. P., Smith, S., & Fairbank, J. C. (2004). Nutrition of the intervertebral disc. *Spine, 29*(23), 2700-2709.

Urban, M. R., Fairbank, J. C., Bibby, S. R., & Urban, J. P. (2001). Intervertebral disc composition in neuromuscular scoliosis: changes in cell density and glycosaminoglycan concentration at the curve apex. *Spine (Phila Pa 1976), 26*(6), 610-617.

Urban, M. R., Fairbank, J. C., Etherington, P. J., Loh, F. L., Winlove, C. P., & Urban, J. P. (2001). Electrochemical measurement of transport into scoliotic

intervertebral discs in vivo using nitrous oxide as a tracer. *Spine (Phila Pa 1976), 26*(8), 984-990.

Ventura, N., Huguet, R., Salvador, A., Terricabras, L., & Cabrera, A. M. (1995). Intervertebral disc calcification in childhood. *Int Orthop, 19*(5), 291-294.

Wallis, G. A., Rash, B., Sweetman, W. A., Thomas, J. T., Super, M., Evans, G., et al. (1994). Amino acid substitutions of conserved residues in the carboxyl-terminal domain of the alpha 1(X) chain of type X collagen occur in two unrelated families with metaphyseal chondrodysplasia type Schmid. *Am J Hum Genet, 54*(2), 169-178.

Warman, M. L., Abbott, M., Apte, S. S., Hefferon, T., McIntosh, I., Cohn, D. H., et al. (1993). A type X collagen mutation causes Schmid metaphyseal chondrodysplasia. *Nat Genet, 5*(1), 79-82.

Watanabe, H., Yamada, Y., & Kimata, K. (1998). Roles of aggrecan, a large chondroitin sulfate proteoglycan, in cartilage structure and function. *J Biochem, 124*(4), 687-693.

Wu, L. N., Genge, B. R., Lloyd, G. C., & Wuthier, R. E. (1991). Collagen-binding proteins in collagenase-released matrix vesicles from cartilage. Interaction between matrix vesicle proteins and different types of collagen. *J Biol Chem, 266*(2), 1195-1203.

Wu, L. N., Ishikawa, Y., Sauer, G. R., Genge, B. R., Mwale, F., Mishima, H., et al. (1995). Morphological and biochemical characterization of mineralizing primary cultures of avian growth plate chondrocytes: evidence for cellular processing of Ca2+ and Pi prior to matrix mineralization. *J Cell Biochem, 57*(2), 218-237.

Wuthier, R. E. (1982). A review of the primary mechanism of endochondral calcification with special emphasis on the role of cells, mitochondria and matrix vesicles. *Clin Orthop Relat Res*(169), 219-242.

Wuthier, R. E., Wu, L. N., Sauer, G. R., Genge, B. R., Yoshimori, T., & Ishikawa, Y. (1992). Mechanism of matrix vesicle calcification: characterization of ion channels and the nucleational core of growth plate vesicles. *Bone Miner, 17*(2), 290-295.

Xi, Y. M., Hu, Y. G., Lu, Z. H., Zheng, H. J., Chen, Y., & Qi, Z. (2004). Gene expression of collagen types IX and X in the lumbar disc. *Chin J Traumatol, 7*(2), 76-80.

Zhang, Y. G., Sun, Z. M., Liu, J. T., Wang, S. J., Ren, F. L., & Guo, X. (2009). Features of intervertebral disc degeneration in rat's aging process. *J Zhejiang Univ Sci B, 10*(7), 522-527.

A P P E N D I X